

**SQUARE WAVE VOLTAMMETRIC DETERMINATION
OF VARIOUS PHARMACEUTICALS**

Thesis submitted to

COCHIN UNIVERSITY OF SCIENCE AND TECHNOLOGY

in partial fulfillment of the requirements for

the award of the degree of

Doctor of Philosophy in Chemistry

by

THERESA C.J.

(Reg. No. 3264)

Department of Applied Chemistry
Cochin University of Science and Technology
Kochi – 682022

February 2015

Square Wave Voltammetric Determination of Various Pharmaceuticals

Ph. D. Thesis under the Faculty of Science

Author:

THERESA C. J.

Assistant Professor

Department of Chemistry, Vimala College

Thrissur – 680009

E mail: theresacj@gmail.com

Research Guide:

Dr. K. GIRISH KUMAR

Professor of Analytical Chemistry

Department of Applied Chemistry

Cochin University of Science and Technology

Kochi – 682022

E mail: giri@cusat.ac.in

Department of Applied Chemistry

Cochin University of Science and Technology

Kochi – 682022, India

February 2015

**DEPARTMENT OF APPLIED CHEMISTRY
COCHIN UNIVERSITY OF SCIENCE AND TECHNOLOGY
KOCHI - 682 022, INDIA**



Dr. K. Girish Kumar

Tel: 0484-2575804

Professor of Analytical Chemistry

E-mail: chem@cusat.ac.in

Date:

Certificate

Certified that the present work entitled “**Square Wave Voltammetric Determination of Various Pharmaceuticals**”, submitted by Ms. Theresa C. J., in partial fulfillment of the requirements for the degree of Doctor of Philosophy in Chemistry to Cochin University of Science and Technology, is an authentic and bonafide record of the original research work carried out by her under my supervision at the Department of Applied Chemistry. Further, the results embodied in this thesis, in full or in part, have not been submitted previously for the award of any other degree.

K. Girish Kumar
(Supervising Guide)

Declaration

I hereby declare that the work presented in this thesis entitled “**Square Wave Voltammetric Determination of Various Pharmaceuticals**” is based on the original work carried out by me under the guidance of Dr. K. Girish Kumar, Professor of Analytical Chemistry, Department of Applied Chemistry, Cochin University of Science and Technology and has not been included in any other thesis submitted previously for the award of any degree.

Kochi – 22

Theresa C.J.

Dedicated to my Parents

Acknowledgements

This thesis is the outcome of a long-time endurance and hardwork, supplemented with the support and blessings of my teachers, friends and family members. I would like to place an accord of all succors bestowed upon me during this tenure.

First and foremost I would like to extend my sincere gratitude to my guide Dr. K. Girish Kumar, Professor, Department of Applied Chemistry, Cochin University of Science and Technology, Kochi. I thank him immensely for his excellent guidance, support and valuable suggestions throughout this endeavour, which nurtured a lot of confidence in me. I am also much indebted to Sir for motivating me to uptake UGC Minor Project. It would be better to state that 'Teacher is a Second Parent' befits him perfectly. Dr. Anitha Girish, Associate Professor, Department of Chemistry, Maharaja's College, Ernakulam assured her constant support with her presence.

I thank all the faculty members of the Department of Applied Chemistry, CUSAT especially Dr. K. Sreekumar, my Doctoral Committee Member for their kind concern and support. I also acknowledge the timely help of various Heads of the Department. Thanks to the Non – teaching staff members who rendered me a lot of support.

I sincerely thank the Principals of Vimala College, Thrissur Dr. Sr. Lissy John Irimpan (Former) and Dr. Sr. Maries V.L. and the C. M. C. Management for their initiative in executing the FDP leave and all supports given to me.

I am indeed grateful to all my dear teachers of the Department of Chemistry of both Vimala College, Thrissur and Sacred Heart College, Thevara who triggered my interest in the subject and was my real inspiration for doing research.

My sincere thanks to Dr. G. Devala Rao, Principal, KVSR College of Pharmacy, Vijayawada for providing pure drug samples for experimental work.

I was very fortunate to have a handful of loving labmates by my side at various stages of my research. Thanks to my seniors Dr. Rema, Dr. Sareena, Dr. Pearl and Dr. Beena. My research days started with the close acquaintance with Dr. Sindhu, Dr. Renjini, Litha, Dr. Leena and Dr. Laina. Our group was further enlightened with the presence of Dr. Sobhana, Divya, Anuja, Soumya, Zafna, and Meera. I thank Divya, Anuja, Ammu, Unni, Jesny Chechi, Sheela Miss and Shalini who stayed by my side during the tough days of my thesis work. I am grateful to Anuja and Jesny Chechi for editing the thesis.

I sincerely thank all my labmates for their sincere co-operation and encouragement. Special thanks to Sindhu, Renjini and Laina for helping me whole – heartedly during the tedious days of my research work. I also thank some of my dear friends who had spent only a short span of time with us but are still so close – Sreejith, Ajilesh, Ajith, Sruthy, Shanty and Ambili. Hope to maintain these valuable relationships wonderful as always.

I thank my parents for prompting me to aim high, workhard and achieve my goals. My dear brothers Mathews and George encouraged me a lot. I remember with gratitude the beautiful days I stayed with my sister

Elezebath, brother – in – law Biju Paul and sweet Paul and Liz during the days of my research work.

I am deeply indebted to my husband Paul for his immense support, care and sacrifices endured to cherish my dream. Our dear little angel, Mary adjusted a lot during these days but her pleasant smile was always a motivation. I have no words to sincerely thank my mother - in - law for substituting my presence at home.

For the financial services rendered I thank CUSAT for University fellowship, DRDO for project fellowship and UGC – JRF fellowship. I also thank UGC for granting FDP to complete my thesis work.

I thank the scientists at STIC, CUSAT for analysis.

Above all, I bow my head in reverence before the God Almighty for all the blessings showered upon me.

Theresa

Preface

Electrochemical analysis is a powerful and versatile analytical technique of immense utility in the field of pharmaceutical analysis. Due to the similarity in the electrochemical and biological reactions, it can be assumed that the oxidation/reduction mechanisms occurring at the electrode surface and in the body have a common theoretical background. Hence biologically active molecules can be investigated by electroanalysis. They are also excellent tools for the determination of pharmaceutical compounds in different matrices. The advance in experimental electrochemical techniques in the field of drug analysis is because of their short duration for analysis and simple operation procedure as compared to other techniques.

Chemical Sensors are devices that transform chemical information, originating from a chemical reaction of the analyte or from a physical property of the investigating system, ranging from the concentration of a specific sample component to total composition analysis, into an analytically useful signal. Among the various types of chemical sensors, Electrochemical sensors are devices capable of transforming the effect of the electrochemical interaction which takes place between the analyte (or the generated species from the interaction of the analyte and a biological compound) and the electrode into an exploitable electric signal (current or potential). Square Wave Voltammetric Sensors falls under the category of electrochemical sensors which are particularly applied for the determination of pharmaceuticals based on Chemically Modified Electrodes (CMEs).

Development of seven square wave voltammetric sensors for pharmacologically important drugs – Metronidazole benzoate, PAM chloride, Guaifenesin, Tamsulosin hydrochloride and Tinidazole with their potential application studies are presented in the thesis. Electrodes modified chemically with Multi - Walled Carbon Nanotube (MWCNT), conducting polymers, gold nanoparticles (AuNPs) and Prussian Blue (PB) acts as a probe for the electrochemical reactions of these drugs at various electrodes.

The thesis is divided into nine chapters. Brief outlines of the chapters are given below:

Chapter 1 outlines a brief introduction to Square Wave voltammetry, principle, instrumentation and applications. A detailed review about the research in the field of voltammetric sensors based on various chemically modified electrodes is incorporated in this chapter.

Chapter 2 gives a brief description about the materials and instruments used for fabrication of sensors. Preparation of the buffer solutions and cleaning procedure for various electrodes are also included in this chapter.

Chapter 3 includes the different parameters optimized to enhance the sensor performance. It also gives an idea of the general procedure for the analysis of drug content in pharmaceutical formulations and also in real samples like urine which was applied to verify the feasibility of the developed sensors.

Chapter 4- Chapter 8 explains the development of various SWV sensors using a three electrode system. Modified gold, platinum and glassy

carbon acts as the working electrode, platinum auxiliary electrode and Ag/AgCl reference electrode. The voltammograms of analytes in different supporting electrolytes were recorded either on CH instrument or BAS Epsilon instrument. The surface modification of the electrodes was confirmed by SEM images and surface area studies.

Chapter 4 details the electrochemical reduction of Metronidazole benzoate (MET) at a poly (p-toulenesulphonic acid) modified glassy carbon electrode [poly(p-TSA)/(GCE)]. The experimental parameters such as the number of cycles for polymerization, pH of the supporting electrolyte and scan rate were optimized. The application study of the developed sensor in the determination of MET in pharmaceuticals and urine samples have also been dealt in detail. A plausible mechanism involving a two electron reduction of the nitro group on MET to nitroso group is suggested.

Chapter 5 Two different voltammetric sensors based on MWCNT and Prussian blue (PB)/Multi-Walled Carbon Nanotube (MWCNT) nanocomposite film on gold electrode was fabricated for the determination of a nerve gas antidote, PAM chloride (PAM). The rapid electron transfer of MWCNT and the synergistic effect between PB and MWCNT accounts for the improved response on the modified electrodes. The response parameters of the newly developed sensor as well as its analytical applications have been discussed in this chapter. The anodic peak may be attributed to the oxidation of the aldoxime group on PAM to the corresponding carbonyl group.

Chapter 6 describes the development of a simple electrochemical sensor for the voltammetric determination of a commonly used expectorant, Guaifenesin (GF) based on MWCNT/Platinum Electrode (PtE). Optimization studies of the developed sensor, response characteristics and analytical applications are explained in detail in this chapter. GF undergoes a two electron oxidation to the corresponding ketone involving a two step mechanism.

Chapter 7 discusses the fabrication of an electrochemical sensor for Tamsulosin (TAM) based on poly (o-phenylenediamine) modified gold electrode. Electrochemical parameters of the oxidation of TAM on the modified electrode were optimised. The methoxy group in TAM is removed together with the ipso substitution of radical cation by water to give a quinone. Application studies of the developed sensor were carried out in body fluid.

Chapter 8 development and performance characteristics of two novel sensors for the drug Tinidazole (TIN) viz, (1) poly (L-Cys) modified glassy carbon sensor and (2) poly (L-Cys)/ AuNP modified glassy carbon sensor are included in this chapter. The nitro group on TIN, which may be considered as the electroactive centre undergoes a two electron reduction to nitroso group. The application studies of the developed sensors in the determination of the drug in pharmaceutical formulations and urine samples are also explained in this chapter.

Chapter 9 presents the summary and important conclusions of the work done. References are included as a separate section at the end of the thesis.



CONTENTS

Chapter – 1	
Introduction.....	1-30
1.1 Interfacial Electrochemistry	2
1.2 Electrochemistry at the interface.....	3
1.3 Electrochemical Sensors	5
1.3.1 Cyclic voltammetry (CV).....	6
1.3.2 Linear Sweep Voltammetry (LSV).....	7
1.3.3 Square Wave Voltammetry (SWV)	7
1.4 Instrumentation - <i>Cell set-up</i>	10
1.4.1 Working electrode (WE).....	10
1.4.2 Reference Electrode.....	12
1.4.3 Auxiliary/Counter Electrode.....	12
1.5 Current in Voltammetric Sensors	12
1.6 Electrochemical sensors and Chemically Modified Electrodes (CMEs).....	13
1.6.1 Conducting polymers.....	15
1.6.2 Multi -Walled Carbon Nano Tube (MWCNT).....	17
1.6.3 Prussian Blue (PB).....	18
1.6.4 Goldnanoparticles (AuNPs).....	19
1.7 Brief review of the literature on voltammetric/ amperometric sensors for pharmaceuticals based on Chemically Modified Electrodes	20
1.8 Scope of the present work	29

Chapter – 2

Materials & Instrumentation.....31-35

2.1	Chemicals and Drugs used	31
2.2	Instruments used.....	32
2.3	Preparation of Urine Sample.....	33
2.4	Pharmaceutical analysis by SWV.....	33

Chapter – 3

Experimental Parameters.....37-41

3.1	Supporting Electrolyte.....	37
3.2	pH of the Supporting Electrolyte.....	38
3.3	Scan Rate Study.....	39
3.3.1	Cottrell Equation	39
3.3.2	Laviron Equation.....	40
3.4	Interference study	41
3.5	Application studies.....	41

Chapter – 4

Voltammetric Sensor for Metronidazole benzoate.....43-62

4.1	Introduction	44
4.2	Experimental.....	46
4.2.1	Modification procedure for GCE.....	46
4.2.2	Preparation of MET solution.....	46
4.2.3	Recording the voltammogram of MET.....	46
4.2.4	Procedure for the assay of Tablet	46
4.3	Designing of a MET Sensor.....	47
4.3.1	Electropolymerisation of p-TSA on GCE.....	47

4.3.2	Dependence of film thickness on MET determination.....	47
4.3.3	Surface Morphology.....	47
4.3.4	Electrochemical behavior of MET.....	48
4.4	Optimization of Experimental Parameters	49
4.4.1	Supporting electrolyte.....	49
4.4.2	Solution pH.....	49
4.4.3	Scan rate study.....	50
4.4.4	Interference study.....	51
4.4.5	Calibration graph for MET	51
4.5	Electroreduction of MET - <i>a plausible mechanism</i>	51
4.6	Application studies of MET Sensor.....	52
4.6.1	Pharmaceutical formulations.....	52
4.6.2	Spiked urine samples	52
4.7	Validation of the Proposed Method	52
4.8	Conclusions.....	53

Chapter – 5

Voltammetric Sensors for PAM Chloride..... 63-87

5.1	Introduction	64
5.2	Method Implemented.....	66
5.2.1	Functionalisation of MWCNT	66
5.2.2	Preparation of MWCNT - Nafion suspension	66
5.2.3	Preparation of MWCNT modified gold electrode.....	66
5.2.4	Preparation of MWCNT/PB modified gold electrode	67
5.2.5	Preparation of PAM solution	67
5.2.6	Analytical Procedure	67
5.3	Results and Discussion.....	68
5.3.1	Surface morphology of the electrodes.....	68
5.3.2	Electrochemical behavior of PAM.....	69

5.3.3	Establishing the experimental parameters	69
5.4	Analytical figures of merit	71
5.4.1	Calibration curve	71
5.4.2	Regeneration and stability of modified electrodes	72
5.5	Probable mechanism for PAM Oxidation	72
5.6	Analytical applications.....	73
5.7	Conclusions.....	74

Chapter – 6

Voltammetric Sensor for Guaifenesin89-106

6.1	Introduction	90
6.2	Fabrication of GF Sensor.....	92
6.2.1	Cleaning of PtE	92
6.2.2	Functionalisation of MWCNT	92
6.2.3	Modification of PtE with MWCNT	92
6.2.4	Preparation of GF solution.....	93
6.2.5	Electrochemical behavior of GF	93
6.3	Establishing the operational parameters of GF sensor	94
6.3.1	Effect of supporting electrolyte.....	95
6.3.2	Scan rate study	95
6.3.3	Amount of MWCNT.....	95
6.3.4	Interference Study.....	96
6.3.5	Linear concentration range	96
6.4	Mechanistic pathway for GF Oxidation.....	96
6.5	Application Studies	97
6.5.1	Analysis of GF in tablet	97
6.5.2	Analysis of GF in urine sample	98
6.6	Conclusions.....	98

Chapter – 7

Voltammetric Sensor for Tamsulosin107-127

7.1	Introduction	108
7.2	Experimental.....	110
7.2.1	Preparation of poly(o-PDA)/GE.....	110
7.2.2	Analytical Procedure	111
7.2.3	Analysis of urine sample.....	111
7.3	Results and Discussion.....	112
7.3.1	Electropolymerisation of o-PDA and mechanism	112
7.3.2	Voltammogram of TAM.....	113
7.3.3	Optimization of experimental parameters	113
7.4	Probable mechanism for TAM oxidation	115
7.5	Application in urine sample	116
7.6	Conclusions.....	116

Chapter – 8

Voltammetric Sensors for Tinidazole129-153

8.2	Introduction	130
8.2	Materials and method	132
8.2.1	Apparatus	132
8.2.2	Cleaning of GCE.....	133
8.2.3	Fabrication of L-Cys/GCE.....	133
8.2.4	Fabrication of AuNP/L-Cys/GCE.....	133
8.2.5	Preparation of TIN solution	134
8.2.6	Preparation of tablet solution	134
8.2.7	Recording the voltammogram for TIN	134
8.3	Results and Discussion.....	134
8.3.1	Morphologies and electrochemical behavior of modified electrodes	134
8.3.2	Optimization of experimental parameters	136

8.4	Determination of Analytical Figures of Merit.....	139
8.4.1	Calibration curve for TIN determination.....	139
8.4.2	Stability of modified electrodes.....	139
8.5	Proposed Scheme for TIN Reduction.....	140
8.6	Analytical Application in Real Samples.....	140
8.6.1	Determination of TIN in pharmaceutical dosage form.....	140
8.6.2	Determination of TIN in spiked urine samples:.....	141
8.7	Summary and Conclusions.....	141

Chapter – 9

Summary & Conclusions..... 155-157

9.1	Objectives of the Work.....	155
9.2	Summary of the work done.....	156
9.3	Conclusions.....	157

References..... 159-177

Research Papers Published.....179

Conference Papers..... 181

LIST OF FIGURES

Figure 4.1	Structure of Metronidazole benzoate	56
Figure 4.2	Electropolymerisation of 1 mM p-TSA on GCE	56
Figure 4.3	Variation of MET peak current with polymerization cycles	57
Figure 4.4	SEM images of a) Bare GCE b) p (p-TSA)/GCE	57
Figure 4.5	Overlay of CVs of a) bare GCE b) poly (p-TSA)/GCE in 2 mM K ₃ [Fe (CN) ₆] solution at scan rates 40 - 400 mV/s Linear relation between i_p and $v^{1/2}$ (<i>figure in inset</i>).....	58
Figure 4.6	SWVs of 1×10^{-3} M MET at a) Bare GCE b) poly (p-TSA)/GCE.....	59
Figure 4.7	Variation of peak current of 1×10^{-3} M MET in 0.1 M PBS of pH 3 - 9	59
Figure 4.8	Overlay of LSVs of 1×10^{-3} M MET on poly (p-TSA)/GCE at scan rate 40 - 400 mV/s	60
Figure 4.9	Variation of MET peak current with $v^{1/2}$	60
Figure 4.10	Linearity between 1×10^{-3} M MET peak current and logarithm of scan rate	61
Figure 4. 11	Overlay of SWVs of MET in 0.1 M PBS in the concentration range 9×10^{-6} M to 1×10^{-4} M on poly (p-TSA)/GCE.....	61
Figure 4. 12	Linear dependence of MET peak current and concentration in the range 9×10^{-6} M to 1×10^{-4} M on poly (p-TSA)/GCE.....	62
Figure 5.1	Structure of PAM chloride.....	77
Figure 5.2	Electropolymerisation of 2 mM PB on GE in 40 cycles.....	77
Figure 5.3	SEM image of a) Bare GE b) MWCNT/GE c) MWCNT/PB/GE	78
Figure 5.4	Overlay of SWVs of a) Bare GE b) MWCNT/GE c) MWCNT/PB/GE in 2 mM ferricyanide solution at different scan rates	79-80
Figure 5.5	SWVs of 1×10^{-3} M PAM at a) Bare GE b) MWCNT/GE c) MWCNT/PB/GE	80
Figure 5.6	Effect of pH on the anodic current of 1×10^{-3} M PAM chloride at a) MWCNT/GE b) MWCNT/PB/GE.....	81

Figure 5.7	Overlay SWVs of 1×10^{-3} PAM at a) MWCNT/GE b) MWCNT/PB/GE at scan from 40 - 240 mV/s.....	82
Figure 5.8	Variation of peak current with square root of scan rate a) MWCNT/GE b) MWCNT/PB/GE.....	83
Figure 5.9	Effect of the amount of MWCNT-Nafion suspension on a) Bare GE b) PB/GE	84
Figure 5.10	Overlay of SWVs of PAM at different concentrations on a) MWCNT/GE b) MWCNT/PB/GE.....	85
Figure 5.11	Calibration graph for PAM chloride at 25 ^o c on a) MWCNT/GE b) MWCNT/PB/GE	86
Figure 5.12	Variation of oxidation potential of 1×10^{-3} M PAM with natural logarithm of scan rate at MWCNT/PB/GE.....	87
Figure 6.1	Structure of Guaifenesin.....	101
Figure 6.2	Square wave voltammogram of 1×10^{-3} M GF on a) Bare PtE b) MWCNT/PtE in 0.1M H ₂ SO ₄	101
Figure 6.3	SEM images of A) Bare PtE B) PtE/ MWCNT	102
Figure 6.4	Overlay of SWVs at a) Bare PtE b) MWCNT/PtE in 2 mM K ₃ Fe(CN) ₆ at scan rates in the range 20 - 120 mV/s	102-103
Figure 6.5	Overlay voltammograms for the oxidation of 1×10^{-3} M GF at different scan rates in the range 40 - 400 mV/s	103
Figure 6.6	Plot of peak current of 1×10^{-3} M GF against the square root of scan rate in the range 40 - 400 mV/s	104
Figure 6.7	Effect of the amount of MWCNT - nafion suspension on the oxidation of GF at MWCNT/PtE.....	104
Figure 6.8	Overlay of SWVs of GF at MWCNT/PtE in the concentration range 1×10^{-4} M - 1×10^{-5} M	105
Figure 6.9	Calibration graph for GF at MWCNT/PtE in the concentration range 5×10^{-5} M - 4×10^{-4} M	105
Figure 6.10	Plot of peak potential of GF against the natural logarithm of scan rate	106

Figure 7.1	Structure of Tamsulosin.....	119
Figure 7.2	Electropolymerisation of o-PDA on GE in 20 cycles	119
Figure 7.3	Mechanism for the polymerisation of o-PDA on GE.....	120
Figure 7.4	Overlay of CVs of 2 mM $K_3[Fe(CN)_6]$ at a) Bare GE b) poly (o-PDA)/GE.....	120-121
Figure 7.5	Variation of peak current of TAM with sq.root of scan rate at a) Bare GE b) poly (o-PDA)/GE.....	121-122
Figure 7.6	SEM images of a) Bare GE b) poly (o-PDA)/GE	122
Figure 7.7	Voltammogram of TAM at a) Bare GE b) p (o-PDA)/GE.....	123
Figure 7.8	Effect of pH on TAM oxidation	123
Figure 7.9	Effect of number of cycles of polymerization on TAM oxidation.....	124
Figure 7.10	Effect of scan rate on TAM oxidation at poly (o-PDA)/GE.....	124
Figure 7.11	Dependence of peak current on square root of scan rate.....	125
Figure 7.12	Plot of peak potential against ln (scan rate)	125
Figure 7.13	Overlay of SWVs of TAM in the concentration range 8×10^{-7} - 1×10^{-5} M.....	126
Figure 7.14	Calibration curves of TAM concentration and oxidation peak current	126
Figure 8.1	Structure of Timidazole.....	144
Figure 8.2	Polymerization of L-Cysteine on GCE in 30 segments from 5 mM L-Cys in 0.1 M PBS.....	144
Figure 8.3	Electrodeposition of AuNP on poly(L-Cys)/ GCE in 20 cycles.....	145
Figure 8.4	SEM images of a) bare GCE b) poly (L-Cys)/GCE c) AuNP/poly (L-Cys)/GCE.....	145-146
Figure 8.5	CVs of a) Bare GCE b) poly (L-Cys)/GCE c) AuNP/ poly (L-Cys)/GCE in 5 mM $Fe(CN)_6^{4-3-}$ at different scan rates	147-148
Figure 8.6	Response characteristic of 1×10^{-5} M TIN on a) Bare GCE b) poly (L-Cys)/GCE c) AuNP/ poly (L-Cys)/GCE.....	148
Figure 8.7	pH dependence of TIN reduction on a) poly (L-Cys)/GCE b) AuNP/ poly (L-Cys)/GCE.....	149

Figure 8.8	Overlay diagrams for TIN reduction at different scan rates in 0.1 M PBS on a) poly (L-Cys)/GCE b) AuNP/ poly (L-Cys)/GCE.....	149-150
Figure 8.9	Ep against ln scan rate for TIN reduction on a) poly (L-Cys)/GCE b) AuNP/ poly (L-Cys)/GCE.....	150-151
Figure 8.10	SWV of TIN at different concentrations on a) poly (L-Cys)/GCE b) AuNP/ poly (L-Cys)/GCE.....	151-152
Figure 8.11	Calibration curve for TIN on a) poly (L-Cys)/GCE b) AuNP/ poly (L-Cys)/GCE.....	152-153

LIST OF SCHEMES

Scheme 4.1	Mechanism for MET reduction involving two electrons	62
Scheme 5.1	Mechanism for PAM oxidation.....	87
Scheme 6.1	Mechanism for the oxidation of GF	106
Scheme 7.1	Mechanism for TAM oxidation	127
Scheme 8.1	Mechanism for Reduction of TIN	153

LIST OF TABLES

Table: 4.1	Influence of various foreign species on the reduction peak current of $1 \times 10^{-3} \text{M}$ MET.....	54
Table: 4.2	Comparison of the developed method for MET determination with the reported works.....	54
Table: 4.3	Determination of MET in tablet	55
Table: 4.4	Determination of MET in urine sample	55
Table: 5.1	Influence of various foreign species on the oxidation peak current of $1 \times 10^{-3} \text{M}$ PAM.....	75
Table: 5.2	Comparison of the developed method for PAM determination with the reported works	75
Table: 5.3	Determination of PAM in urine sample	76
Table 5.4	Comparison of the results obtained by developed sensors and standard method in urine sample.....	76
Table 6.1	Interference by the foreign species in the determination of GF	99
Table 6.2	Comparison of the developed method with the reported works	99
Table 6.3	Tablet study of GF using developed method and standard method...	100
Table 6.4	Recovery % of GF in urine sample using MWCNT/PtE	100
Table 7.1	Interference by the foreign species in the determination of TAM	117
Table 7.2	Comparison of the developed method with the reported works for TAM determination	117
Table 7.3	Recovery % of TAM in urine sample at poly (o-PDA)/GE.....	118
Table 8.1	Effect of interferents on the reduction of TIN at various modified electrodes.....	142
Table: 8.2	Comparison of the developed method for TIN determination with the reported works	142
Table 8.3	Determination of TIN in pharmaceutical formulations.....	143
Table 8.4	Determination of TIN in urine sample on modified electrodes	143

Chapter - **1**

INTRODUCTION

Contents

1.1	Interfacial Electrochemistry
1.2	Electrochemistry at the interface
1.3	Electrochemical Sensors
1.4	Instrumentation – Cell set-up
1.5	Current in Voltammetric Sensors
1.6	Electrochemical sensors and Chemically Modified Electrodes (CMEs)
1.7	Brief review of the literature on voltammetric/ amperometric sensors for pharmaceuticals based on Chemically Modified Electrodes
1.8	Scope of the present work

Recent advancements in the field of material science and characterization techniques has bloomed ‘Electrochemistry’ as a multidisciplinary branch procured from Physics, Chemistry, Biology and Chemical Engineering. Metamorphosis of Electrochemistry from 18th century to the current stage is ascribed to the kinetic, thermodynamic and quantum mechanical study possible at the ‘**Surface**’ both experimentally and theoretically. The increasing thrust for the development of various materials has further glorified this branch of Chemistry.

1.1 Interfacial Electrochemistry

Electrochemistry is defined as the branch of chemistry that scrutinizes various phenomena resulting from combined chemical and electrical effects. The facet of physical electrochemistry including ion-solvent and ion-ion interactions, activity coefficients, the Debye Huckel theory, ionic mobility and conductivity, transport number etc. falls under the category of ‘Bulk Electrochemistry’.

In contrast, the application of electrochemical processes to measure the quantity of an analyte species (Analytical Electrochemistry) is dependent to larger extent on their thermodynamics (entropy and enthalpy change of the reaction), kinetics (rate of a reaction), and mass transport effects. This branch of electrochemistry is termed as ‘Interfacial electrochemistry’ which gained importance in the latter half of the 20th century with two Nobel Prize highlights: Heyrovsky in 1959 for polarography and Marcus in 1992 for the theory of electron transfer. Upon inducing a charge at the electrode/electrolyte interface, a potential difference develops due to the charge separation between the two layers resulting in enormous field strength. This is regarded as the core of Interfacial Electrochemistry.

The interfacial region in the vicinity of the electrode surface has been described by various models. A ‘double layer’ model was envisaged by Helmholtz. According to him, the excess charge on the metal is neutralized by unimolecular layer of oppositely charged ions [1]. Guoy-Chapman significantly improved the double layer by introducing a ‘diffuse model’. Combining these two models, Stern [2] proposed the possibility of two elements for a double layer.

- 1) An inner element known as a compact layer or Helmholtz layer which is charge free and is in the atomic dimension.
- 2) Outer element or diffuse layer or Guoy- Chapman layer with unequally distributed anions and cations obeying Boltzmann and Poisson laws.

Currently the most accepted model is the one proposed by Grahame with three distinct regions. The regions are

- 1) Inner Helmholtz Plane (IHP) passing through the centre of specifically adsorbed ions.
- 2) Outer Helmholtz Plane (OHP) passing through the centre of fully solvated ions which is the site for electron transfer.
- 3) Extending outside OHP to the bulk solution is the diffuse layer with a maximum width of 100 \AA . The actual potential felt by the reactant is influenced by this layer.

1.2 Electrochemistry at the interface:

Charge transfer at the interface, which is motivated by the gradients in electrical and chemical potentials triggers an electrochemical reaction. Electron Transfer (ET) reactions at the electrode/solution interface are affected by applied electrode potential, temperature, mass transport and structure of the double layer. All electrochemical reactions are regarded as activated processes (by applied potential as in voltammetry) that can overcome the activation energy barrier which acts as a driving force for the ET reaction at the interface. Interfacial ET processes can be either oxidation or reduction involving an electron transfer either to or from the highest occupied level (Fermi level).

The two approaches of ET reaction include macroscopic phenomenological approach describing the electron transfer kinetics in terms of rate equation and current – potential relationship, which is based on the activated complex theory of chemical reaction. The latter being microscopic molecular based approach. The basic principle of electrochemical kinetics is based on Butler – Volmer equation which describes the dependence of electrical current on an electrode to the electrode potential. The ET reaction can be summed up to the following stages: diffusion of the species to the reaction site, rearrangement of ionic atmosphere, re-orientation of solvent dipoles and finally the ET.

The current flow at the interface can be either Faradaic or Non – Faradaic. Faradaic current is the charge transferred across the electrified interface as a result of an electrochemical reaction obeying Faraday’s law. This can be simply illustrated as follows: if the applied potential is greater than the potential of the electroactive species, reduction occurs at the working electrode. As a result electroactive species diffuses from the bulk solution to the electrode surface and the reduction product simultaneously diffuses towards the bulk solution to the electrode surface. The magnitude of this current depends on the rate of the electrochemical reaction which is directly a measure of mass transport and rate of electron transfer at the electrode surface.

Non – Faradaic current is the charge associated with the movement of electrolyte ions, adsorption, desorption etc at the interface. In voltammetric measurements this short – lived charging current is termed as the background current. Apart from these two currents, in the absence of an analyte, a small residual current may flow due to the oxidation or reduction of the trace impurities or charging/discharging of the capacitor at the interface.

1.3 Electrochemical Sensors

Wolfbeis [3] defined chemical sensor as “small sized devices comprising a recognition element, a transduction element and a signal processor capable of continuously and reversibly reporting a chemical concentration”. Depending on the transducer type they are categorized as electrochemical, optical, mass – sensitive and heat - sensitive sensors.

Action of an electrochemical sensor may be stated in the following steps:

- Analyte species drifting towards the sensing element
- Analyte being bound selectively to the sensor surface
- Generation of signal at the sensor surface
- Transmission of this signal to the electrochemical instrument to be displayed as the output signal.

Electrochemical sensors can be categorized as potentiometric, voltammetric or conductometric depending on their signal transduction. In potentiometric sensors, the recognition element converts the analytical signal into a potential signal generated from an electrochemical reaction at the interface. Most commonly used potentiometric sensor is an Ion- Selective Electrode (ISE) where the potential of an analyte is measured selectively against an indicator electrode. At the interface between the ion selective membrane and the solution a potential due to the charge separation arises. This potential is measured under condition of zero current and it varies logarithmically with the activity (concentration) of the species generated according to the Nernst equation.

In conductometric sensors the electrolyte conductivity at the device which can be altered by the presence of certain chemical species is measured. The two components of a conductometric sensor are a sensitive conducting layer and contact electrodes. The sensing effect is based on the change of the number of mobile charge carriers in the electrolyte arising from adsorption, catalysis or diffusion at the electrode surface. As the measured conductivity is a linear function of the ion concentration, it can be used for sensor applications [4].

Voltammetry (varying voltage) provides an electroanalytical method, in which the current varies linearly with the concentration of the electroactive species (analyte) involved in a chemical or biological recognition process at a scanned potential. Amperometry is a type of voltammetry in which current is registered at a potential that is maintained constant throughout the analysis.

Electrochemical, particularly voltammetric sensors are fabricated in the present investigation. Among the various potentiodynamic voltammetric techniques cyclic voltammetry, linear sweep voltammetry and square wave voltammetry are employed in the present work.

1.3.1 Cyclic voltammetry (CV)

It was first reported in 1938 and theoretically explained by Randles. In CV, the working electrode is subjected to a triangular potential sweep whereby the initial potential E_i rise to a final potential E_f and returns back to the start potential at a constant potential sweep rate. The current density is plotted against a function of applied potential and is obtained as a resultant voltammogram. Depending on the nature of the electroactive species an oxidation or reduction peak is obtained on a cyclic voltammogram. The

current corresponding to the oxidation/reduction is a characteristic signal of the analyte and is proportional to its concentration. Peak height and width of the voltammogram depends on the electrolyte concentration, nature of the electrode material and potential sweep rate. Applying this principle, sensor for various analytes has been developed.

1.3.2 Linear Sweep Voltammetry (LSV)

LSV is closely related to CV, but the potential is swept linearly in only one direction. So LSV is particularly useful to study irreversible reactions. As in CV, the potential of the working electrode is ramped from E_i to E_f and the peak current varied linearly with the square root of scan rate. The voltammogram depends on the rate of electron transfer reaction, chemical reactivity of the electroactive species and the scan rate. Being a highly sensitive method, LSV has been applied for the development of sensors for various analytes.

1.3.3 Square Wave Voltammetry (SWV)

SWV is a potential electrochemical technique among the various pulse techniques for analytical applications, study of electrode mechanisms and their kinetics [5 – 7]. It is regarded as an advanced technique unifying the pulse technique with CV and impedance techniques [8]. In SWV, the potential modulation comprises of a staircase potential ramp combined with square – shaped potential pulses [9].

SWV originated from Barker's polarography as early as 1957 [10] is still regarded as the simplest among these techniques. Here a symmetric square wave of frequency and amplitude riding on either a ramp or slow

staircase waveform is recorded. The difference in currents at the ends of two successive half cycles is measured.

With the advent of electronic technology, a Kalousek commutator [11], in which a potential is switched between a slowly varying ramp and a constant value to study the reversibility of electrode reaction was developed. The current is measured only on the reverse half cycle of the voltammogram.

The most common format of SWV is Osteryoung method [12] as the whole measurement process can be carried out using a very rapid voltage scan rate. Unlike the other wave forms, in Osteryoung method the base potential increases after each full cycle by a potential ΔE . As the experimental time increases the initial potential changes from E_0 to E_{SW} , where E_{SW} is SWV amplitude, and held for a pulse duration. Thereafter the potential falls down to $E_0 - E_{SW}$ in the same pulse range. At the end of each pulse the current is measured as i_f (forward current) and i_b (backward current). Thus in the course of a single potential cycle, the electrode reaction is driven to both anodic and cathodic reactions which gives an insight into the electrode mechanism. The difference between these two currents is displayed as the typical SWV response of a particular analyte. The resultant of all net currents corresponding to each potential cycle sum up to gave a bell – shaped curve with an output current that increases linearly with scan rate.

In the recent years, SWV has emerged as a viable technique replacing the lengthy and expensive chromatography, spectrophotometry etc. It is a versatile method for the quantification of important class of compounds such as proteins [13], vitamins [14], pesticides [15], alkaloids [16], metal traces [17] and drugs [18].

The wide range of applications of SWV is mainly due to their advantages over other voltammetric techniques. A few of them as reported by Topal et al. [19] are listed below:

- ◆ SWV is the most pronounced pulse techniques as the response can be found at a higher effective scan rate (500 mVs^{-1}).
- ◆ Analytical determinations can be made at lower concentrations even upto 10 nM.
- ◆ Higher sensitivity because of its efficient discrimination of capacitance current.
- ◆ Speed of analysis is not more than 5 seconds.
- ◆ As the difference of currents is larger than either component currents the height of the peak can be easily interpreted thus enhancing the accuracy of the technique.
- ◆ Surface fouling at the electrode is minimized due to the lower time of analysis.

SWV is regarded as an excellent tool for the simultaneous determination of compounds with close redox potentials due to their outstanding resolution. Tian et al. [20] reported the simultaneous determination of ascorbic acid, dopamine and uric acid at an AuNP modified graphite electrode.

A new approach for the evaluation of the kinetics of a surface confined electrode reaction was developed by Wang et al. [21, 22]. This is based on Fourier transformed SWV (FT-SWV) depending on a quasi-reversible maximum. They are also an excellent choice for assessing the

number of bacterial culture in real samples. E. coli population has been detected by SWV on a MWCNT modified GCE [23].

An insight to the redox mechanisms of various enzymes is included in protein – film voltammetry. This coupled with SWV provides detailed information regarding the mechanism, kinetics and thermodynamics of important proteins in the human body [24].

In pharmaceutical formulation analysis the prior importance is the determination of drugs in biological fluids following their administration in human. Electrochemical methods, especially SWV are a remarkable choice in this regard.

1.4 Instrumentation – Cell set-up

Voltammetric measurements are conducted in a three electrode system which offers the advantage of maintaining a stable reference potential. The three electrodes are working electrode, reference electrode and auxiliary/counter electrode.

1.4.1 Working electrode (WE)

WE form an ideal phase interface for electron transfer reaction. They have a large potential range suitable for both anodic and cathodic reactions. WE should possess long term stability and an easily reproducible surface for their excellent analytical application.

They are often made of unreactive metals or carbon and are broadly classified as solid type and liquid type. Carbon based (glassy carbon, carbon paste, graphite, TiO₂ etc) and metal based (Pt, Au, Ag) electrodes are included in the category of solid electrodes. Example for liquid electrodes are dropping

mercury electrode, hanging mercury drop electrode, static mercury drop electrode etc. Glassy carbon, platinum and gold electrodes with chemical modifiers are chosen as the working electrodes for the determination of various pharmaceuticals in the present work.

a) *Platinum Electrode (PtE):*

Due to the ease of fabrication into various forms and electrochemical inertness, Pt surface acts as a platform for the redox reaction of the different electroactive analyte species. But even in the presence of trace amount of acid or water in the electrolyte, H⁺ ions are reduced to hydrogen gas at fairly modest negative potentials. As a result any useful analytical signal of the analyte may be obstructed. This has limited their applicability in the field of sensor fabrication.

b) *Gold electrode (GE):*

GEs are inert like PtE, but are particularly useful for the preparation of modified electrodes with Self Assembled Monolayers (SAM). Oxidation at its surface in the positive potential range restricts their application in that range.

c) *Glassy Carbon Electrode (GCE):*

GCE possess the properties of both glassy and ceramic materials combined with graphite. The application of GCE as a WE for voltammetry was proposed initially by Zittel and Miller [25]. Their specific surface orientation, extreme resistance to chemical attack and impermeability to gases and liquids renders them suitable as an electrode material for sensor fabrication. The advantage of GCE over other electrodes is that they can operate in positive as well as negative potentials.

1.4.2 Reference Electrode

It is the reference point against which the potential of other electrodes can be measured. They should have a well – defined, stable equilibrium electrode potential unaffected by the electrolyte species. Most common primary reference electrode is Standard Hydrogen Electrode (SHE). But due to the difficulty in constructing and maintaining SHE a secondary reference electrode (Ag/AgCl, Calomel electrode) is often preferred in voltammetric measurements. Ag/AgCl electrode is composed of a Ag wire immersed in a solution saturated with AgCl and KCl.

1.4.3 Auxiliary/Counter Electrode

Counter electrode permits the passage of current in an electrochemical reaction through it without disturbing the potential of the reference electrode. Platinum electrode is often the best choice in this regard due to its inertness and speed with which most electrode reactions occur at its surface.

1.5 Current in Voltammetric Sensors

The basic principle of voltammetric sensors is the effect of concentration of the detecting species on the current – potential characteristics of the reduction or oxidation reaction involved. The mass transfer rate of the analyte onto the electrode surface and the kinetics of the electron transfer at the electrode surface directly affect the current - potential characteristics. But the simultaneous assessment of mass transfer and kinetics is rather complicated. Hence voltammetric measurements are carried out hydrodynamically.

The three modes of mass transport are:

- **Migration** of charged species due to a potential gradient
- **Convection** due to the movement of species by mechanical means
- **Diffusion** of the analyte from the bulk solution to the electrode surface arising from a concentration gradient.

In voltammetry, the current that flows through the WE depends upon the kinetics of the overall electrode process and its magnitude is based on the rate of the slowest mass transfer rate. By eliminating the effect of migration by a supporting electrolyte and that of convection by an unstirred electrolyte solution, the limiting current depends only on diffusion.

1.6 Electrochemical sensors and Chemically Modified Electrodes (CMEs)

The concept of chemically modified electrode (CME) was first introduced by Murray and co-workers [26] in 1975 to describe electrodes that had foreign molecules deliberately immobilized on their surfaces. This added a new dimension to the sensing technique in voltammetry.

According to IUPAC definition [27] CME is *an electrode made of a conducting or semiconducting material that is coated with a selected monomolecular, multimolecular, ionic, or polymeric film of a chemical modifier and that by means of faradaic (charge-transfer) reactions or interfacial potential differences (no net charge transfer) exhibits chemical, electrochemical, and/or optical properties of the film.*

The various strategies adopted [28] for the preparation of CMEs on electrode surface includes the following:

Irreversible Adsorption

The modifier species may be spontaneously adsorbed on the surface of an inert electrode from its solution as the substrate environment is energetically more favourable.

Covalent Attachment

Covalent bonds are formed between the specific functional groups on the electrode surface and the molecule to be attached to the surface. This is applicable to electrode surfaces such as SnO₂, TiO₂, RuO₂, platinum, gold, etc.

Formation of polymer layer

Coating the electrode surface with polymer film is proven to be the most versatile approach for preparing CMEs. These polymers belong to four general categories - redox polymer, ion – exchange polymer, co-ordination polymer and electronically conductive polymer. Polymer film can be coated by the following methods:

- Dip the surface to be coated into a solution of the polymer followed by evaporation of the solvent. Even though simple to execute, here the amount of material to be coated cannot be controlled.
- Alternatively, the surface is coated with a measured volume of the modifier.
- Film of uniform thickness can be achieved on semi-conductor materials by spin – coating.
- Electropolymerisation of the monomer unit on the electrode surface by cyclic voltammetry.

Coating inorganic material on electrode surface

Considering the well – defined microstructures of clay and zeolite coupled with their ability to withstand high temperatures and oxidizable environment, they are chosen as electrode modifiers. Transition metal hexacyanoferrates (eg: Prussian blue) are also good candidates due to their interesting electrochemical and optical properties.

Langmuir – Blodgett (LB) Method

LB method entails the use of a surfactant to create a highly ordered monolayer film at the air/water interface and transferring these films to substrate surfaces. The multiple transfers ultimately results in the formation of multilayer films at the surface.

Many of the biologically important compounds, even though electro active requires a higher overpotential at solid electrode surfaces for analysis. This may result in larger background current resulting in a poor detection limit of the analyte species. CMEs can impart the desired properties on to the electrode by suitable chemical reagents which otherwise will restrict their applicability. Various chemical modifiers used in the present study include MWCNT, Prussian blue, Goldnanoparticles and conducting polymers of L-Cysteine, p - toluenesulphonic acid and o-phenylenediamine on gold, platinum and glassy carbon electrodes.

1.6.1 Conducting polymers

Conducting polymers or synthetic metals are materials which possess both electrical property of metals and exceptional properties of polymers such as resistance to corrosion, chemical attack, less expensive [29] etc. Shirakawa et. al was the first to report about a conducting polymer, polyacetylene which

exhibited dramatic magnification in electrical conductivity on treatment with oxidizing or reducing agents [30].

Electrochemical polymerization is the most popular method for the synthesis of conducting polymers as homogeneous polymer films can be formed directly at the electrode surface, possessing a wide range of applications. Polymerization can be achieved by three different modes: galvanostatic (constant current), potentiostatic (constant potential) or potentiodynamic (cyclic or pulse voltammetric technique is applied). Based on the conduction mechanism, they are categorized as:

- Conducting polymer composites (polypyrrole, polyaniline etc)
- Organometallic polymer conductors (metallophthalocyanine and their polymers)
- Polymeric charge transfer complexes (tetrathiafulvalene)
- Inherently conducting polymers (polyacetylene)

The common feature of conducting polymers is the existence of an extended π – conjugated system. Unlike in metals, the conductivity of polymers cannot be explained by simple band theory. Radical cation, formed during the course of polymer growth is delocalized only over a small segment called a polaron. The energy associated with this species is higher than that in the valence band, which is of the order of energy of the band gap of metals attributing to the conductivity of polymers. This excellent conductivity makes them suitable for electron transfer [31], ion recognition [32] and electroanalysis [33].

1.6.2 Multi –Walled Carbon Nano Tube (MWCNT)

Chemistry of nano structured carbon materials emanated with the discovery of C₆₀ fullerene in 1985. Iijima [34] revolutionized the branch of material science with the introduction of carbon nanotube in 1991. Geim and Novoselov [35] further enlightened the world of carbon by developing graphene in 2010. Basically, all the three nanomaterials are based on the same structural unit with a single – layer of sp² hybridized graphene sheet. This sheet may be wrapped, rolled or left flat as in fullerene, carbon nanotube and graphene respectively.

CNTs can be synthesized by arc discharge method [36], laser ablation method [37], chemical vapours deposition method [38], flame synthesis method [39] or silane solution method [40]. Among the two types of CNTs, MWCNT has greater application than SWNT (single – walled nano tube) [41] as they can be prepared in bulk with high purity in the presence of a catalyst. Also a chance of occurrence of defect is relatively less in MWCNT and cannot be easily twisted due to their complex structure.

Two decades, since their discovery CNT have a broad range of applications in the field of medicine, polymer science, super capacitors etc [42]. The use of CNTs onto inert electrodes for pharmaceutical analysis has been achieved by voltammetry. The salient features of CNTs which makes them remarkable as electrode modifiers are:

- Greater electron transport rate through quantum effect due to their nano scale dimensions, which will be propagated along the axis of the tube.
- Highly symmetric structure with basic graphene units.
- A greater length to diameter ratio of 1,000,000.

A technical barrier in the use of CNTs is their reduced solubility which can be improved by functionalisation. This is achieved by adsorption, electrostatic interaction or covalent bonding of CNT with molecules that render hydrophilicity. Apart from enhancing the solubility of CNTs, functionalisation leads to better biocompatibility and reduction in aggregation of the individual tubes through vander Waals forces [43].

1.6.3 Prussian Blue (PB)

PB is an inorganic polycrystalline substance possessing electrochromic, photophysical, electrocatalytic and magnetic properties. Chemically PB has the structure $\text{Fe}^{\text{III}}_4 [\text{Fe}^{\text{II}}(\text{CN})_6]_3$ and can be prepared by chemical, electrochemical and sonochemical method [44 – 46].

In electrocatalysis, PB has a great potential for hydrogen peroxide sensing. This is achieved on glassy carbon, graphite, platinum and gold electrodes modified with PB [47 -50]. The deposition of PB on solid electrodes was first reported by Neff et. al in 1978 [51]. Further their electrochemical stability is improved by various electroactive materials such as cetyltrimethyl ammonium bromide [52], MWCNT [53], screen printed electrodes [54] etc.

The peculiar electrochemical nature of PB is attributed to its stability and structure wherein low molecular weight species penetrate and get reduced at the metal hexacyanoferrate. This structure may be comparable to a biological binding component with all the advantages of an inorganic species attributing to their application as a CME [55].

Farah et al. determined H_2O_2 on a PB/graphene oxide modified GCE by CV [56]. A disposable electronic tongue using PB film electrodeposited

onto CD-R gold surfaces for recognizing milk adulteration was reported recently [57]. Persulphate anions were analyzed [58] voltametrically on a PB modified platinum disc electrode. But their instability in neutral medium often ruptures the modified PB layer after a few scans. This restricts their application in sensor development.

The use of protective layers such as nafion, surfactants, chitosan, nanohybrids etc has improved their operational stability amazingly. Kumar et. al [59] prepared a Au – PB nanocomposite film on GCE from a solution containing ferricyanide and HAuCl₄ for analysis of peroxide. A glucose biosensor [60] based on the co-deposition of glucose oxidase and chitosan – gold nanoparticle on a Au – PB modified GCE exhibited wide linear range, fast response time and satisfactory operational stability.

1.6.4 Goldnanoparticles (AuNPs)

The history of AuNPs date back to the first report about colloidal gold by Faraday [61] in 1857. Since then, AuNPs are the most extensively studied nanoparticles [62] with several application possibilities in catalysis, therapeutics, diagnostics and sensing. The development of new sensing platforms employing AuNPs is exclusively based on their optical and electrochemical properties [63 – 66].

Among the various methods for AuNP syntheses [67, 68], electrochemical deposition is superior as it has the ability to monitor the size and distribution of nanoparticles on the electrode surface [69, 70]. AuNPs occur in various size ranging from 2 – 100 nm and are categorized [71] as gold nanorods/nanoshells/nanocages/nanospheres or SERS nanoparticles.

AuNPs has triggered a new genre for the development of novel sensors for the voltammetric analysis of various species due to their high aspect ratio, electrical conductivity and biocompatibility.

1.7 Brief review of the literature on voltammetric/ amperometric sensors for pharmaceuticals based on Chemically Modified Electrodes

A poly (carmine)/GCE sensor was fabricated [72] to investigate the electrochemical behavior of tinidazole by voltammetry. A well-defined reduction peak was observed at 606 mV after 90s accumulation with a constant potential of 0 mV. The cathodic peak current is proportional to the concentration of tinidazole between 1.0×10^{-7} M - 5.0×10^{-5} M. The lower limit of detection of tinidazole at the fabricated sensor was found to be 5.0×10^{-8} M.

Amperometric sensor for sophoridine [73] based on L - Theanine modified GCE was developed. The electrode process was studied by CV and amperometry. The results revealed that the poly (L - Theanine) membrane effectively decreased the anodic potential of sophoridine and greatly increased its response current. Linear concentration range of the method was 1.0×10^{-6} M – 1.4×10^{-4} M at the developed sensor.

A poly (3-methylthiophene) modified GCE with nafion/single – walled carbon nanotube film was fabricated and used for the selective and sensitive determination of dopamine. Scanning Electrochemical Microscopy of the electrode surface established the uniform dispersion of CNT on the conductive polymer. The hybrid film on the electrode remarkably enhanced the electrochemical response of dopamine with a detection limit of 5 nM. Moreover the influence of ascorbic acid and uric acid were diminished

notably. Analyte species was successfully determined in dopamine hydrochloride injection and human serum [74].

Santos et. al [75] developed a voltammetric sensor for amoxicillin based on glutaraldehyde cross- linked poly(glutamic acid) modified GCE. Amoxicillin can be determined at a lower potential based on its pre – concentration by cathodic accumulation. In 0.1 mol L⁻¹ acetate buffer solution (pH 5.2) with an accumulation period of 60 sec, amoxicillin can be determined at a lower concentration of 0.92 μ mol L⁻¹. Application studies of the analyte were carried out in urine sample at the developed sensor.

Sensitive determination of domperidone [76] using a conducting polymer layer of 4-amino-3-hydroxynaphthalene sulphonic acid on GCE in acidic solution is reported recently. Domperidone exhibited a well-defined oxidation peak at 840 mV at the modified electrode with a detection limit of 12 nM. The determination was highly effective with no interference from common metabolites such as ascorbic acid, uric acid, xanthine and hypoxanthine. The developed sensor had a high analytical utility as confirmed by its application in body fluids and tablets for the determination of domperidone.

GCE was modified with poly (p-aminobenzenesulphonic acid) under a controlled potential between -1500 mV and +2000 mV for 24 segments by cyclic voltammetry. Electrochemical behavior of tryptophan at this modified electrode showed an improved response when compared with bare GCE. Under the optimized conditions, the anodic peak current of tryptophan varied linearly with concentration in the range $1.0 \times 10^{-7} - 1.4 \times 10^{-6}$ mol L⁻¹. The proposed method is successfully applied for the determination of tryptophan in a commercial amino acid oral solution [77].

Amperometric response of the common interferents such as ascorbic acid, hydrogen peroxide and paracetamol in many enzymatic biosensors were studied at a polyaniline (PANI) modified platinum electrode. Aniline was electropolymerised on the electrode surface at a controlled potential of 800 mV from an acidic solution containing aniline monomer. The electrochemical behavior of paracetamol and hydrogen peroxide retarded significantly at the modified platinum electrode, whereas ascorbic showed an enhanced activity due its adsorption through the PANI pores onto the electrode surface [78].

The electrochemical behavior of two tricyclic anti – depressants viz; imipramine HCl and amitriptyline HCl were investigated using a carbon paste electrode modified with poly (N- vinylimidazole). The current density of imipramine HCl increased with the polymer layer on the electrode and amitriptyline HCl gained electro activity upon modification. Developed sensor was applied for the determination of these analytes in tablets [79].

Paracetamol was determined voltammetrically [80] on a composite film of poly (4-vinyl pyridine) and MWCNT at a glassy carbon electrode. The notable enhancement in the kinetics of oxidation of paracetmol was attributed to the combined effect of the conducting property of the polymer with the physical property of the nanotube. The exceptional change in electrochemical response after modification include 300 fold higher peak current, nanomolar detection limit, stable for more than 60 days, no influence from physiologically common interferences and application in real samples.

Sindhu et al. [81] reported the voltammetric determination of pyridine-2-aldoxime methochloride (PAM chloride) on a poly (p-toluene sulfonic acid) modified glassy carbon sensor. Compared to the bare electrode, the modified electrode showed an enhancement in oxidation peak current of

PAM. The peak current for PAM oxidation varied linearly with concentration in the range 1×10^{-3} M - 1×10^{-7} M and detection limit was found to be 3×10^{-8} M for PAM. Application studies of the developed sensor was conducted in body fluids.

A novel sensor based on electropolymerization of β - cyclodextrin and L - arginine on carbon paste electrode for determination of various fluoroquinolones (ofloxacin, ciprofloxacin, norfloxacin and gatifloxacin) was reported. The proposed method [82] exhibited excellent electrocatalytic activity towards the oxidation of these drugs. Concentration of all the four fluoroquinolones was determined in pharmaceutical formulations and human serum samples by the fabricated sensor.

Electrocatalytic oxidation of some cephalosporins [83] was carried out on poly (o-anisidine)/SDS/Ni modified carbon paste electrode by cyclic voltammetry. Addition of SDS (sodium dodecyl sulphate) to the monomer solution enhanced the polymer growth rate on the electrode surface. Kinetic parameters such as charge transfer coefficient catalytic reaction rate for oxidation were also determined. Application studies were conducted in pharmaceutical formulation with the developed sensor.

Zhao et al. [84] reported the voltammetric determination of Promethazine on MWCNT coated gold electrode (MWCNT/Au). Promethazine exhibited a sensitive oxidation peak at the modified electrode in pH 4 phosphate buffer solution at 660 mV (vs. SCE). Under the optimized conditions, the anodic peak current is linear to promethazine concentration in the range from 5.0×10^{-8} M - 1.0×10^{-5} M with a detection limit of 1.0×10^{-8} M. This method has been successfully applied for the determination of the analyte in medicine sample.

Simultaneous determination of ascorbic acid and caffeine in pharmaceutical preparation is of prime importance as in combination they possess analgesic and antipyretic effects. Gupta et al. achieved this on MWCNT modified glassy carbon electrode by square wave voltammetry. Oxidation of these species involved equal number of protons and electrons. In view of the high sensitivity, the developed technique has been used for the reliable determination of ascorbic acid and caffeine in tea leaves, coffee, cold drink (mountain dew), pharmaceutical preparations and urine sample [85].

A novel composite film of CNT and cysteic acid was coated on GCE for the electroanalytical determination of nimesulide by differential pulse voltammetry. Cysteic acid was formed by the electrochemical oxidation of L-cysteine at the electrode surface. Prior to its determination, nimesulide was subjected to strong accumulation. Developed sensor was found to be highly selective, sensitive, stable and is applicable for nimesulide determination in pharmaceutical formulation and human serum samples [86].

Oxidative behavior of amlodipine besylate [87] was studied at a gold electrode and (oxidized-MWCNT)/gold electrode by cyclic voltammetry and square wave anodic stripping voltammetry. AFM analysis showed that oxidized – MWCNT covered the electrode surface homogeneously. The linear dependency of anodic current versus concentration of amlodipine besylate was in the range 13.80 – 19.61 μgmL^{-1} .

Silva et al [88] reported a novel vertically aligned carbon nanotube/graphene oxide on a titanium substrate for the determination of atorvastatin calcium by differential pulse adsorptive stripping voltammetry. The film was developed by a microwave plasma chemical vapour deposition method followed by oxygen plasma treatment. This resulted in the improved

wettability of the film which enhanced the response of atorvastatin calcium at the developed sensor. Optimization studies were carried out and feasibility in real sample was analysed.

The voltammetric oxidation of valganciclovir [89] was investigated at MWCNT modified glassy carbon electrode sensor using cyclic voltammetry and differential pulse voltammetry. Various operational parameters were optimized and the calibration curve was linear in the concentration range $7.5 \times 10^{-9} - 1.0 \times 10^{-6}$ M with a lower detection limit of 1.52×10^{-9} M. Probable mechanism for oxidation of valganciclovir is an irreversible electrochemical process with a diffusion under adsorption – controlled system. Sensitive and selective determination of the analyte in its dosage forms was also conducted.

An ultra-sensitive voltammetric sensor for trace analysis of carbamazepine [90] on a MWCNT/glassy carbon electrode sensor was developed. When compared to bare electrode, the electroactivity of carbamazepine enhanced significantly on modification with nanotube. Results obtained were comparable with those obtained by chromatographic technique. The method was successfully applied for its determination in real pharmaceutical tabulations, spiked and unspiked waste water samples.

Electrocatalytic determination of tryptophan based on (Copper-Cobalt) hexacyanoferrate film modified graphite electrode was reported by Liu et. al. The experimental parameters such as scan cycles, ratio of Cu(II) and Co (II), pH and applied potential were investigated in detail. The linear concentration range of tryptophan was found to be $10 \mu\text{M} - 900 \mu\text{M}$ with a lower limit of detection of $6 \mu\text{M}$. The developed sensor was successfully applied for the determination of tryptophan in milk [91].

The spontaneous deposition of Prussian blue particles onto conducting material such as multi - walled carbon nanotube was carried out by Shiu et. al. [92] this was confirmed by AFM and SEM. CNT/Prussian blue composite modified GCE exhibited an electrocatalytic property for hydrogen peroxide reduction. The high sensitivity of the fabricated sensor for peroxide reduction may be due to the synergistic effect of CNT with Prussian blue. This was further developed as an amperometric glucose biosensor with good selectivity, sensitivity and short response time.

Laina et al [93] fabricated a Prussian blue /MWCNT nanocomposite modified glassy carbon electrode sensor for the determination of Hesperidin by differential pulse voltammetry. The electrochemical reduction of the bio - flavanoid was shown to be a diffusion controlled process involving the reduction of the keto group to the corresponding hydroxyl group. Application studies were conducted in spiked urine samples.

Sanghavi et al. [94] prepared a graphene – gold nanoparticle composite on the surface of glassy carbon electrode by electrochemical co – reduction of a mixture of graphene oxide and chloroauric acid. Characterization studies of the sensor were conducted by scanning electron microscopy, uv-visible spectrophotometry, x-ray diffraction, cyclic voltammetry, chronocoulometry and electrochemical impedance spectroscopy. This nano composite on GCE was then decorated with a film of nafion. Sumatriptan, a drug for migraine treatment was voltammetrically determined using this developed sensor with a sub-nano molar detection limit of 7.03×10^{-10} M. practical application of the developed sensor were demonstrated in commercially available tablets, urine and blood serum samples.

Gold film was coated on platinum electrode from chloroauric acid by pulse plating technique. The ultra - stable chemically modified electrode thus fabricated was characterized by electrochemical impedance spectroscopy. Based on the thin gold film electrode, a voltammetric sensor for oxidation of ketamine was developed. The method was found to be highly accurate, reliable and useful for the quality control of ketamine hydrochloride injection [95].

Highly efficient electrochemical sensor based on modified carbon paste electrode was fabricated recently for the determination of olanzapine hydrochloride. The modifiers include glutamine and gold nanoparticles in the presence of sodium dodecyl sulphate medium of pH 7. Limit of detection and limit of quantification were found and calculated to be 3.58×10^{-9} M and 1.19×10^{-8} M respectively. After optimizing the various operational parameters, the proposed method was applied for the determination of analyte in pharmaceutical dosage form and human urine. The developed sensor was successful for olanzapine analysis together with fluoxetine, ascorbic acid and uric acid [96].

A novel graphene – AuNP modified gold electrode sensor was fabricated for the determination of an antiepileptic drug, carbamazepine. Various electrochemical studies employed to study the oxidation of carbamazepine are CV, LSV and electrochemical impedance spectroscopy. The electrocatalytic effect of a graphene-AuNP modified electrode may be attributed to π - π stacking interaction between carbamazepine and the sp^2 hybridized carbon in graphene, which makes the electron transfer feasible. In addition, gold nanoparticles may act as nanoantennas, enhancing the tunneling of electrons toward the nanostructured surface. The lower detection limit of the analyte at the modified electrode was found to be 3.03×10^{-6} M [97].

Atta et al. [98] reported a AuNP modified carbon paste electrode sensor for the voltammetric determination of terazosin, an antihypertensive drug. The effect of parameters including pH and scan rate on the response was investigated. A linear range from 8.0×10^{-9} to 5.4×10^{-5} molL⁻¹ with correlation coefficient of 0.9995 and detection limit of 1.2×10^{-10} molL⁻¹ was obtained. This sensor was used for determining terazosin spiked in urine, and excellent recovery results are achieved.

The electrochemical oxidation of atenolol at AuNP/ MWCNT modified glassy carbon electrode (GCE) was studied by various voltammetric techniques. The enhanced peak current of atenolol at this sensor may be attributed to the synergetic effects of AuNPs and MWCNT. The proposed sensor was successfully applied to the determination of atenolol in pharmaceutical samples, human urine and blood serum as real samples. The method was also applied to monitor atenolol in urine samples of a dosage-received volunteer [99].

The electrochemical behaviour of celecoxib at a graphene/AuNP based carbon ionic liquid electrode was studied by means of cyclic voltammetry and differential pulse voltammetry. The excellent electrocatalytic activity of the developed sensor towards the reduction of celecoxib in phosphate buffer solution was attributed to the larger surface area and greater electron transfer ability. The calibration curve was linear in the concentration range of 0.5 to 15 μ M and the detection limit was about 0.2 μ M. Celecoxib was determined in real samples with the developed method [100].

Promethazine was analysed voltammetrically at an AuNP modified carbon paste electrode sensor in 0.1 M PBS (pH 6). The oxidation peak current of promethazine at the surface of Au-NPs/CPE is 2.25 times larger than the

bare electrode, and the peak potential at the Au-NPs/CPE is shifted 42 mV to more negative values. The diffusion coefficient and kinetic parameters such as the electron transfer coefficient (α), ionic exchanging current (i_0) and catalytic rate constant, for promethazine were determined using electrochemical approaches. The modified electrode was applied to determine promethazine in real samples with satisfactory results [101].

1.8 Scope of the present work

The analytical investigations of bulk materials, drug formulations and impurities are of prime importance to improve the efficiency, safety and economy of drug therapy. This has resulted in rating pharmaceutical analysis among the versatile branch of applied analytical chemistry. Almost three decades ago, the only method for the determination of all the antibiotics was by microbiological method. But this has been replaced by more sensitive and sophisticated techniques such as HPLC, voltammetry, potentiometry etc.

Voltammetry may be regarded as an excellent electroanalytical technique for pharmaceutical analysis as they are easily portable with instrumental simplicity, short analysis time and low cost. Voltammetric sensors are routinely used to probe the chemical reactivity of an oxidized/reduced moiety in a drug. The development of various nanomaterials, conducting polymers etc has added a new dimension to sensor technology. Chemically modified electrodes as voltammetric sensors are of remarkable significance as they can lower the peak potential of the analyte species and increase their selectivity and sensitivity.

From the proficiency acquired by our group in the field of electroanalytical techniques by developing quiet a number of sensors [102 –

Chapter – 1

107] for various analytes, the present work is aimed at the determination of Metronidazole, PAM chloride, Gauifenesin, Tamsulosin and Tinidazole using various modifiers on gold, platinum or glassy carbon electrode.



MATERIALS AND INSTRUMENTATION

2.1	Chemicals and Drugs used
2.2	Instruments used
2.3	Preparation of Urine Sample
2.4	Pharmaceutical analysis by SWV

A brief description about the reagents and chemicals used for the voltammetric analysis of various pharmaceuticals, method adopted for the electrochemical determination, various preparation procedures and the instruments used are included in this chapter.

2.1 Chemicals and Drugs used

All the reagents and solvents used throughout were of the analytical grade. Milli-Q water from Millipore Direct-Q instrument were used for sample preparation when required. The modifiers MWCNT, PB, o-phenylene diamine, p- toluenesulphonic acid, HAuCl₄ and L-Cysteine were purchased from Sigma-Aldrich, SRL Chemicals, Lancaster and s.d fine Chemicals. All chemicals were used as received except MWCNT and o-PD. MWCNT was carboxylated and o-PD subjected to twice recrystallization from water before use.

Pure drugs used for the analysis viz Metronidazole benzoate (MET), PAM Chloride (PAM), Guaifenesin (GF), Tamsulosin hydrochloride (TAM) and Tinidazole (TIN) were obtained as gift samples. Pharmaceutical formulations used for tablet study was purchased from local distributors.

Excellent voltammetric response of the drugs except TAM and GF were observed in 0.1 M phosphate buffer solution (PBS) at the modified electrodes and that of TAM in 0.1 M acetate buffer solution (ABS) and GF in 0.1 M H₂SO₄. Preparation of these buffer solutions are tabulated as Table 2.1 and Table 2.2.

2.2 Instruments used

Either BAS Epsilon electrochemical analyzer or CH instrument was used for voltammetric analysis. IUPAC mode was chosen for displaying the voltammogram with anodic positive and cathodic negative. A conventional three electrode system with working electrode (gold, platinum or glassy carbon) of various modifications, Ag/AgCl reference electrode and platinum auxiliary electrode were employed. In addition to SWV (Square Wave Voltammetry) technique, Cyclic Voltammetry (CV) and Linear Sweep Voltammetry (LSV) were adopted for the analysis.

pH measurements were performed on a Metrohm and ELICO pH meter. Electrode cleaning and sample dissolutions were carried out in an Ultrasonicator (Oscar Ultrasonics Pvt. Ltd., Mumbai). SEM images were recorded using JOEL 6390 LV at STIC, CUSAT, Kochi. Spectrophotometric determinations were carried out on an Evolution 201 UV-Visible spectrophotometer.

2.3 Preparation of Urine Sample

Urine sample was prepared by dissolving the chemicals given in Table 2.3. in 25 mL aqueous solution.

2.4 Pharmaceutical analysis by SWV

Stock solutions of the analyte prepared were serially diluted with the appropriate supporting electrolyte. This was taken in an electrochemical cell immersed with the three electrodes and the voltammogram recorded in the SWV mode. The analyte exhibited either an oxidation or reduction at the modified electrodes. Further, mechanisms of the electrochemical reactions were studied by LSV and surface area by CV.

Table 2.1 Preparation of 0.1 M Phosphate buffer solution

pH	NaH ₂ PO ₄ (in grams/100 mL)	Na ₂ HPO ₄ (in grams/100 mL)
2	1.3799	0.0001
3	1.3790	0.0003
4	1.3780	0.0036
5	1.3615	0.0360
6	1.2143	0.3218
7	0.5836	1.5466
8	0.0940	2.497
9	0.010	2.6605
10	0.0010	2.6781

Table 2.2 Preparation of 0.1 M Acetate buffer solution

pH	CH ₃ COOH (in grams/100 mL)	CH ₃ COONa. 3H ₂ O (in grams/100 mL)
2	0.5994	0.0024
3	0.5900	0.0237
4	0.5098	0.2054
5	0.2161	0.8711
6	0.0319	1.2885
7	0.0036	1.3534
8	0.0034	1.3602
9	0.00038	1.3609
10	0.0000	1.3609

Table 2.3 Preparation of urine sample

No:	Compound	Quantity
1	$\text{NH}_4\text{H}_2\text{PO}_4$	0.7725 g
2	NaCl	1.27 g
3	KCl	0.715 g
4	CaCO_3	0.078 g
5	$\text{MgCl}_2 \cdot 6\text{H}_2\text{O}$	0.1045 g
6	HCl	2.175 mL
7	H_2SO_4	0.1675 mL
8	Urea	4.625 mg



3.1	Supporting Electrolyte
3.2	pH of the Supporting Electrolyte
3.3	Scan Rate Study
3.4	Interference study
3.5	Application studies

Various experimental parameters such as supporting electrolyte, pH, scan rate, and influence of various interferents for optimizing the developed sensor is described in this chapter. Application studies that illustrate the feasibility of the sensor are also discussed here.

3.1 Supporting Electrolyte

IUPAC definition - An electrolyte containing chemical species that are not electroactive (within the range of potentials used) and which has an ionic strength and conductivity much larger than those due to the electroactive species added to the electrolyte. Commonly used supporting electrolytes include chlorides, nitrates, sulphates and perchlorates of lithium, sodium, potassium, tetra alkyl ammonium salts, acids, bases and buffer solutions.

The two modes of transport operating in a quiescent solution are diffusion and migration. But in voltammetry, ‘diffusion – only’ conditions are generally preferred as they are easily reproducible and more accurate [108]. By varying the applied potential at the working electrode, electrolysis occurs which induces a potential gradient and concentration gradient which migrates and diffuses chemical species respectively in solution.

With the addition of a suitable supporting electrolyte [109, 110] with a concentration 10 to 100 fold excess that of the analyte, the resistivity of the solution decreases thus screening the effect of the potential gradient in solution. Bard et al. [111] demonstrated voltammetry to be purely diffusional as the electrons ‘bypass’ potential gradient by quantum mechanical tunneling.

As part of present investigations, voltammetric measurements of the analyte is carried out in 0.1 M concentrations of different supporting electrolytes such as KCl, NaOH, H₂SO₄, PBS, ABS, BRB, citrate buffer etc. They also have the ability to determinate the potential range of the analyte in a voltammetric measurement. The electrolytic solution in which the analyte species gives the lowest peak potential is chosen as the supporting electrolyte for the drug for further studies with the developed sensor.

3.2 pH of the Supporting Electrolyte

Voltammetric measurements carried out in aqueous solutions are likely to be pH dependent as the addition/removal of an electron from the analyte molecule may induce the uptake or loss of a proton. Hence the pH studies are conducted with the analyte in the chosen supporting electrolyte ranging its pH from acidic to neutral to basic. Optimal pH for the analysis is fixed as the one which gave a stable voltammogram with lower peak potential

and enhanced current response for the drug of interest at the modified electrode sensor.

pH studies establish the feasibility of the developed sensor for the particular analyte in acidic/basic media. This may eventually be a supporting factor while predicting the mechanism of the reaction.

3.3 Scan Rate Study

3.3.1 Cottrell Equation

For diffusion controlled square wave voltammetric experiment, the current measured depends only on the rate at which the analyte diffuses to the electrode surface. In 1903, Frederick Gardner Cottrell [112] derived a relation between electric current and time in an electrochemical experiment based on Fick's second law of diffusion. According to Cottrell equation,

$$i_p = \frac{nFAc\sqrt{D}}{\sqrt{\pi t}}$$

where D is the diffusion coefficient (m²/s), c is the concentration in bulk solution (mM), A is the surface area of the electrode (m²), F - Faraday's constant, t - time in seconds and n being the number of electrons transferred. Practically this equation may be simplified as

$$i_p = k/\sqrt{t}$$

where k is the collection of constants for a given system. Further 1/√t is replaced with v^{1/2}, v being the scan rate ranging from 20-2000 mV/s. Thus any deviation from linearity in the plot of peak current of the analyte at the

developed sensor against $\nu^{1/2}$ indicates that the electrochemical process drifts away from diffusion characteristics.

3.3.2 Laviron Equation

In electrode kinetics electron transfer coefficient is a very useful parameter for investigating the mechanism. Butler and Volmer defined electron transfer coefficient as the fraction of electrostatic potential energy affecting the reduction rate in an electrode reaction, with the remaining fraction affecting the corresponding oxidation state.

$$\alpha = \frac{RT}{nF} \left(\frac{d \ln j}{dE} \right)$$

The term $\left(\frac{dE}{d \ln j} \right)$ is the anodic Tafel slope (b), n is the number of electrons involved in oxidation or reduction and other terms has their usual meaning. The equation was simplified by Laviron as

$$b = \frac{RT}{\alpha nF}$$

and is strictly applicable only for elementary one electron transfer step ($n = 1$).

For a totally irreversible electrode reaction, the value of αn is estimated from the slope of the plot of peak potentials against the logarithm of various scan rates (ν). The value of α alone is obtained from the slope of $\log I_p$ against $\log \nu$. For diffusion controlled process $\alpha = 0.5$, and any deviation from this can be deduced from the experimental value. The number of electrons involved 'n' can then be calculated which will give an insight to the reaction mechanism. Based on the value of 'n' and previous reports a plausible mechanism for the various analytes chosen is established in the present work.

3.4 Interference Study

The selectivity of the developed sensor is dependent on the interferences from the various compounds. It is highly probable that many co-existing surface active compounds capable of competing with the analyte of interest may increase or decrease the peak response in the chosen supporting electrolyte. The influence of these species was studied by recording the voltammogram of the analyte in the presence of various foreign species under identical experimental condition as the developed method. The tolerance limit was assumed as the maximum concentration of the foreign substances which caused an approximately $\pm 5\%$ relative error in the determination.

3.5 Application Studies

The feasibility of a fabricated electrochemical sensor can be examined by their application in real samples. Concentration studies are conducted in the tablet solution of the analyte with the developed sensor. Peak current is plotted as a function of concentration and unknown concentrations are determined graphically. Replicate number of experiments is conducted and standard deviations of analyses are tabulated. Results obtained are then compared with that of a standard method.

Similarly application studies are carried out in spiked urine sample. 2 mL of prepared urine (as described in chapter 2) is mixed with 8 mL of the chosen buffer solution. Concentration studies are conducted as in tablet solution.



Chapter - 4

VOLTAMMETRIC SENSOR FOR METRONIDAZOLE BENZOATE

Contents

4.1	Introduction
4.2	Experimental
4.3	Designing of a MET Sensor
4.4	Optimization of Experimental Parameters
4.5	Electroreduction of MET – <i>a plausible mechanism</i>
4.6	Application studies of MET Sensor
4.7	Validation of the Proposed Method
4.8	Conclusions

A simple and sensitive electrochemical method for the determination of metronidazole benzoate (MET) based on poly (p-toluenesulphonic acid) modified glassy carbon electrode (GCE) is described in this chapter. MET yielded a well defined reduction peak at -560 mV on the modified GCE which was 100 mV potential less than that on a bare GCE. The peak current was proportional to MET concentration in the range 9×10^{-6} M – 1×10^{-4} M and the detection limit was found to be 6.0×10^{-7} M. Various operational parameters of the sensor such as supporting electrolyte, pH, scan rate etc were optimized by experimental technique. Application studies of the developed sensor were carried out in pharmaceutical formulation and spiked urine samples.

4.1 Introduction

Metronidazole benzoate (figure 4.1), (MET) [1-(2-benzyloxyethyl)-2-methyl-5-nitroimidazole] is a nitroimidazole derivative. This drug has proven to be effective against dysentery, vaginitis, periodontitis and several other microbial infestations [113]. It is also used to battle less common infections like giardiasis or beaver fever and trichomoniasis, a sexually transmitted disease.

MET is used in combination with other acid-suppressing agents for the treatment of gastric *Helicobacter pylori* infections. It is metabolized primarily in the liver yielding two oxidative products – hydroxyl derivative and acetic acid derivative. The acetic acid metabolite does not possess any pharmacological activity and is passed off through the urine.

MET exerts its antimicrobial effects through the production of free radicals that are toxic to microbes. It inhibits nucleic acid synthesis by disrupting the DNA of microbial cells. This function occurs only when MET is partially reduced and this is observed only in anaerobic cells which are attacked by the reaction intermediates such as nitro anionic radical and hydroxyl amine derivative [114]. The microorganism protozoa and anaerobic bacteria usually cause infections in the gum, pelvic cavity and abdomen where oxygen is not essential for cell growth. Even though safe in human beings, prolonged use of MET may be carcinogenic to animals. So the use of MET has been banned by the US Government in animals that will be used for human food.

MET may be administered orally or intravenously for the treatment of severe infections. It has the ability to block the alcohol digestion in the body

leading to the accumulation of acetaldehyde in the blood stream. This may be very dangerous as the extend of possible reactions are unpredictable. So even a trace amount of alcohol should be avoided during MET medication.

Methods for the assay of MET in pharmaceutical dosage forms include capillary electrophoresis [115], chromatography [116], nuclear magnetic resonance spectrometry [117] and spectrophotometry [118]. Compared with these methods, electroanalytical techniques are far more superior in terms of simplicity, time constrain and cost. Additionally MET contains a nitro group, which may be treated as the active centre for electrochemical sensing.

There are a few reports for MET determination in electroanalytical research based on the reduction of the nitro group on the electrode surface. But the intermediates formed during reduction often poison the electrode surface. So various electrode modifiers have been used for MET determination on GCE including β -cyclodextrin/ AuNP/poly-L-cysteine [119], carbon nanotube [120], porphyrin [121], graphene composite [122] and DNA [123].

Our focus here is on poly (p-toluenesulphonic acid) [poly (p-TSA)] modified GCE for the determination of MET, as the conducting polymer layer of p-TSA may be strongly adhered to the surface forming a stable film due to their negatively charged surface. The resultant modified electrode exhibited a better performance for MET determination and can be used for analyses of the drug in pharmaceutical samples and urine.

4.2 Experimental

4.2.1 Modification procedure for GCE

GCE was polished with 0.05 μm alumina slurry on a polishing pad, rinsed thoroughly with water. Polished GCE was then sonicated in methanol, 1:1 HNO_3 and acetone consecutively, washing with water each time. The electrode was subsequently placed in a solution containing 0.1 M NaCl/1 mM p-TSA and a cyclic potential sweep was applied in the range -2000 mV to +2500 mV [124] at a scan rate of 100 mV/s in 30 cycles. The modified electrode was then washed with Milli Q water and a blue film appeared on the surface after drying. The electrode surface was then activated in 0.1 M PBS by CV from -800 mV to +800 mV.

4.2.2 Preparation of MET solution

A 1×10^{-2} M solution of MET was prepared by dissolving 41.7 mg of the sample in 10 mL methanol. Diluted solution was prepared daily from this stock solution with the chosen supporting electrolyte.

4.2.3 Recording the voltammogram of MET

The voltammetric behavior of MET was carried out by sweeping the potential from -800 mV to 0 mV at 100 mV/s in the square wave mode on a CHN electrochemical workstation with a conventional three electrode system including poly (p-TSA)/ GC working electrode, a platinum wire counter electrode and an Ag/AgCl reference electrode.

4.2.4 Procedure for the Assay of Tablet

Ten tablets were accurately weighed and finely powdered. An amount required for the preparation of 1×10^{-3} M MET solution was transferred from

the powdered sample into a 25 mL standard flask and made up in methanol. Appropriate solutions of the tablet were prepared by taking the micro amount of the aliquots of the supernatant liquid in the supporting electrolyte.

4.3 Designing of a MET Sensor

4.3.1 Electropolymerisation of p-TSA on GCE

The cyclic voltammogram for the electro polymerization of p-TSA on GCE is depicted in figure 4.2. Three reduction peaks appeared at +358 mV, -528 mV and -1156 mV and an oxidation peak at + 1520 mV. As reported by Nabais et al [125] the multiple reduction peaks in the first cycle corresponds to the reduction of monomer but a prominent oxidation peak appeared only from the third cycle onwards. The larger peaks observed in the subsequent cycles reflects the continuous growth of the uniform polymeric film.

4.3.2 Dependence of film thickness on MET determination

The thickness of poly (p-TSA) film on GCE surface can be controlled by regulating the number of cyclic scans for polymerization. The current response (i_p) of MET at the modified electrode by varying the number of cycles from 10 to 40 for polymerization is given in figure 4.3. As the value of i_p ceases to increase after 30 cycles, this was chosen appropriate for electro polymerization of p-TSA on GCE.

4.3.3 Surface Morphology

The SEM images of bare and modified GCE are given in figure 4.4. Obviously surface modification has occurred which can serve as a platform for catalyzing MET reduction on poly (p-TSA)/GCE.

Surface modification of the electrode is further established by comparing the effective surface areas of both bare GCE and poly (p-TSA)/GCE. The CV of 2 mM potassium ferricyanide solution was recorded at these electrodes in the potential range 0 – 600 mV at various scan rates as given in figure 4.5.

The linear relation between peak current and square root of scan rate is given in the inset of figure 4.5. The corresponding regression equations are:

$$i_p = 1.51052 v^{1/2} - 2.58851 \quad (R^2 = 0.99781) \quad \text{- for bare GCE and}$$

$$i_p = 5.24442 v^{1/2} - 11.20681 \quad (R^2 = 0.99051) \quad \text{- for poly (p-TSA)/GCE}$$

The surface area of the electrodes are then estimated from the slope of the curve applying Randles Sevcik equation,

$$i_p = 2.69 \times 10^5 A n^{3/2} D^{1/2} c v^{1/2}$$

where A- effective surface area in cm^2 , D- diffusion coefficient in cm^2/s , n – number of electrons transferred per mole of the electroactive species and c – concentration of the solution. The effective surface area of 0.1021 cm^2 for bare GCE is increased to 0.3543 cm^2 when modified with p-TSA. From the above observation, it was assumed that MET can be reduced easily on the surface of poly (p-TSA)/GCE as the conducting polymer layer offers a modified surface of thrice enhanced surface area.

4.3.4 Electrochemical behavior of MET

The electrochemical behavior of MET at poly (p-TSA) film coated GCE have been examined using SWV in 0.1 M PBS. A 1×10^{-3} M MET solution gave a reduction peak at -676 mV in bare GCE which decreased to -560 mV on the surface of poly (p-TSA)/GCE. Also the peak current enhanced

from 25.96 μA to 82 μA with a polymeric film of p-TSA on the surface of GCE (figure 4.6). The absence of an oxidation peak in the reverse scan of MET by CV confirms that the reduction is totally irreversible.

The surface activity of polymer modified electrode is dependent on the charge exerted by them. Thus the reduction of MET may be ascribed to the electrostatic interaction between the positively charged $-\text{NO}_2$ group of MET and the high electron density of the sulphonyl group of poly (p-TSA). This would ultimately lead to an increase in the concentration of MET around the surface of the modified electrode. The outcome is the facile reduction of MET on poly (p-TSA)/GCE which is manifested by the better peak current and reduced peak potential.

4.4 Optimization of Experimental Parameters

4.4.1 Supporting electrolyte

The electrochemical reduction of 1×10^{-3} M MET at poly (p-TSA)/GCE have been carried out in various supporting electrolytes. MET exhibited a well – defined reduction voltammogram in 0.1 M solutions of NaCl, KOH, PBS and ABS; but not in HCl. As the best current response with lowest reduction potential appeared in PBS, this was preferred as the supporting electrolyte for MET determination throughout the experiment.

4.4.2 Solution pH

The reduction of MET was carried out in PBS of pH varying in the range 3 – 9 and is illustrated in figure 4.7. At lower pH ($\text{pH} < 7$), multiple peaks appeared in the voltammogram establishing the fact that the reaction proceeds via intermediate steps. Also peak potential was dependent on pH in this range which is suggestive of protonation [126] as the initial step prior to

reduction. But at a higher solution pH, potential remains almost independent of pH and only a single peak appeared in the voltammogram. Absence of multiple peaks for MET reduction is attributed to the overlap of the various reduction peaks of the intermediates formed in the reaction of only slightly varying potentials. This behavior is very common among the heterocyclic nitroimidazoles. Considering all these observations into account together with the peak current response, pH 7 was chosen optimal for MET determination.

4.4.3 Scan rate study

The effect of potential scan rate on the reduction of MET was studied in PBS containing 1×10^{-3} M MET. LSV of this solution was carried out in the range 40 – 400 mV/s and the overlay voltammograms are given in figure 4.8. Moreover a linear relation between peak current and square root of scan rate indicates that the process is diffusion controlled (figure 4.9). Also the peak current remains unaltered with the accumulation time which justifies the diffusional behavior.

According to Laviron's conclusion, the relation between the peak potential E_p and $\ln v$ for MET determination on the modified electrode was examined graphically (figure 4.10). These parameters showed a linear relationship with a slope b . The number of electrons involved in the MET reduction (n_a) is given by the equation:

$$b = RT/\alpha n_a F$$

where $\alpha = 0.5$ for a totally irreversible electrode process. The value of n_a is calculated as 1.6 (~2) which confirms that two electrons are involved in MET reduction.

4.4.4 Interference study

The effect of the foreign species on the determination of 1×10^{-3} M MET was investigated by SWV and is given in table 4.1. NaCl, dextrose, urea, ascorbic acid and tinidazole were chosen for the study of selectivity of the proposed method. A 100 fold excess of NaCl, dextrose and urea did not interfere with MET analysis on the poly (p-TSA)/GCE sensor. Analyte solution containing an equimolar concentration of ascorbic acid had no effect on MET determination. But, tinidazole a drug chemically very similar to MET interfered severely.

4.4.5 Calibration graph for MET

Under the optimized experimental conditions, the SWV demonstrating the excellent response of poly (p-TSA)/GCE for MET determination with concentration is given in figure 4.11. The reduction peak current was found to be linear to MET concentration in the range 9×10^{-6} M – 1×10^{-4} M (figure 4.12) with a detection limit of 6.5×10^{-7} M. Also the developed sensor is remarkably excellent for MET determination in terms of detection limit when compared to the works reported earlier (Table 4.2).

4.5 Electroreduction of MET – a plausible mechanism

Nitroimidazoles can undergo reduction to the corresponding amines in a complex process involving six electrons [127] or a four electron reduction [128] to nitro derivatives and hydroxyl amine. However protonated nitroimidazoles undergoes reduction to nitrosyl accepting only two electrons [129]. As the number of electrons involved in the reduction is calculated to be two by Laviron equation, the most probable mechanism is the reduction of NO_2 group of MET to nitrosyl group (Scheme 4.1).

4.6 Application Studies of MET Sensor

4.6.1 Pharmaceutical formulations

The SWV determination of MET in pharmaceutical formulation was conducted on poly (p-TSA)/GCE using the solution prepared from the tablet as in section 4.2.4. The solution was diluted in 0.1 M PBS to concentrations comparable to those in the calibration curve for MET and the concentration of drug in the tablet determined graphically. The declared amount of MET in the tablet was in agreement with the results tabulated from these concentrations (Table 4.3).

4.6.2 Spiked Urine Samples

The feasibility of fabricated sensors for MET in urine sample was analysed. Various concentration of the drug solution in PBS containing fixed amount of urine sample was prepared. The electrochemical behaviour of drug solution on the modified electrodes was studied by SWV and the unknown concentrations determined from the calibration graph. The recovery percentage is in the range 98 – 103 % (table 4.4).

4.7 Validation of the Proposed Method

The developed method for the determination of MET using poly (p-TSA)/GCE by SWV was validated with the standard method from European Pharmacopeia [130]. The absorbances of the MET tablet solution in the concentration range 1×10^{-5} M to 1×10^{-4} M was measured between 220 – 350 nm and plotted graphically. From the calibration graph, unknown concentrations were determined. The results obtained by the developed method and standard method were in good agreement (Table 4.3), thus validating the application of poly (p-TSA)/GCE sensor for MET reduction.

4.8 Conclusions

A poly (p-TSA)/GCE sensor was fabricated for the voltammetric determination of MET by SWV. MET gave a reduction peak at - 560 mV with a high peak current of 82 μ A. The electrostatic interaction between the negatively charged poly (p-TSA) film and the cationic species of MET contributes to the improved response of MET at this electrode. Various experimental parameters of the fabricated sensor were optimized. The MET reduction involved an irreversible, diffusion controlled, two electron mechanism. A possible mechanistic pathway for MET reduction was proposed. Application studies of the developed sensor were carried out in pharmaceutical tabulations and spiked urine samples

Table: 4.1 Influence of various foreign species on the reduction peak current of 1×10^{-3} M MET

Foreign species	Concentration (M) Upper Limit	Signal change (%)
Sodium chloride	1×10^{-1}	5.7
Potassium Sulphate	1×10^{-1}	4.8
Dextrose	1×10^{-1}	2.8
Urea	1×10^{-1}	4.7
Ascorbic acid	1×10^{-3}	3.7
Tinidazole	1×10^{-3}	>60

Table: 4.2 Comparison of the developed method for MET determination with the reported works

No:	Method adopted	Lower detection limit (M)
1	Flow injection spectrophotometry [131]	4.08×10^{-3} M
2	Kinetic Spectrophotometry [132]	2.4×10^{-4} M
3	Spectrophotometry [133]	5.2×10^{-7} M
4	HPLC [134]	7.2×10^{-8} M
5	Gas Chromatography [135]	2.5×10^{-3} M
6	Reverse Phase liquid chromatography [136]	7.2×10^{-5} M
7	Voltammetry [137]	5.8×10^{-12} M
8	Voltammetry [121]	4.36×10^{-6} M
9	Voltammetry (<i>present method</i>)	6.00×10^{-7} M

Table: 4.3 Determination of MET in tablet

Sample	Method adopted	Declared amount	Found amount	SD	CV
Metrogyl (Unique, India)	Present method	200 mg	202 mg	0.51	0.25
	Standard method	200 mg	200 mg	0.53	0.26

Table: 4.4 Determination of MET in urine sample

Amount of MET added in urine sample	Amount of MET found in urine sample	Recovery %
3.00×10^{-5} M	3.11×10^{-5} M	103.3
6.00×10^{-5} M	6.02×10^{-5} M	100.4
9.00×10^{-5} M	8.86×10^{-5} M	98.5

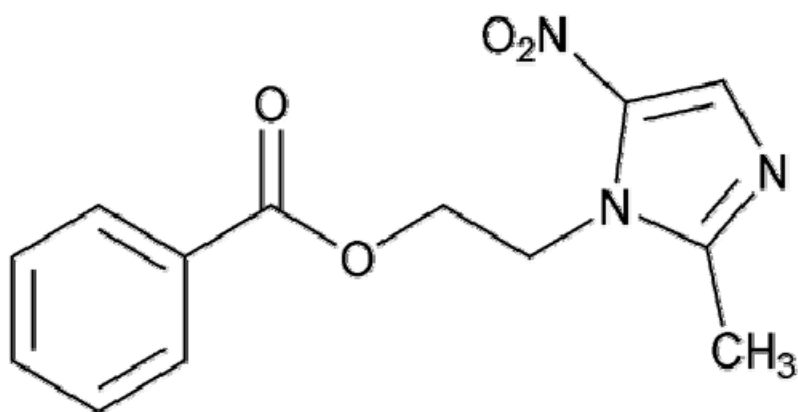


Figure 4.1 Structure of Metronidazole benzoate

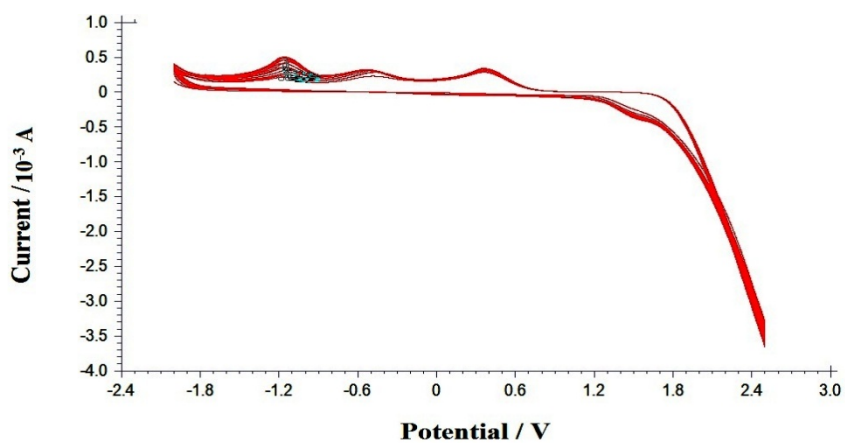


Figure 4.2 Electropolymerisation of 1 mM p-TSA on GCE

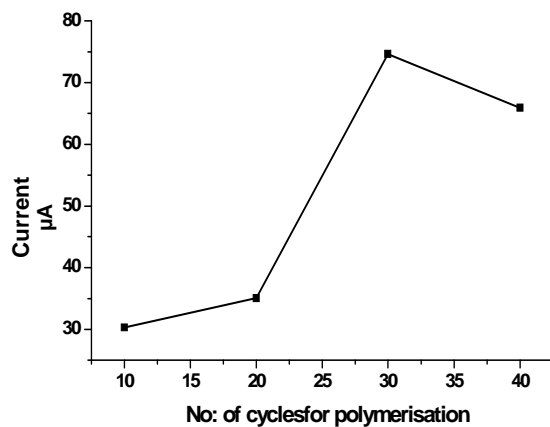


Figure 4.3 Variation of MET peak current with polymerization cycles

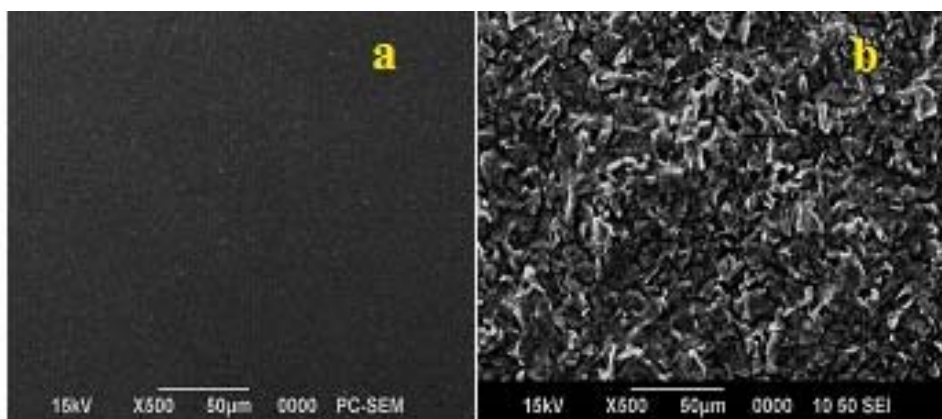
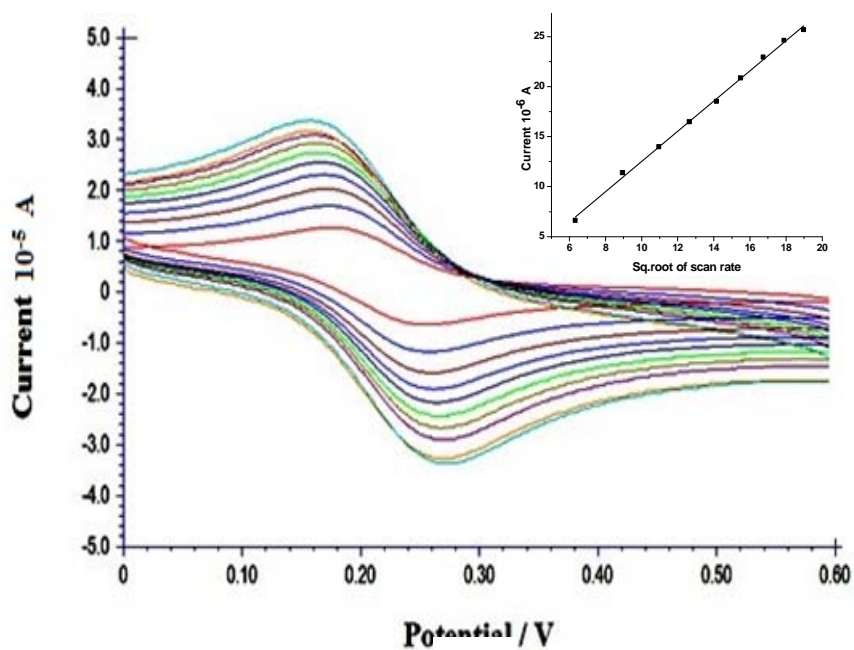
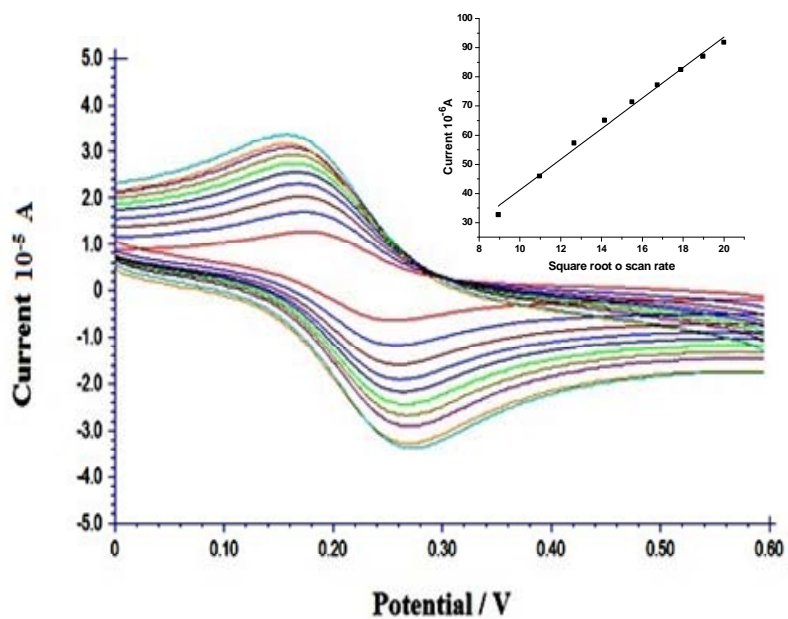


Figure 4.4 SEM images of a) Bare GCE b) poly (p-TSA)/GCE



(a)



(b)

Figure 4.5 Overlay of CVs of a) bare GCE b) poly (p-TSA)/GCE in 2 mM $K_3 [Fe (CN)_6]$ solution at scan rates 40 – 400 mV/s Linear relation between i_p and $v^{1/2}$ (figure in inset)

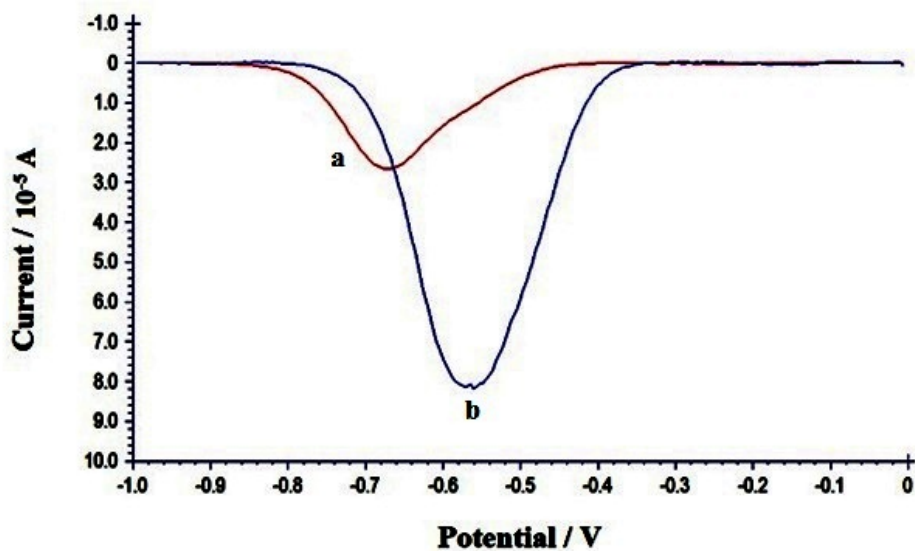


Figure 4.6 SWVs of 1×10^{-3} M MET at a) Bare GCE b) poly (p-TSA)/GCE

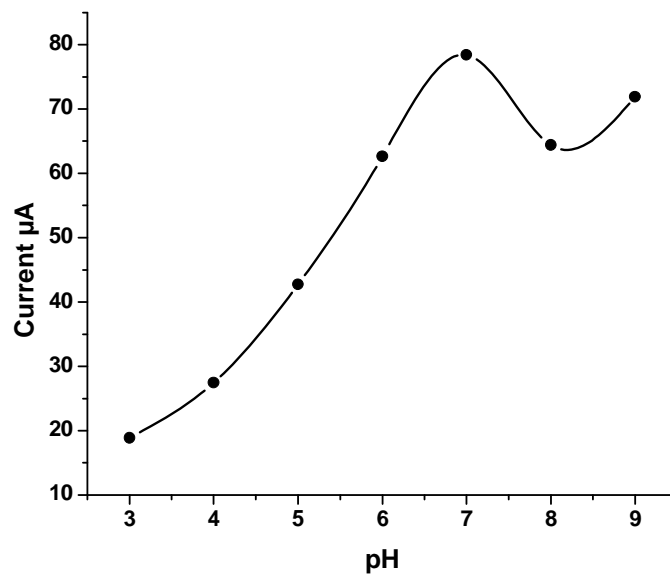


Figure 4.7 Variation of peak current of 1×10^{-3} M MET in 0.1 M PBS of pH 3 – 9

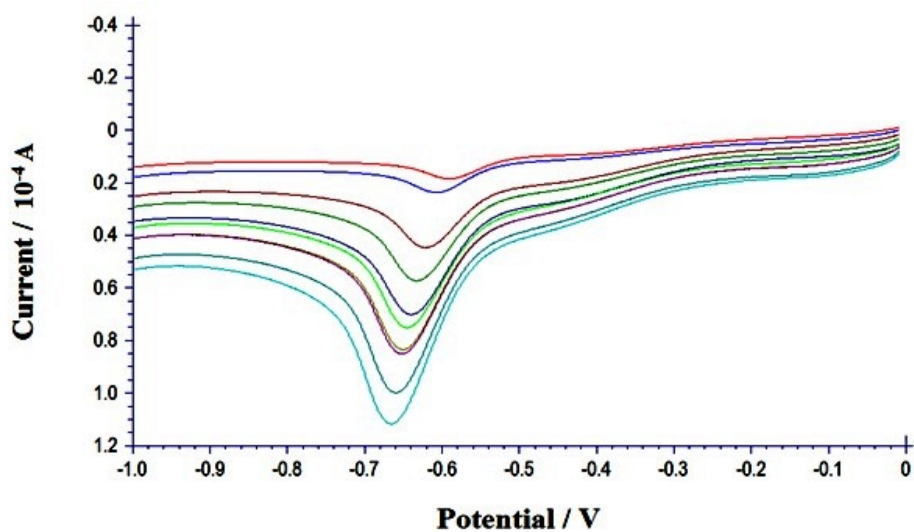


Figure 4.8 Overlay of LSVs of 1×10^{-3} M MET on poly (p-TSA)/GCE at scan rate 40 – 400 mV/s

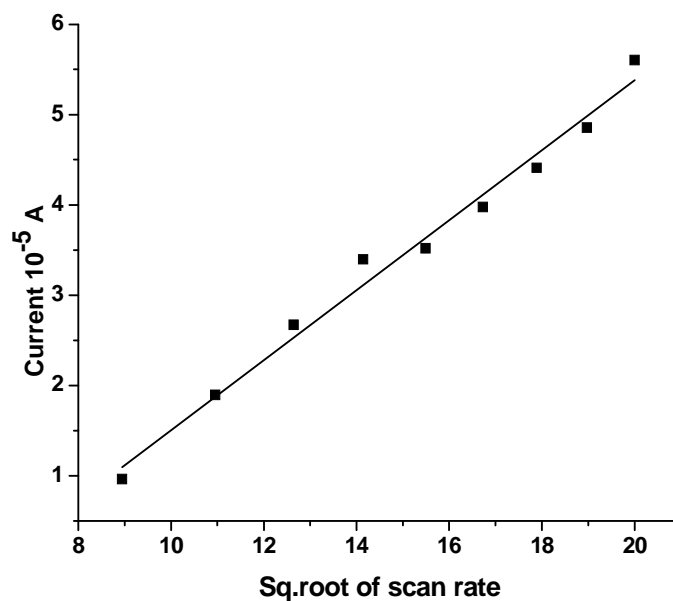


Figure 4.9 Variation of MET peak current with $v^{1/2}$

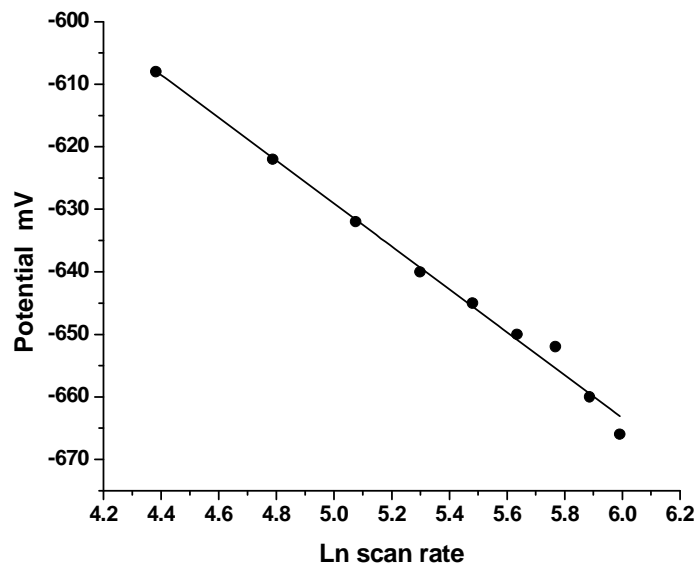


Figure 4.10 Linearity between 1×10^{-3} M MET peak current and logarithm of scan rate

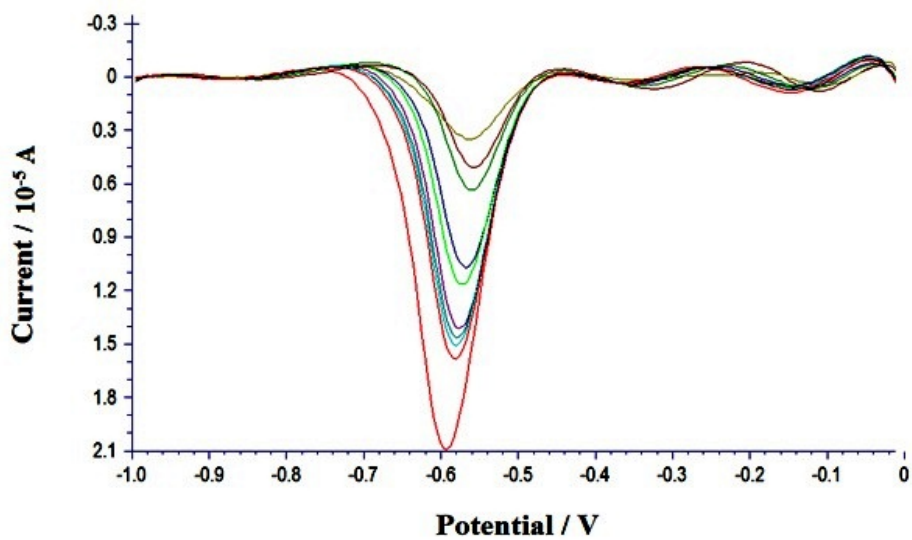


Figure 4.11 Overlay of SWVs of MET in 0.1 M PBS in the concentration range 9×10^{-6} M to 1×10^{-4} M on poly (p-TSA)/GCE

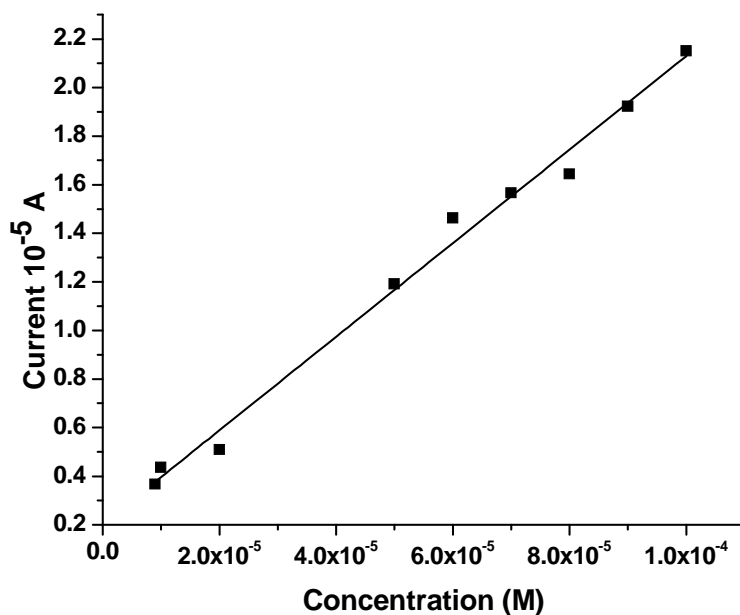
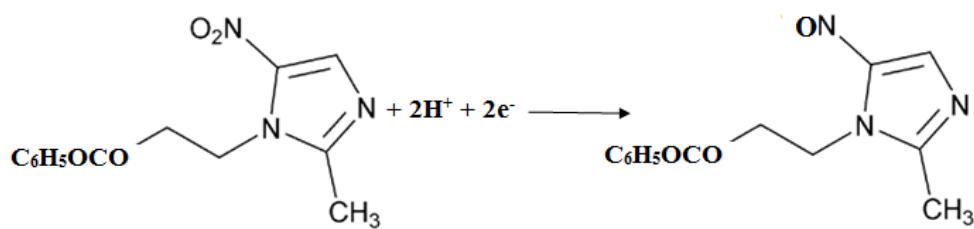


Figure 4. 12 Linear dependence of MET peak current and concentration in the range 9×10^{-6} M to 1×10^{-4} M on poly (p-TSA)/GCE



Scheme 4.1 Mechanism for MET reduction involving two electrons

* ★ ☞ ◇ ☞ ★ *

Chapter - **5**

VOLTAMMETRIC SENSORS FOR PAM CHLORIDE

Contents

5.1	Introduction
5.2	Method Implemented
5.3	Results and Discussion
5.4	Analytical figures of merit
5.5	Probable Mechanism for PAM Oxidation
5.6	Analytical Applications
5.7	Conclusions

This chapter deals with the development of two different electrochemical sensors for 2- pyridine aldoxime methyl chloride (PAM), an antidote used in the treatment of organophosphate poisoning. SWV technique is adopted here for the voltammetric determination of PAM on MWCNT/GE and MWCNT/PB/GE. The anodic peak potential of 592 mV for PAM on MWCNT/GE decreased to 456 mV on incorporating Prussian blue (PB) film onto this surface. The parameters affecting the sensor response were optimized and a calibration curve was plotted. Both the sensors exhibited a nano level detection limit for PAM. Application studies of the developed sensors were carried out in urine sample.

5.1 Introduction

2 - pyridine aldoxime methyl chloride (Figure 5.1) or pralidoxime chloride (PAM) is used as an antidote for organophosphate poisoning. Organophosphates are a diverse group of chemicals used in both domestic and industrial purposes as insecticides, nerve gases, ophthalmic agents, herbicides and antihelmintics. Among these nerve agents are highly toxic, manmade compounds that have been manufactured for use in chemical warfare. The principal nerve agents are sarin, soman and tabun.

In 1800s, organophosphates were first synthesized and used as pesticides. But in 1930, German military developed it as a chemical warfare agent. During World War II, in 1941 the original use of organophosphates as pesticides was re-introduced. Still they continue to be of wide concern as chemical weapon in this era of terrorist activity. They inhibit the enzyme cholinesterase from hydrolyzing the neurotransmitter acetylcholine. Consequently, acetylcholine accumulates and causes prolonged stimulation of the affected tissues resulting in involuntary urination and defecation, muscle twitching/fasciculation seizures, coma and ultimately death.

PAM impels the organophosphate bound to acetylcholine to change their confirmation, resulting in the cleavage of organophosphate – enzyme bond. Ultimately the enzyme is regenerated and their activity retained.

Despite its widespread use in chemical warfare, the determination of PAM gained importance only very recently. Various methods of analysis include spectrophotometry [138], capillary zone electrophoresis [139], isotachopheresis [140], ion pair chromatography [141] and polarography [142]. The voltammetric determination of PAM using modified platinum and

glassy carbon electrode have been reported [143 -144]. Gold electrode (GE) as a probe for the voltammetric determination of PAM has been reported by our group [145] with MWCNT/SAM (self assembled monolayer) as an electrode modifier.

In the electroanalytical field, MWCNTs are widely used as electrode modifier materials as they exhibited good performance in promoting electron transfer reactions. There are several reports where the substrate electrodes used for preparing CNT – modified electrodes were generally glassy carbon and graphite electrode. Metal substrate electrodes such as gold and platinum were rarely utilized probably due to the inconvenience of immobilizing MWCNTs on metal surfaces.

Recently, electrochemical sensors based on the combination of MWCNT and PB on electrodes has gained great interest for the excellent synergistic electrocatalytic effect offered by the composite MWCNT/PB material [146 - 147]. Also PB is an excellent electron transfer mediator in the modified electrodes because of its fine reversibility and stability. Attachment of PB species to the electrode surface can be achieved by electrodeposition [148], adsorption [149], encapsulating in sol gels [150] or entrapping into polymer matrices [151].

The electrochemistry and analytical applications of PB and its analogues were reported by Karyakin in his review paper [152]. The electroanalytical devices with PB is expected to have a long term operational stability with improved selectivity and sensitivity for monitoring food additives, chemical threat agents and key metabolites of life pathways.

Considering the electrocatalytic activity of MWCNT and MWCNT/PB composite, the present investigation is aimed to explore the voltammetric behavior of PAM on MWCNT/GE and MWCNT/PB/GE. PAM gave a well defined oxidation peak at 592 mV and 456 mV on MWCNT/GE and MWCNT/PB/GE respectively by SWV. After optimizing the various parameters for sensor response, the application studies of both the fabricated sensors were carried out in body fluids.

5.2 Method Implemented

5.2.1 Functionalisation of MWCNT

MWCNT was refluxed in 100 mL 6 mol L⁻¹ nitric acid for 10 hours to eliminate metal oxide catalyst within the nanotubes and segment MWCNT for easier and better dispersion. The resulting suspension was diluted with 200 mL of water and MWCNT was filtered and washed with double distilled water. The washed nanotube was collected and dried. This treatment caused segmentation of MWCNT and generation of –COOH groups at their terminus and sidewalls.

5.2.2 Preparation of MWCNT – Nafion suspension

5 mg of acid treated MWCNT was dispersed in 13 % (v/v) nafion – water solution (2.3 mL) to give a 0.22 % (w/v) black homogeneous solution.

5.2.3 Preparation of MWCNT modified gold electrode

Prior to modification, GE was polished with alumina (<50 nm) slurries, rinsed with double distilled water and methanol, and then ultrasonicated for 5 minutes in a water bath. Mechanically cleaned GE was then subjected to electrochemical cleaning by cycling between 0 – 1500 mV in

0.5 M H₂SO₄ in 40 cycles. MWCNT/GE was then fabricated by dropping 4 μL MWCNT suspensions on the GE surface and evaporating the solvent.

5.2.4 Preparation of MWCNT/PB modified gold electrode

Prussian blue was electrodeposited on GE from a solution containing 2 mM PB and 0.1 M HCl/ 0.1 M KCl as supporting electrolyte. A cyclic scan was applied between a potential of 0 mV and 1200 mV in 40 cycles [153] for electrodepositing PB on the surface of GE (Figure 5.2). After drying, 4 μL of MWCNT suspension was dropped on to this electrode to develop PB – MWCNT composite modified GE.

5.2.5 Preparation of PAM solution

The stock solution of 1×10^{-1} M PAM was prepared by dissolving 0.172 g drug in 10 mL water. By suitably diluting the stock solution using PBS as supporting electrolyte, solutions of various concentration of the analyte were prepared.

5.2.6 Analytical Procedure

A 10 mL of PBS (100 mM, pH=8) with appropriate amount of PAM for various concentrations, was transferred into a cell, and then the modified electrode was immersed into the solution. The circuit was completed with platinum auxiliary electrode and Ag/AgCl reference electrode. A potential scan between 0 - 1000 mV was triggered, and the anodic peak was recorded using SWV on MWCNT/GE and MWCNT/PB/GE. The electrode was regenerated by successive potential scan between 0 – 1000 mV in a blank solution for reuse. All experiments were carried out at room temperature.

5.3 Results and Discussion

5.3.1 Surface morphology of the electrodes

5.3.1.1 SEM images

The SEM images of bare and modified GEs are given in the Figure 5.3. The modified electrode has many spherical particles on the surface which is not detected in the bare GE. This established the enhanced number of catalytic sites for PAM oxidation on the electrode surface. The particle diameter is of the order 2 - 5 microns rather than the expected nanometer range. This is due to the hydrophobic nature of CNTs resulting in a spontaneous aggregation [154] that increases the possibility of bundling and close packing on the surface.

5.3.1.2 Estimation of electrode areas

The dependence of peak current on scan rate in a solution of 2 mM $K_3Fe(CN)_6$ on MWCNT/GE and MWCNT/PB/GE was studied by CV and SWV respectively and is depicted in Figure 5.4. When scan rate changed from 40 to 400 mVs^{-1} , the peak current was linear to the square root of scan rate (v). According to Randles Sevcik equation,

$$i_p = 2.69 \times 10^5 n^{3/2} AD^{1/2} C_0 v^{1/2}$$

Supposing the diffusion coefficient (D) of $K_3Fe(CN)_6$ as $7.6 \times 10^{-6} cm^2s^{-1}$ and for one electron transfer, n being 1, the electrode area (A) of MWCNT/GE was estimated to be $0.16 cm^2$ and $0.18 cm^2$ for MWCNT/PB/GE. This calculation is based on the slope of i_p (peak current) versus $v^{1/2}$ (square root of scan rate) relation. The areas thus obtained were 1.5 times the effective area of the bare GE. Therefore in comparison with the bare

GE, both the modified electrodes can prompt the electro active species for a better sensitive response.

5.3.2 Electrochemical behavior of PAM

The SWV response of 1×10^{-3} M PAM was recorded by scanning the potential from 0 – 1000 mV with a scan rate of 100 mV/s in a solution of 0.1 M PBS. A comparison of PAM response at the various electrodes may be drawn from Figure 5.5. At MWCNT/GE, PAM exhibited a well-defined and sensitive oxidation peak at 592 mV, which was a 100 mV less than for the bare GE. Also, the oxidation peak current of PAM at the modified electrode had a 15 times enhancement from $1 \mu\text{A}$ to $15 \mu\text{A}$. This may be attributed to the rapid electron transfer due to the conductivity of MWCNT wires imbedded onto the GE which can promote the electron transfer and enhance the accumulation of PAM.

On sandwiching PB between GE and MWCNT, the oxidation potential of PAM decreased notably from 684 mV to 448 mV which may be ascribed to the synergistic effect of these modifications. The peak current also exhibited a remarkable enhancement to $25 \mu\text{A}$ with PB on GE. The absence of a reduction peak for PAM in the reverse sweep at both the modified electrodes establishes the irreversibility of the electrochemical process.

5.3.3 Establishing the experimental parameters

The performance characteristic of the developed sensors are greatly dependent on various experimental parameters such as supporting electrolyte and its pH, scan rate, amount of MWCNT and interference by the foreign species. The optimization of these parameters is discussed in the preceding sections.

5.3.3.1 Influence of supporting electrolyte

The electrochemical behavior of 1×10^{-3} M PAM on both the modified electrodes was studied by SWV in 0.1 M concentration of different electrolytes such as KNO_3 , H_2SO_4 , NaCl , NaOH and PBS solution. PAM gave no response in KNO_3 and H_2SO_4 buffer solutions. As PAM gave the best oxidation peak in PBS solution; it was used as the supporting electrolyte throughout the experiment.

5.3.3.2 Influence of pH

The influence of solution pH on the peak current (Figure 5.6) and potential for PAM determination was investigated from pH 2 - 10. There was no peak in the acidic pH range but the peak current increased gradually in neutral media and attained a maximum at pH 8. Thereafter peak current decreased with the increase in pH. So 0.1 M PBS of pH 8 was optimal for PAM determination. Thus it was concluded that PAM oxidation is favoured only in non- acidic medium.

5.3.3.3 Influence of scan rate

The influence of scan rate on the electrochemical behavior of PAM was investigated (Figure 5.7) in the range from 40 – 240 mVs^{-1} . The peak current of PAM increased with an increase in scan rate followed by a positive shift in the peak potential. The peak current increased linearly with the square root of scan rate (Figure 5.8) indicating a diffusion controlled process of PAM oxidation on the surface of MWCNT/GE and MWCNT/PB/GE.

5.3.3.4 Dependence of peak current on amount of MWCNT

When the amount of MWCNT-nafion suspension was 1 - 4 μL , the peak current of PAM increased gradually (Figure 5.9) on both the modified electrodes as the analyte got adsorbed on the surface. However, nafion being an insulator and can produce uncompensated resistive effects and prohibit the charge transfer of PAM at the modified electrodes. So when the amount exceeded 4 μL the oxidation peak current decreased as too much of nafion retarded the electron transfer and mass transportation of PAM.

5.3.3.5 Influence of foreign species

The influence of some foreign species in the oxidation of PAM at the modified electrodes was analyzed. The results (Table 5.1) showed that a 100 - fold excess of glucose, K_2SO_4 , NaCl, lactose and urea does not interfere with the determination of PAM, while ascorbic acid interfered severely. These results indicated that the film electrodes have good selectivity for the determination of PAM.

5.4 Analytical Figures of Merit

The analytical performance characteristics such as linear range, detection limit and stability under optimized conditions of the developed sensors were assessed for its practical applicability.

5.4.1 Calibration curve

Under the selected optimized experimental conditions, (0.1 M PBS, pH=8, 0 - 1000mV potential) the increase in oxidation peak current with PAM concentration (Figure 5.10) was investigated. The result showed that when the concentration (Figure 5.11) changes from $8 \times 10^{-7} \text{ M}$ – $1 \times 10^{-5} \text{ M}$, the anodic

peak current is linear to PAM concentration at MWCNT/GE with a detection limit of 78 nM. The peak current of PAM varied linearly with concentration in the range 2×10^{-7} M – 3×10^{-6} M on MWCNT/PB/GE. The lower detection limit of PAM on this electrode was 16 nM. Thus these modified electrodes are superior to the existing methods (Table 5.2) for PAM determination in terms of nano molar detection limit.

5.4.2 Regeneration and stability of modified electrodes

Modified electrodes were regenerated by repetitive cycling in a blank solution. A 1×10^{-3} M PAM solution was determined successively several times with the same electrode and regenerated after every determination. The slight variation of peak current in the consecutive determination established that the electrode surface can be easily regenerated.

The response of the same electrode decreased only slightly even after repetitive use for several days. This may be due to the loss of MWCNT from the electrode surface. The consistency in the electrode response indicated that the modified electrode had high stability. On the other hand, the porous structure and large surface area of the film electrode encouraged PAM to penetrate the interfacial layer easily, which is not beneficial for subsequent determination. So the modified electrode was cleaned and used after each determination.

5.5 Probable Mechanism for PAM Oxidation

Useful information regarding the mechanism of a reaction can be acquired from the relation between peak potential and scan rate. On increasing the scan rate, the oxidation potential of PAM shifted towards more positive values on MWCNT/PB/GCE but varied irregularly on MWCNT/GE. The plot

of oxidation potential E_p versus natural logarithm of scan rate ($\ln v$) was linear with a correlation coefficient of 0.9923 (Figure 5.12) and their relation can be expressed as:

$$E_p = 24.925 \ln v + 354.87$$

For an irreversible electrode process, according to Laviron equation the slope of the above equation $b = RT/\alpha nF$, where α is 0.5 for an irreversible electrode process and other symbols have their usual meanings. Substituting the value of b as 24.925, the number of electrons transferred in PAM oxidation is calculated as 2.06 (~2).

The mechanistic scheme for PAM oxidation at MWCNT/PB/GE is given in Scheme 5.1. The electroactive centre of PAM is the aldoxime group. The oxidation of aldoxime proceeds via the formation of iminoxy radicals which then dimerises [155] and reacts subsequently to give the corresponding carbonyl group. The whole mechanism involves the transfer of two electrons which reduces the carboxylic group on MWCNT [156].

5.6 Analytical Applications

The feasibility of the MWCNT/GE and MWCNT/PB/GE for PAM determination in urine sample was analyzed. Various concentration of the drug solution in PBS containing fixed amount of urine sample was prepared. The electrochemical behavior of the prepared solution on modified electrodes was studied by SWV (Table 5.3) and the unknown concentrations were determined from the calibration graph. The recovery percentage is in the range 96.7 – 104.5 %.

The recovery obtained by the developed sensors was compared (Table 5.4) with the standard spectrophotometric method [157] by recording the absorbance of varying concentrations of PAM spiked in urine sample. The measurement was carried out in 1 M NaOH in the range 200 – 400 nm. Unknown concentrations were determined graphically from the plot of absorbance against PAM concentration. The good agreement between the recoveries obtained by these methods establishes the acceptability of the developed sensors for PAM determination.

5.7 Conclusions

Voltammetric behavior of PAM was investigated at MWCNT-nafion modified GE and MWCNT-PB composite GE by SWV. Oxidation of PAM was found to be an irreversible, two electron process involving diffusion controlled process. Both MWCNT and MWCNT-PB showed electrocatalytic action for the oxidation of PAM, characterized by the enhancement of the peak current and the reduction of peak potential, which was probably due to the larger effective surface area of MWCNT and the stronger adsorption of PAM together with the synergic effect of MWCNT and PB. Thus a very sensitive and simple electrochemical method for the determination of PAM was developed and applied for PAM determination in urine samples.

Table: 5.1 Influence of various foreign species on the oxidation peak current of 1×10^{-3} M PAM

Foreign species (0.1 M)	Signal change (%) on	
	MWCNT/GE	MWCNT/PB/GE
Sodium chloride	3.94	2.6
Potassium Sulphate	2.88	3.16
Dextrose	3.18	3.06
Urea	0.34	2.1
Ascorbic acid	15.24	11.9

Table:5.2 Comparison of the developed method for PAM determination with the reported works

No:	Method adopted	Lower detection limit (M)
1	Spectrophotometry [138]	1.00×10^{-5} M
2	Capillary zone electrophoresis [139]	1.00×10^{-7} M
3	Isotachophoresis [140]	1.5×10^{-7} M
4	Ion pair chromatography [141]	2.8×10^{-5} M
5	Voltammetry [143]	3.0×10^{-7} M
6	Voltammetry [144]	3.0×10^{-8} M
7	Voltammetry [145]	1.0×10^{-8} M
8	Voltammetry (<i>present method</i>)	16×10^{-9} M, 78×10^{-9} M

Table: 5.3 Determination of PAM in urine sample

Developed sensor	Amount of PAM added in urine sample (M)	Amount of PAM found in urine sample (M)	Recovery %
MWCNT/GE	6.00×10^{-6}	5.82×10^{-6}	96.7
	8.00×10^{-6}	7.88×10^{-6}	98.5
	9.00×10^{-6}	9.05×10^{-6}	100.4
MWCNT/PB/GE	5.00×10^{-6}	4.96×10^{-6}	99.2
	7.00×10^{-6}	7.32×10^{-6}	104.5
	9.00×10^{-6}	8.84×10^{-6}	98.2

Table 5.4 Comparison of the results obtained by developed sensors and standard method for PAM determination in urine sample

Method adopted	Recovery (%)	C.V.
Standard	99.4	1.91
MWCNT/GE	98.5	1.68
MWCNT/PB/GE	100.6	3.36

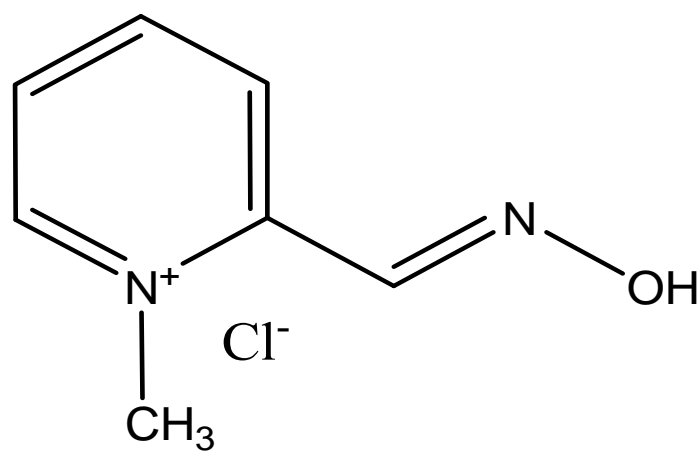


Figure 5.1 Structure of PAM chloride

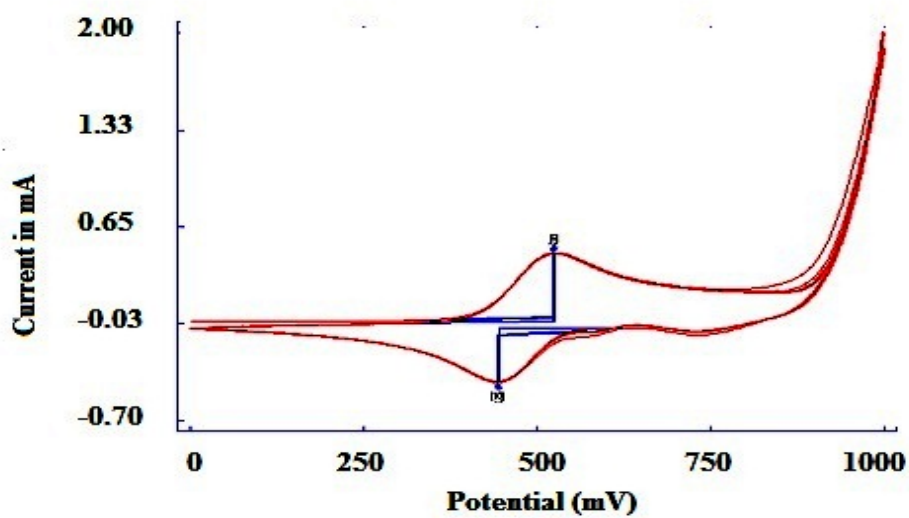


Figure 5.2 Electropolymerisation of 2 mM PB on GE in 40 cycles

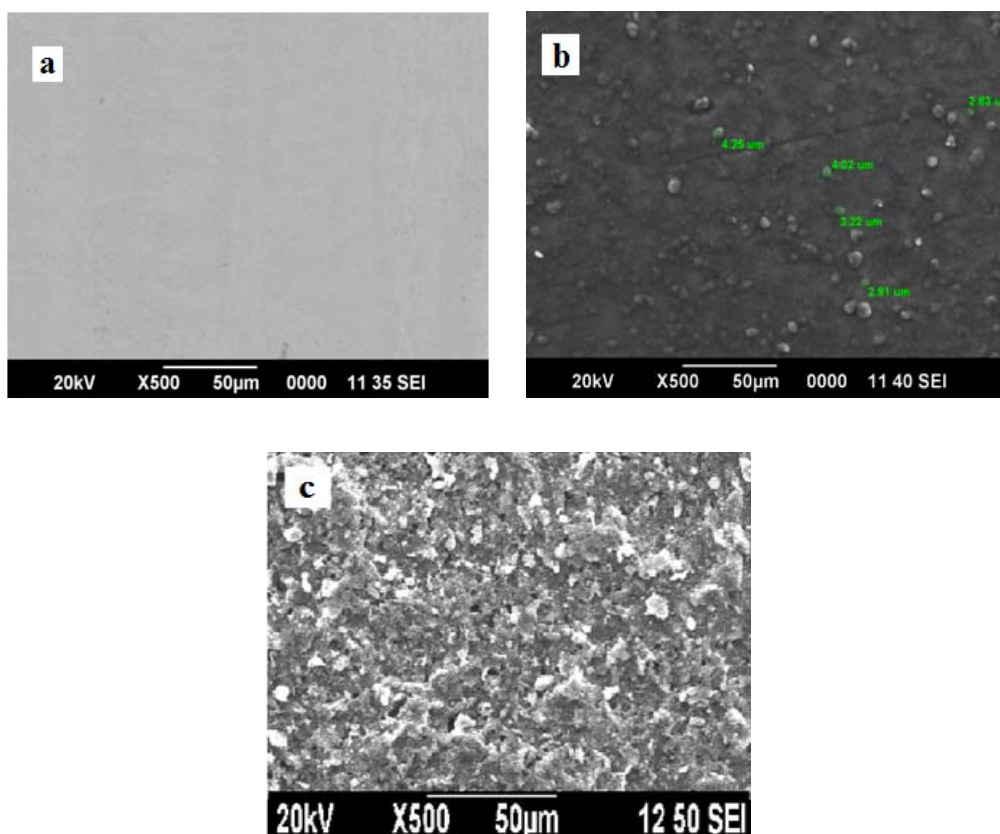
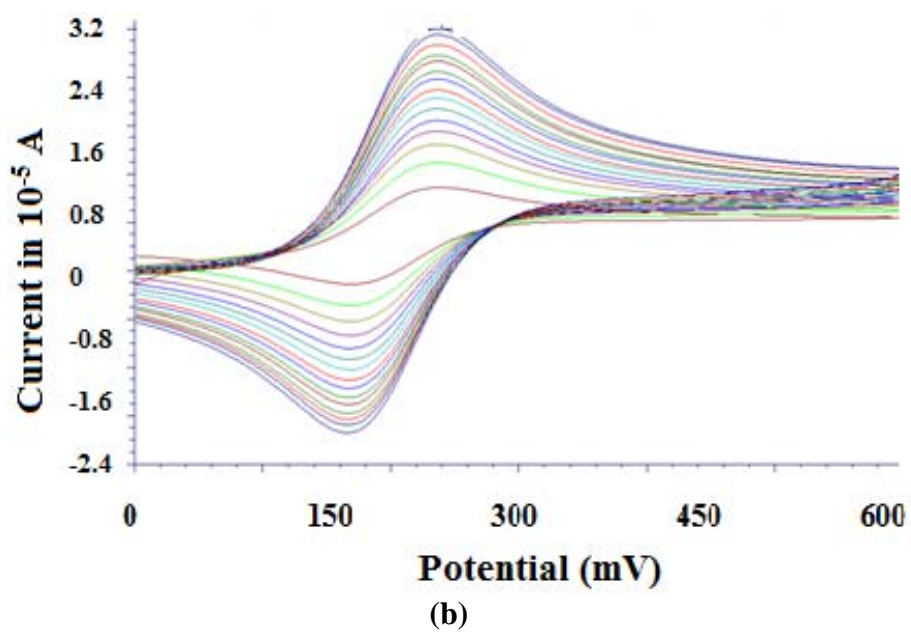
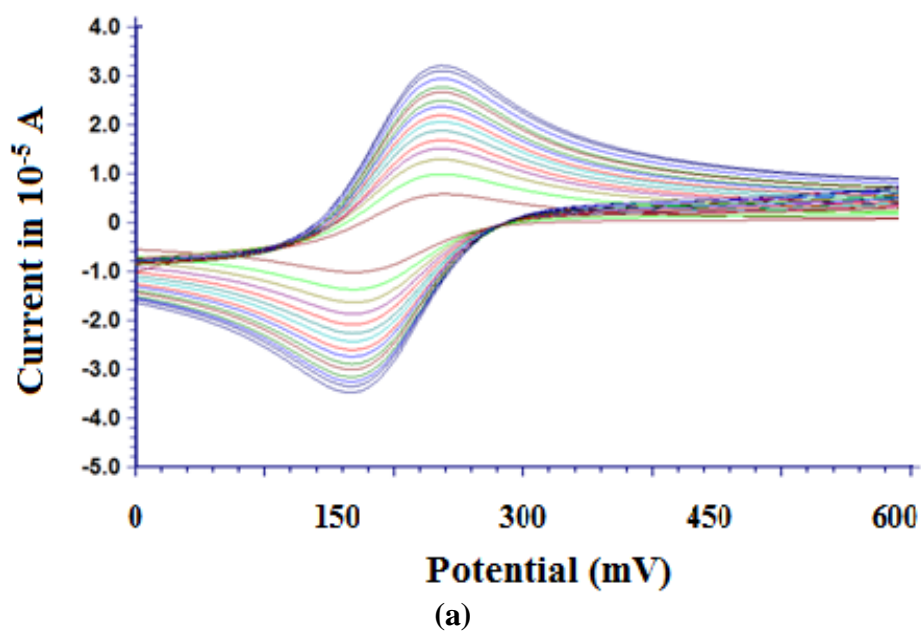
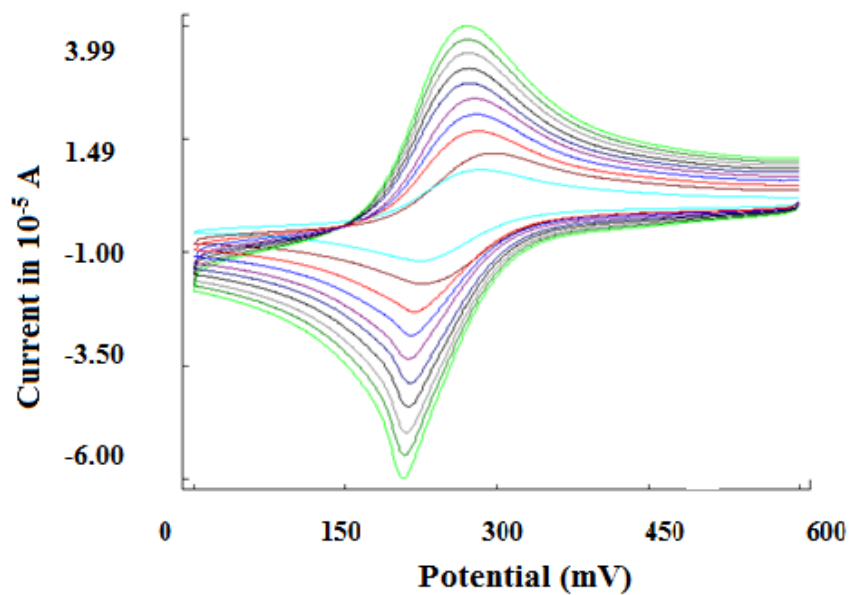


Figure 5.3 SEM image of a) Bare GE b) MWCNT/GE c) MWCNT/PB/GE





(c)
 Figure 5.4 Overlay of SWVs of (a) Bare GE (b) MWCNT/GE (c) MWCNT/ PB/ GE in 2 mM ferricyanide solution at different scan rates

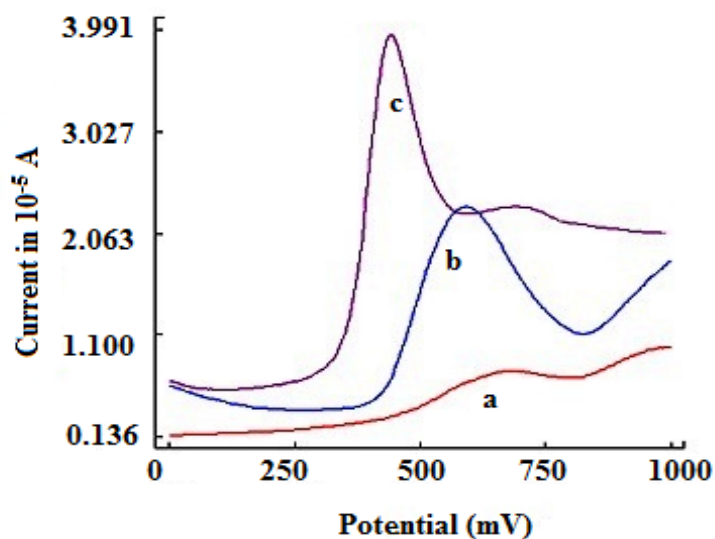
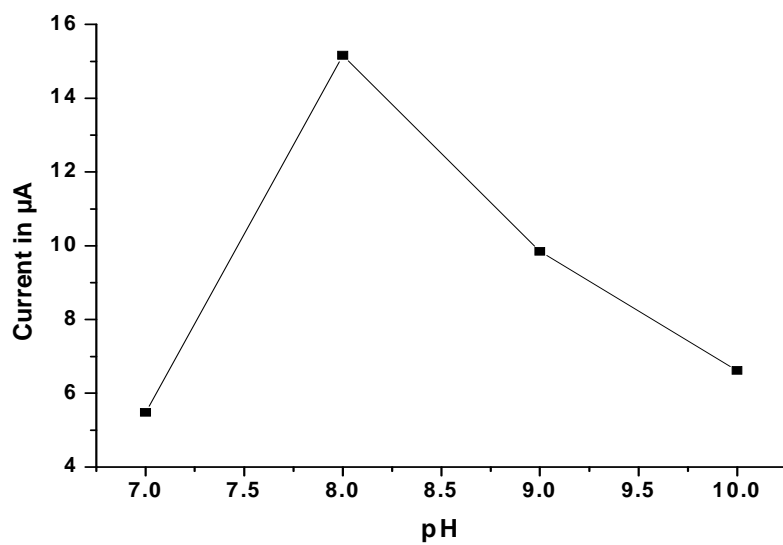
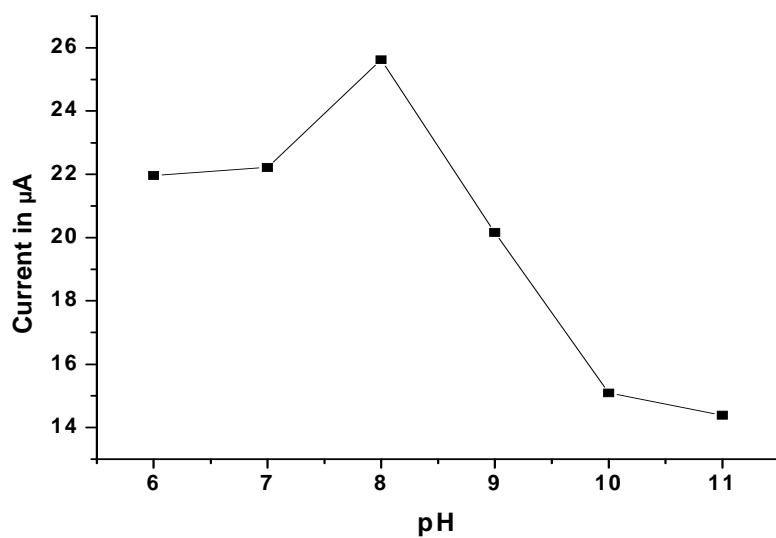


Figure 5.5 SWVs of 1×10^{-3} M PAM at a) Bare GE b) MWCNT/GE c) MWCNT/PB/GE



(a)



(b)

Figure 5.6 Effect of pH on the anodic current of 1×10^{-3} M PAM chloride at a) MWCNT/GE b) MWCNT/PB/GE

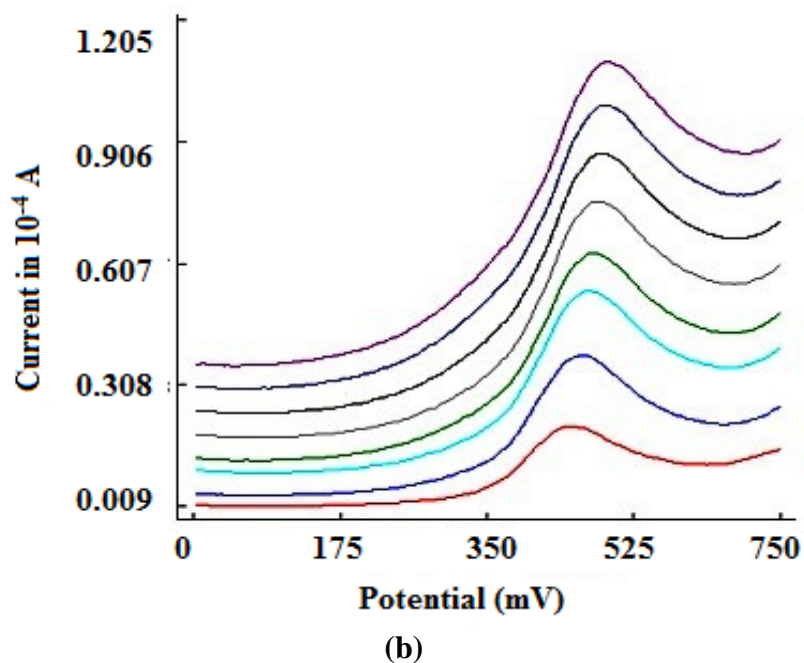
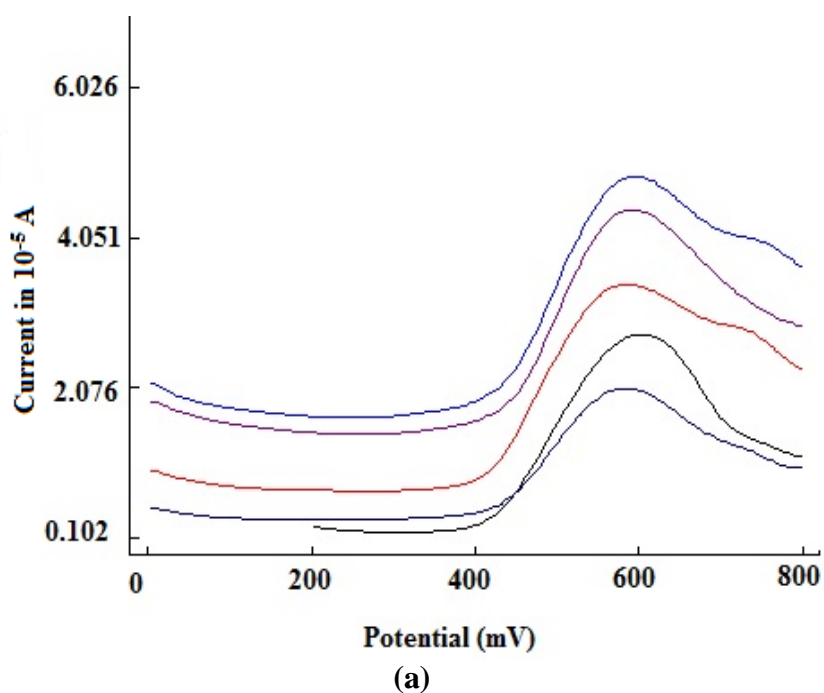
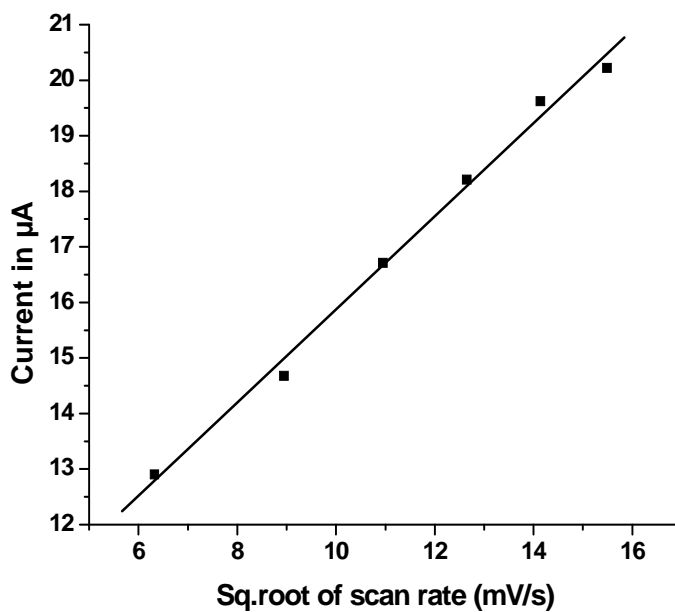
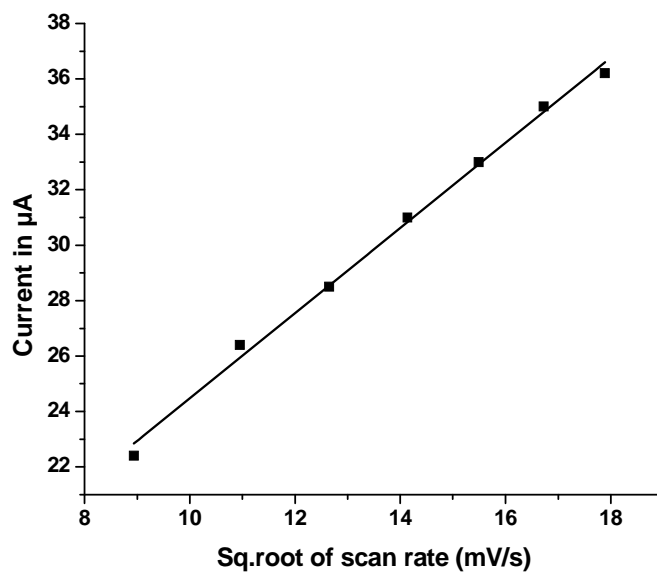


Figure 5.7 Overlay SWVs of 1×10^{-3} PAM at a) MWCNT/GE
b) MWCNT/PB/GE at scan from 40 – 240 mV/s

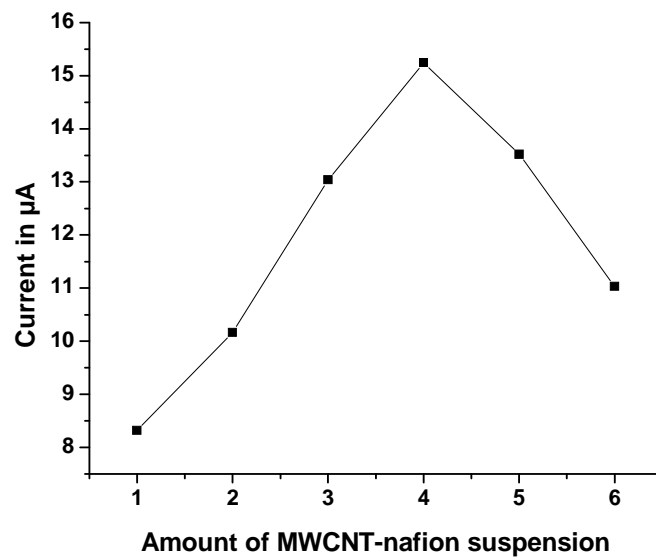


(a)

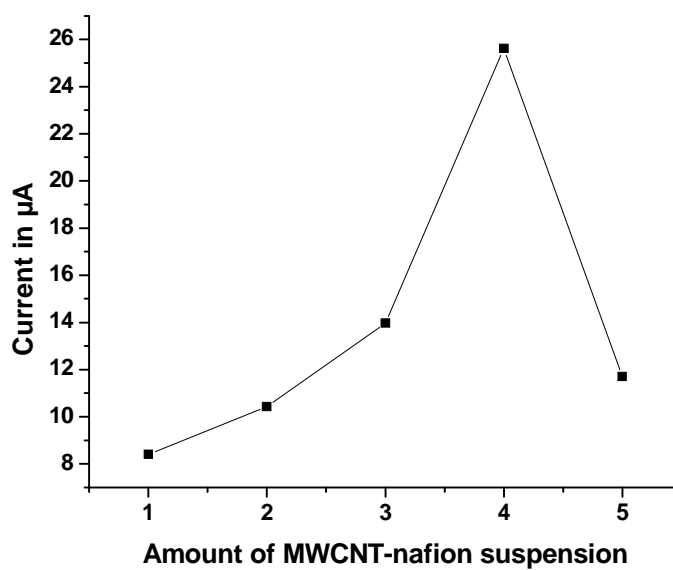


(b)

Figure 5.8 Variation of peak current with square root of scan rate
a) MWCNT/GE b) MWCNT/PB/GE

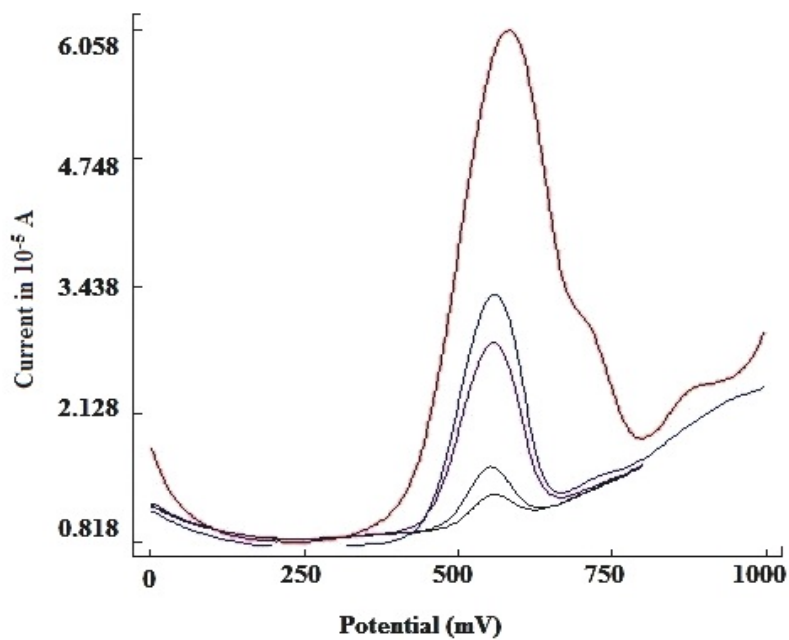


(a)

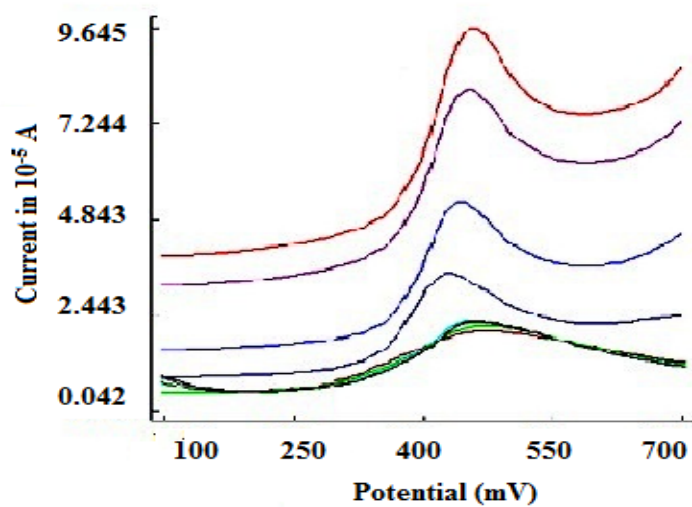


(b)

Figure 5.9 Effect of the amount of MWCNT-Nafion suspension on
a) Bare GE b) PB/GE

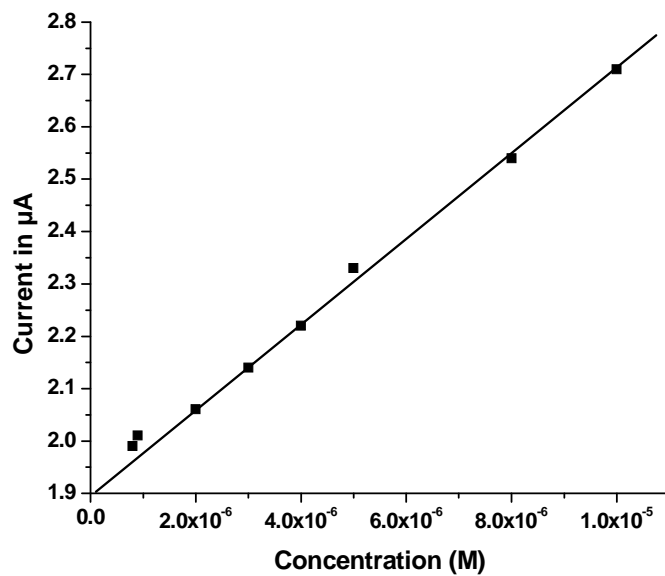


(a)

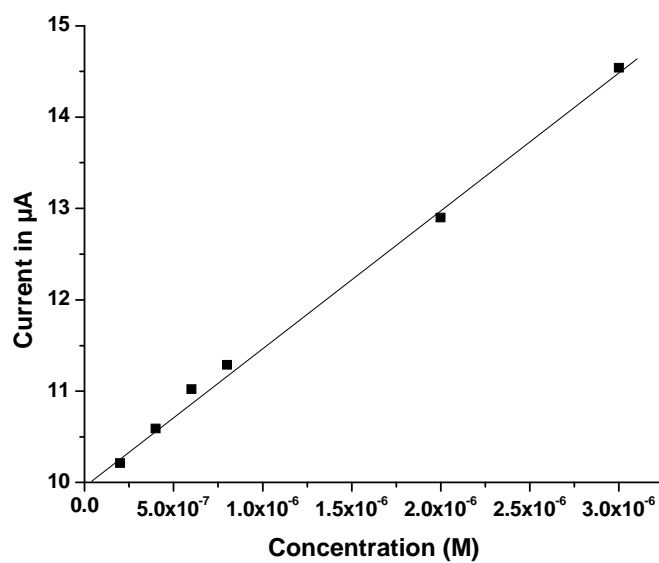


(b)

Figure 5.10 Overlay of SWVs of PAM at different concentrations on a) MWCNT/GE b) MWCNT/PB/GE



(a)



(b)

Figure 5.11 Calibration graph for PAM chloride at 25°C on a) MWCNT/GE b) MWCNT/PB/GE

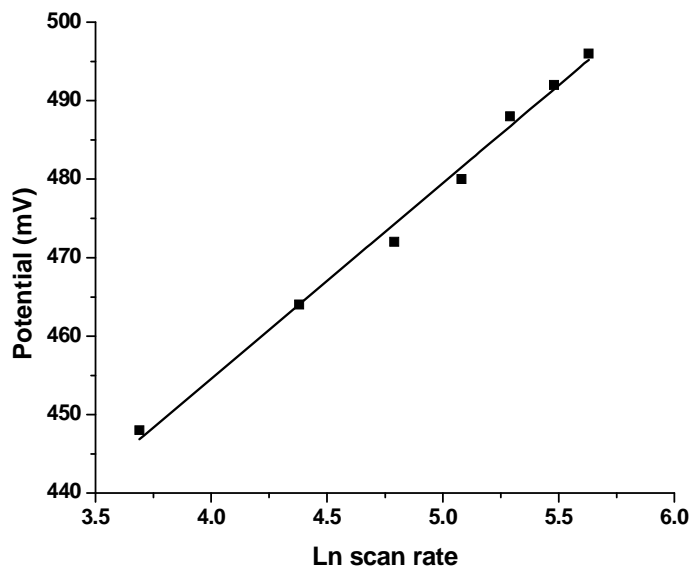
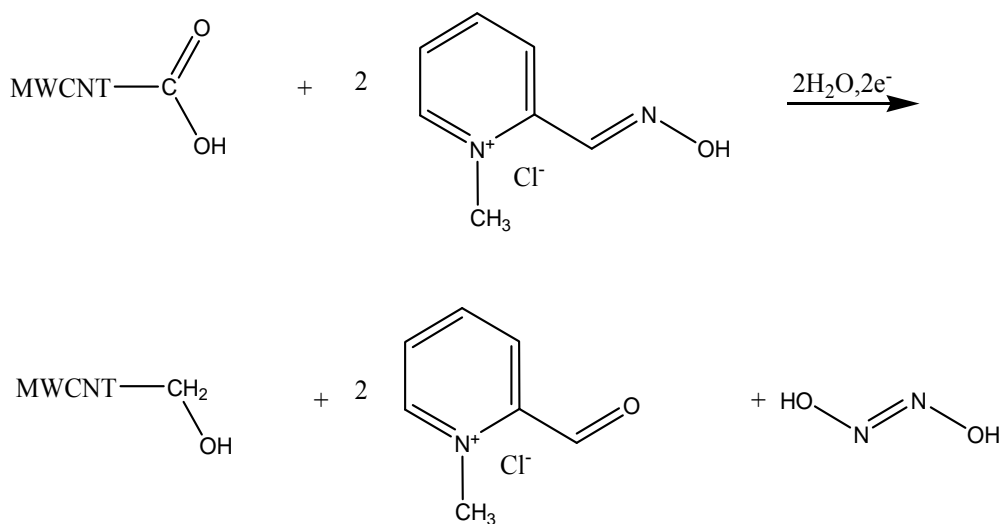


Figure 5.12 Variation of oxidation potential of 1×10^{-3} M PAM with natural logarithm of scan rate at MWCNT/PB/GE



Scheme 5.1 Mechanism for PAM oxidation



VOLTAMMETRIC SENSOR FOR GUAIFENESIN

6.1	Introduction
6.2	Fabrication of GF Sensor
6.3	Establishing the operational parameters of GF sensor
6.4	Mechanistic pathway for GF Oxidation
6.5	Application Studies
6.6	Conclusions

The electrocatalytic activity of multi – walled carbon nanotube (MWCNT) towards the oxidation of guaifenesin (GF) on Platinum electrode (PtE) by SWV is explained in this chapter. GF yielded a well-defined oxidation peak at 1100 mV at the MWCNT-film coated PtE in 0.1 M H₂SO₄ buffer. Compared with bare PtE, the MWCNT/PtE significantly enhanced the oxidation peak current of GF from 19.4 μA to 78.8 μA. The conditions such as effect of supporting electrolyte, pH, scan rate, range of linear response and interference study for the sensor were optimised. The proposed method was successfully applied for determination of GF in tablet and urine sample.

6.1 Introduction

Guaifenesin (GF), 3-(2-Methoxyphenoxy)-1, 2-propanediol (Figure 6.1), is an expectorant which acts by increasing the volume and reducing the viscosity of secretions in the trachea and bronchi. It is derived from a tree bark extract called 'guaiaicum' and was approved as an expectorant by FDA (Food and Drug administration) in 1952. But it was termed 'Guaifenesin' only in 1990s after the production of tablets from the extract.

Opera singers consider GF as the "wonder drug" for its ability to promote secondary mucosal secretion in the respiratory system. GF is also administered to ease the congestion of cold, flu, rhino sinusitis and extreme condition such as fibromyalgia and COPD (chronic obstructive pulmonary disease). The drug is widely used by women to facilitate conception by thinning and increasing the amount of cervical mucus.

GF acts by drawing water into the bronchi which in turn helps to thin the mucus and lubricate the air passage into the lungs. This facilitates the removal of mucus from the chest by coughing. So it is advisable to drink plenty of water during GF medication. GF is reported to possess only minor side effects and so physician's first choice as an expectorant.

There are various analytical methods for the determination of GF in pharmaceutical formulations including chemometrics [158], spectrophotometry [159 - 161], LC [162], HPLC [163] and capillary electrophoresis [164]. But all these methods are either expensive or time consuming which may be resolved by voltammetric technique. Tapsoba et al [165] reported the voltammetric determination of GF on bare PtE. The present work is aimed to determine GF on modified electrodes and to explore a mechanism for its oxidation.

Initial attempt was to determine GF voltammetrically using a metalloporphyrin modified carbon paste electrode. Even though good results were obtained, the acidic medium destroyed the electrode material. In basic medium no peak was obtained for GF on the same electrode. Next choice was gold electrode which had improved sensing for the drug; but the electrode showed a peak around the same potential in the supporting electrolyte as the drug which affected the analysis. Finally, improved response of GF was observed on multi – walled carbon nanotube (MWCNT) modified PtE.

Multi-walled carbon nanotubes (MWCNTs) are one among the most researched materials of 21st century owing to its wide range of applications. MWCNT has revolutionized the branch of electrochemistry as a viable nano material due to their extra ordinary electronic, chemical and structural characteristics. In the electro analytical field, MWCNTs are widely used as electrode modifiers. The subtle 1 - D character [166] of MWCNTs suggests that it can mediate electron transfer reactions with electro active species in solution when used as modifiers.

The insolubility of MWCNTs in most of the solvents hindered their applications in electroanalysis in the early ages of their discovery [167]. But MWCNTs can be homogeneously dispersed in nafion solution because of the hydrophobic side chains and polar head groups of nafion. This polymeric backbone enhanced the stability of MWCNT and accounts for their electroanalytical applications. J Wang et. al reported the preparation of amperometric biosensors by solubilising MWCNT in nafion [168]. Sensitive determination of caffeine was carried out on a nafion/MWCNT composite film coated glassy carbon electrode [169].

In view of the electrocatalytic activity of MWCNT, the determination of GF was carried out on MWCNT/PtE sensor. The response characteristics of the developed sensor were established and validated with a standard method.

6.2 Fabrication of GF Sensor

6.2.1 Cleaning of PtE

Prior to modification, the electrode was mechanically polished with alumina slurries on a flat pad. The slurry clinging on to the surface was removed by sonicating in absolute ethanol. The polished electrode was then subjected to an electrochemical cleaning by performing CV in the range 0 – 1500 mV in 0.5 M sulphuric acid.

6.2.2 Functionalisation of MWCNT

MWCNT was refluxed in 100 mL 6 mol L⁻¹ nitric acid for 10 hours to eliminate metal oxide catalyst within the nanotubes and segment MWCNT for easier and better dispersion. If not removed properly the metal residual particle significantly changes the behavior of MWCNT- based devices [170]. The resulting suspension was diluted with 200 mL of water and MWCNT was filtered and washed with double distilled water. The washed nanotube was collected and dried. This treatment caused segmentation of MWCNT and generation of –COOH groups at their terminus and sidewalls.

6.2.3 Modification of PtE with MWCNT

5 mg of acid treated MWCNT was dispersed in 13 % (v/v) nafion – water solution (2.3 mL) to give a 0.22 % (w/v) black homogeneous solution. 4 µL of the dark solution was dropped on to the surface of cleaned PtE and allowed to dry to form a uniform film of MWCNT on the surface.

6.2.4 Preparation of GF solution

A 1×10^{-1} M solution of GF was prepared by dissolving 0.198 g of the drug in 10 mL methanol solution. Required concentrations of GF were prepared from the stock solution by suitably diluting with the selected supporting electrolyte.

6.2.5 Electrochemical behavior of GF

The electrochemical behaviour 1×10^{-3} M GF at MWCNT modified PtE was investigated by SWV. The cell set up included MWCNT/PtE as the working electrode, Pt auxiliary electrode and Ag/AgCl reference electrode. The voltammogram of GF was recorded in the potential range 0 – 1200 mV in 0.1 M H₂SO₄ as supporting electrolyte.

A well - defined and sensitive oxidation peak of GF appeared at 1100 mV on MWCNT/PtE which was 70 mV less than that on bare PtE. Compared with the bare PtE, there was also an enhancement of oxidation peak current of GF from 19 μ A to 78 μ A at the modified PtE. Figure 6.2 displays the comparison of oxidation peak of 1×10^{-3} M GF in 0.1 M sulphuric acid at both the electrodes. No reduction peak is observed for GF in the reverse sweep of CV indicated an irreversible electrochemical process.

The appearance of oxidation peak at a lower potential of GF on the modified electrode undoubtedly proved the electrocatalytic activity of MWCNT on PtE. The MWCNT film coated on PtE greatly enhances the electron transfer contributing to the facile oxidation of GF.

The modification of PtE with MWCNT is supported by the following surface morphological studies.

a) SEM image

SEM images of both bare PtE and MWCNT/PtE are shown in Figure 6.3. The modified electrode has many spherical particles on the surface which is not detected in the bare PtE. Particles on the surface are bigger with a diameter in the order of microns [171] due to the aggregation of the CNTs. The enhanced oxidation activity of GF on the modified electrode is due to the increased number of catalytic sites on the surface and also due to the electrocatalytic activity of MWCNT.

b) Surface area study

SWVs of 2 mM $K_3Fe(CN)_6$ was recorded in the potential range 0 – 600 mV on bare PtE and MWCNT/PtE at different scan rates (Figure 6.4). A linear plot of peak current (i_p) against square root of scan rate (ν) was plotted. By applying Randles- Sevcik equation, peak current

$$i_p = 2.69 \times 10^5 A n^{3/2} D^{1/2} c \nu^{1/2}$$

where A- effective surface area in cm^2 , D- diffusion coefficient in cm^2/s , n – number of electrons transferred per mole of the electroactive species and c – concentration of the solution. The surface area of both bare and modified PtE was calculated and it was found that on modification with MWCNT there is a fourfold increase in surface area from $0.20 cm^2$ to $0.76 cm^2$. This is a strong evidence for the successful and effective modification of PtE using MWCNT.

6.3 Establishing the Operational Parameters of GF Sensor

The performance characteristics of the developed sensor is dependent on parameters such as supporting electrolyte chosen, scan rate, interference by foreign species, amount of MWCNT used for modification and the linear

working range of the sensor. The effects of these factors are discussed in the next section.

6.3.1 Effect of supporting electrolyte

Supporting electrolyte played an important role in the electrochemical response of GF. Therefore 0.1 M concentrations of acetate buffer (ABS), phosphate buffer (PBS), H₂SO₄, HCl, HNO₃, KNO₃ and NaOH was tested as supporting electrolytes for GF oxidation by SWV. It was observed that the peak current is highest and the peak shape is well defined in 0.1 M sulphuric acid. Hence 0.1 M sulphuric acid was chosen as the experimental medium for the voltammetric studies of GF.

At pH > 5, despite the fact that an oxidation wave was observed, the shape and the reproducibility were poor. The inhibition of GF oxidation waves is obvious at higher pH.

6.3.2 Scan rate study

The effect of scan rate on the oxidation peak current of GF was studied by Linear Sweep Voltammetry (LSV). It was found that oxidation peak current of 1×10^{-3} M GF increased with scan rate in the range 40 - 400 mV/s. The overlay of voltammograms for the oxidation of GF at different scan rates is given in Figure 6.5. As the peak current of GF varied linearly with square root of scan rate (Figure 6.6), the oxidation mechanism of GF at MWCNT/PtE is diffusion controlled.

6.3.3 Amount of MWCNT

The oxidation peak current of GF on the modified electrode with different amount of MWCNT was measured and is plotted graphically in

Figure 6.7. As the maximum response for GF was obtained with 4 μL of MWCNT, this amount was dropped onto PtE for further determinations.

6.3.4 Interference study

In order to investigate the selectivity of the method, the effects of some biologically important compounds on the electrochemical oxidation of 1×10^{-3} M GF (Table 6.1) have been evaluated. It was found that glycine, sodium chloride, potassium chloride, glucose and urea when present upto 1×10^{-1} M have almost no influence on the current response of 1×10^{-3} M GF. However ascorbic acid interfered severely.

6.3.5 Linear concentration range

Variation of anodic peak current with the concentration of GF was studied by SWV using the modified electrode under optimized conditions. The lower working concentration range of the developed sensor was found to be 5×10^{-6} M. The peak current exhibited linearity in the range 4×10^{-4} to 5×10^{-5} M concentration of GF (Figure 6.8). From the calibration curve plotted between GF concentration and peak current (Figure 6.9) the detection limit was found to be 1.34×10^{-6} M. From the comparison of the lower detection limits of the proposed method with other reported works is compiled in Table 6.2.

6.4 Mechanistic Pathway for GF Oxidation

To calculate the number of electrons involved in GF oxidation peak potential against the natural logarithm of scan rate is plotted (Figure 6.10). According to Laviron theory, the slope of this linear graph $b = RT/\alpha nF$, where $\alpha = 0.5$ for an irreversible diffusion controlled process, n gives the number of

electrons transferred and other symbols have their usual meanings. From this equation the value of $n = 1$, which suggests oxidation of GF in accordance with the mechanism proposed by Gholivand et al. [172].

The peak may be attributed to the oxidation of secondary alcohol group in GF to ketone group involving a two step mechanism as given in Scheme 6.1. The formation of the free radical may be considered as the rate determining step, which involves the transfer of one electron. The $-\text{COOH}$ terminus of the acid treated MWCNT may accept this electron from GF and get reduced to the corresponding carbonyl group. This involvement of MWCNT in the oxidation of GF results in the enhanced electrochemical response of GF on MWCNT/PtE than on bare electrode.

6.5 Application Studies

6.5.1 Analysis of GF in tablet

Pharmaceutical sample preparation - An accurately weighed portion of finely powdered tablets equivalent to about 1×10^{-3} M GF was transferred into a 100 mL standard flask and the content diluted with water. The content of the flask was shaken vigorously on a mechanical shaker for 10 min and sonicated for 10 min. The solution was filtered into a 100 mL flask; the residue washed several times with water and made upto the mark. For voltammetric analysis, the solution was diluted to the linear concentration range.

Using MWCNT/PtE, the proposed method was applied for the determination of GF in pharmaceutical dosage forms. As can be seen from the results shown in Table 6.3, the methods gave satisfactory recovery data with

no significant differences between the declared and experimental data. The standard deviations for the assay results show good precision.

In order to test the reliability of the method, results obtained by MWCNT/PtE sensor were compared with those obtained by standard pharmacopeia method [173]. The solution of GF used for tablet study is taken in chloroform and the absorbances measured with varying concentrations. Close agreement between the two methods confirmed the novelty of the developed method.

6.5.2 Analysis of GF in urine sample

The applicability of MWCNT modified electrode for the determination of GF in urine was also investigated. Various concentrations of the drug solution in 0.1 M H₂SO₄ solution containing fixed amount of urine sample were prepared. The electrochemical behavior of the prepared solution on the MWCNT/PtE was studied by SWV and the unknown concentrations were determined from the calibration graph. The recovery percentage is in the range 96.8 – 99.4 %.

6.6 Conclusions

Incorporating the intrinsic conducting property of MWCNT on PtE, a voltammetric sensor for the determination of GF has been developed. The high electron transfer rate due to the conductivity of the MWCNT wires imbedded onto PtE, enhanced the oxidation peak current of GF involving a one electron diffusion controlled process. The modified electrode has remarkable advantages such as wide linear dynamic range, low detection limit and applicability in real samples. Hence it may be suggested that the developed sensor has potential to be used for the accurate determination of GF in pharmaceuticals.

Table 6.1 Interference by the foreign species in the determination of GF

Foreign species	Signal change (%)
K ⁺	4.8
Na ⁺	1.6
SO ₄ ²⁻	4.8
Cl ⁻	1.6
Citric acid	1.5
Urea	2.7
Glucose	1
Ascorbic acid	23

Table 6.2 Comparison of the developed method with the reported works

No:	Method adopted	Lower detection limit (M)
1	Chemometrics [158]	1.45×10^{-6}
2	Colorimetric method [159]	1.3×10^{-5}
3	Derivative spectrophotometry [160]	2.48×10^{-7}
4	First and second derivative uv spectrophotometry [161]	9.8×10^{-6}
5	Reverse Phase - HPLC [163]	1.04×10^{-6}
6	Capillary electrophoresis [164]	1.02×10^{-5}
7	Voltammetry [165]	1.5×10^{-8}
8	Voltammetry (<i>Present method</i>)	1.34×10^{-6}

Table 6.3 Tablet study of GF using developed method and standard method

Sample	Declared amount	Method adopted	Found
EXPAL (Mech Pharma, India)	100 mg	MWCNT/Pt electrode	101.5 mg
	100 mg	Standard method	99.8 mg

Table 6.4 Recovery % of GF in urine sample using MWCNT/PtE

GF added (M)	GF found (M)	Recovery %
2×10^{-5} M	1.98×10^{-5} M	99.0
4×10^{-5} M	3.87×10^{-5} M	96.8
9×10^{-5} M	8.95×10^{-5} M	99.4

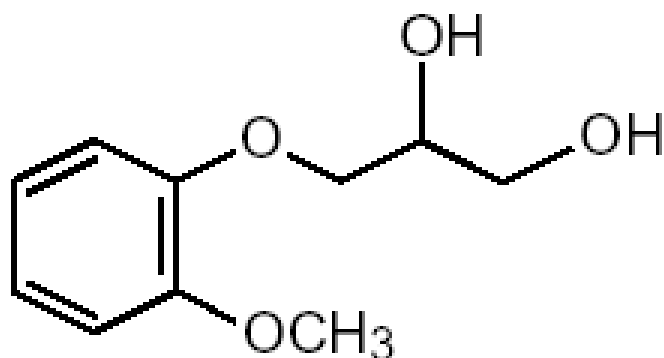


Figure 6.1 Structure of Guaiifenesin

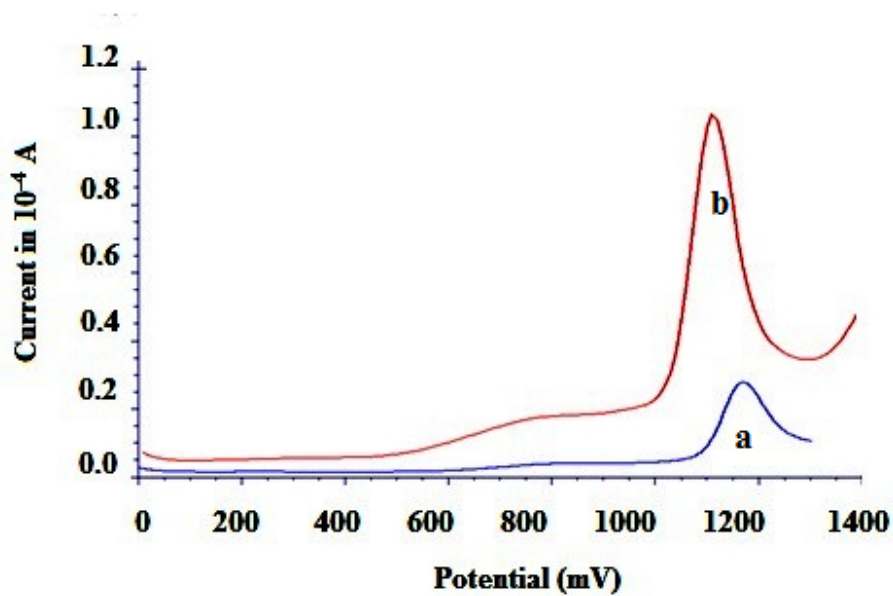
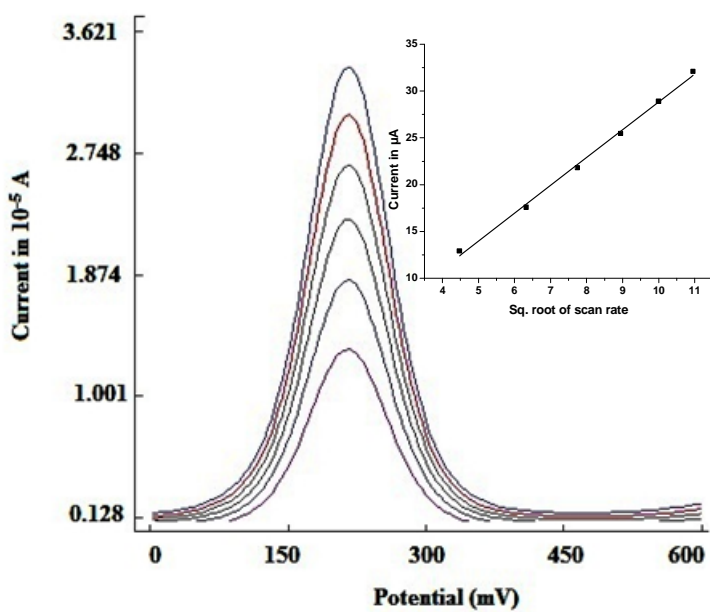
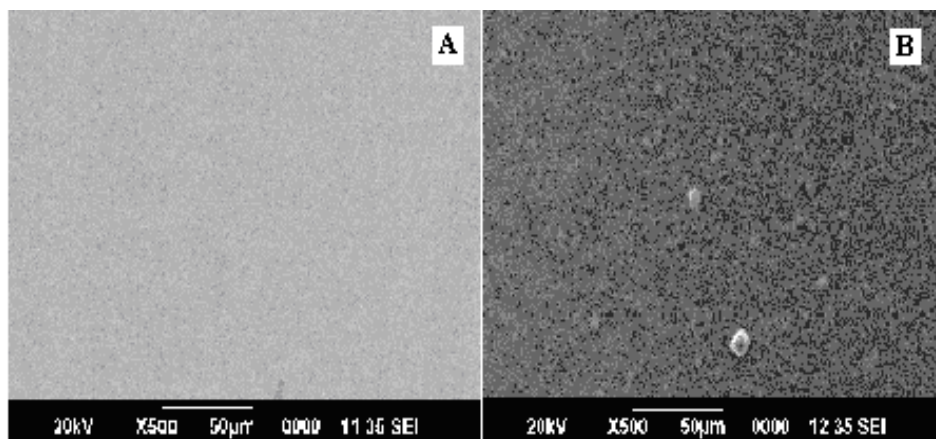
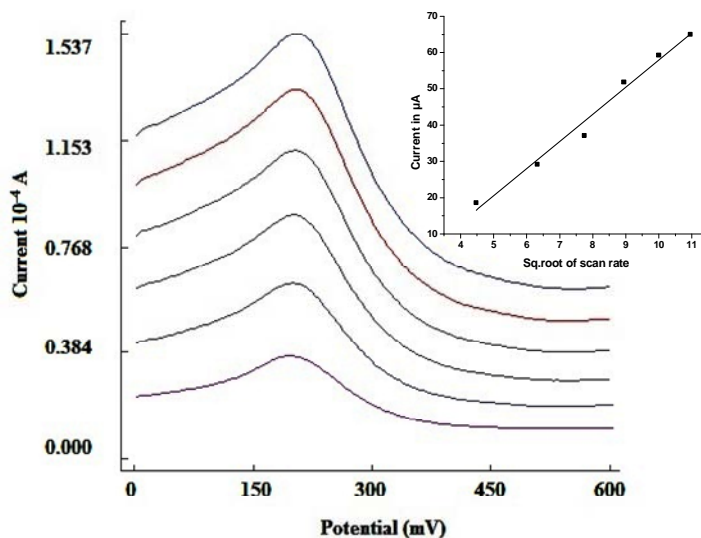


Figure 6.2 Square wave voltammogram of 1×10^{-3} M GF on a) Bare PtE b) MWCNT/PtE in 0.1M H₂SO₄





(b)

Figure 6.4 Overlay of SWVs at a) Bare PtE b) MWCNT/PtE in 2 mM $K_3Fe(CN)_6$ at scan rates in the range 20 – 120 mV/s. Variation of square root of scan rate with peak current from the overlay diagram (*inset*)

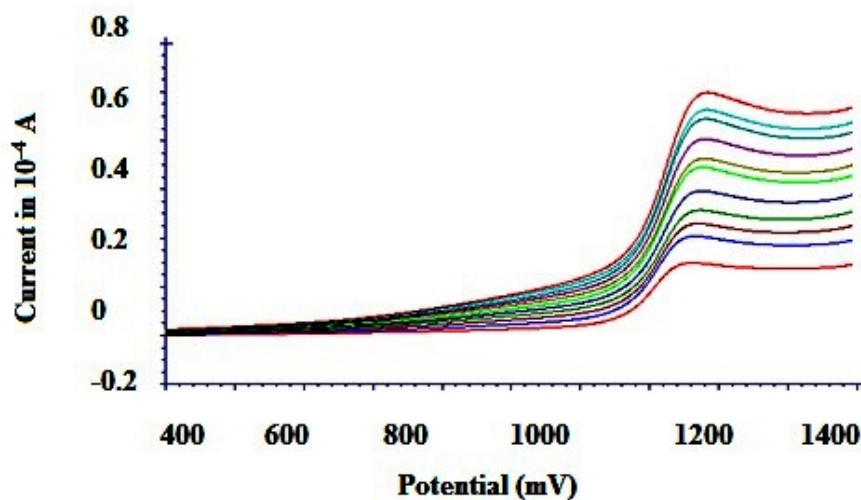


Figure 6.5 Overlay voltammograms for the oxidation of 1×10^{-3} M GF at different scan rates in the range 40 – 400 mV/s

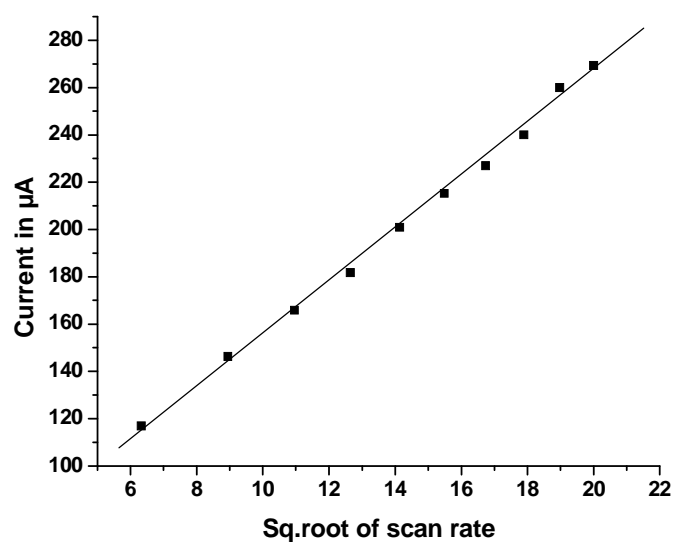


Figure 6.6 Plot of peak current of 1×10^{-3} M GF against the square root of scan rate in the range 40 – 400 mV/s

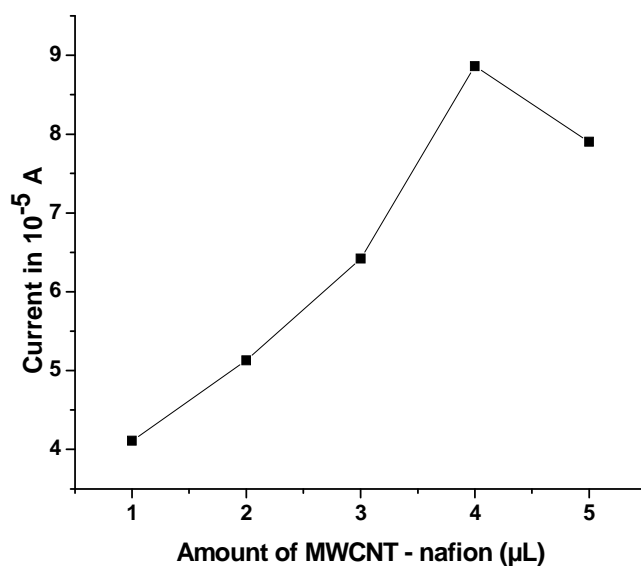


Figure 6.7 Effect of the amount of MWCNT – nafion suspension on the oxidation of GF at MWCNT/PtE

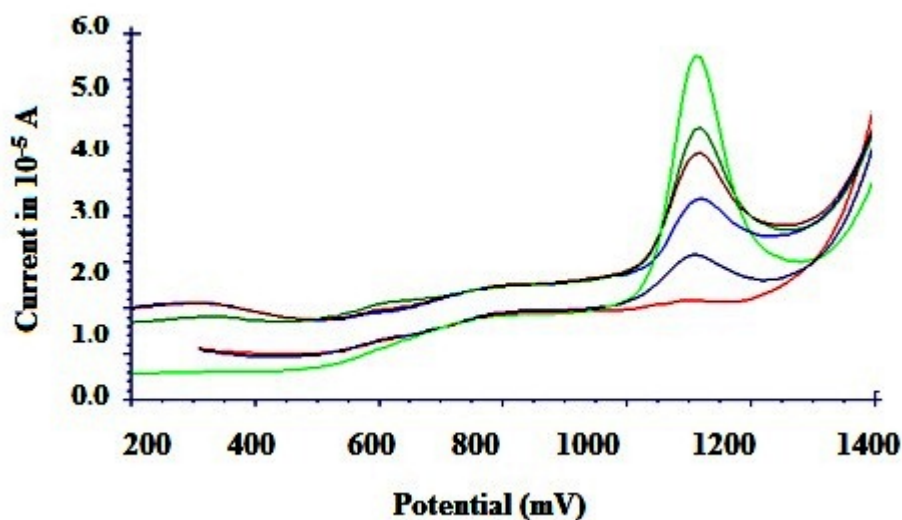


Figure 6.8 Overlay of SWVs of GF at MWCNT/PtE in the concentration range $4 \times 10^{-4} \text{ M} - 5 \times 10^{-5} \text{ M} - 4 \times 10^{-4} \text{ M}$

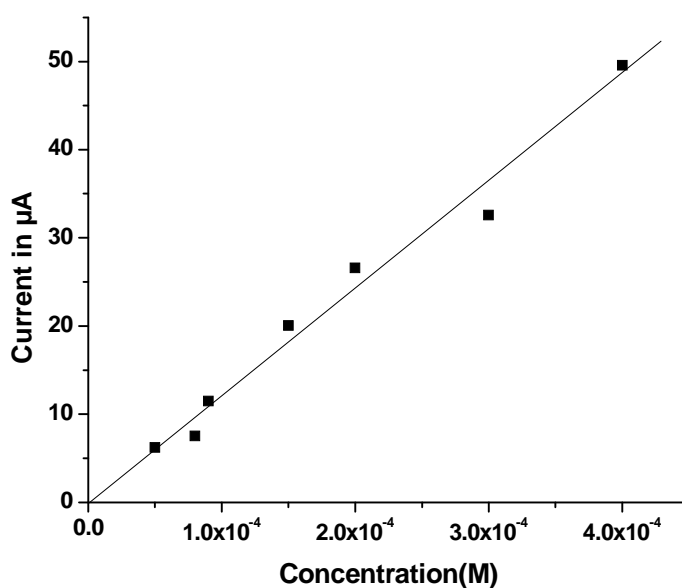


Figure 6.9 Calibration graph for GF at MWCNT/PtE in the concentration range $5 \times 10^{-5} \text{ M} - 4 \times 10^{-4} \text{ M}$

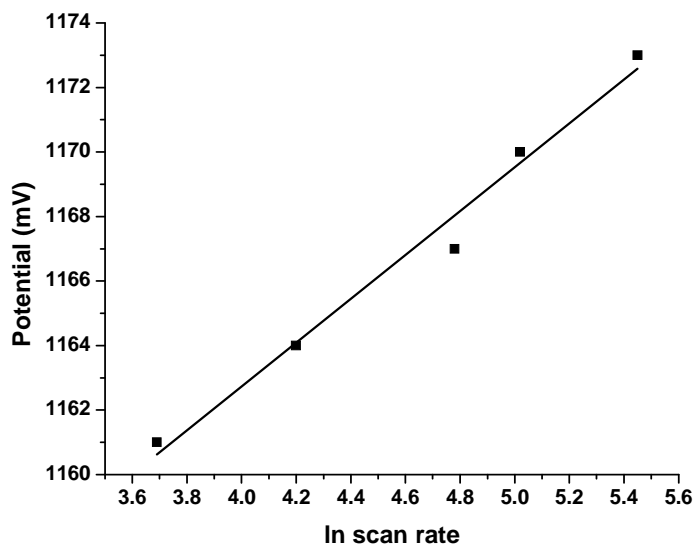
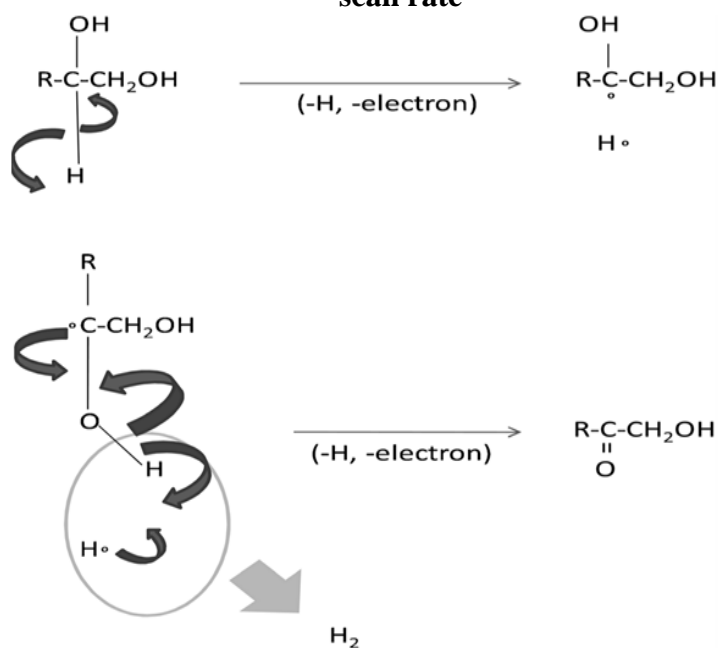


Figure 6.10 Plot of peak potential of GF against the natural logarithm of scan rate



Scheme 6.1 Mechanism for the oxidation of GF

* ★ ❧ ❧ ❧ ★ *

VOLTAMMETRIC SENSOR FOR TAMSULOSIN

7.1	Introduction
7.2	Experimental
7.3	Results and Discussion
7.4	Probable Mechanism for TAM Oxidation
7.5	Application in Urine Sample
7.6	Conclusions

The electrooxidative behavior and determination of Tamsulosin hydrochloride (TAM), one of the α_1 -adrenoceptor antagonist, on a poly-o-phenylene diamine [poly (o-PDA)] modified gold electrode (GE) by SWV is explained in this chapter. TAM showed an irreversible oxidation peak at 864 mV in 0.1 M acetate buffer (pH 5) solution. The anodic peak which is due to the oxidation of the methoxy group on the phenyl ring of TAM showed a 10-fold enhancement on GE when modified with a polymeric film of o-PDA. The peak current was proportional to TAM concentration in the range 8×10^{-7} M to 1×10^{-5} M with a detection limit of 7.4×10^{-8} M. The influence of pH, scan rate, supporting electrolyte, foreign species and number of cycles for polymerization on the oxidation peak current of TAM were studied. The developed sensor was applied for the determination of TAM in urine sample.

7.1 Introduction

Tamsulosin hydrochloride (TAM), chemically 5-[(2*R*)-2-[[2-(2-Ethoxyphenoxy) ethyl]amino]propyl]-2-benzenesulfonamide hydrochloride (Figure 7.1) is an α_1 -adrenoceptor blocking agent which exhibits selectivity for α_1 receptors in the human prostate. It was approved by FDA (Food and Drug administration) in 1997. Of the two enantiomeric forms of TAM, R-isomer is the active component pharmaceutically.

TAM is used to treat the symptoms of an enlarged prostate, a condition technically known as BPH (Benign Prostatic Hyperplasia) which results in the enlargement and tightening of muscles that can obstructs the flow of urine by compressing the urethra. The muscle tightening is caused by a chemical released by the adrenergic nerve. TAM has the ability to block the effect of this chemical on the muscles and thus to relax them. Among the various drugs used for blocking alpha adrenergic nerves, TAM is best preferred to treat BPH as it has lesser side effects and therapy can be started at an optimum dose.

TAM has been studied and determined by a number of procedures: liquid chromatography-mass spectrometry [174, 175], liquid chromatography with fluorescence detection [176], radio receptor assay [177], spectrofluorimetry [178], high performance thin layer chromatography [179, 180], RP - HPLC method [181], and spectrophotometry [182]. But these reported methods were influenced by interference of endogenous substances and potential loss of drug in the re-extraction procedure and involving lengthy, tedious and time- consuming plasma sample.

Electrochemically generated conducting or non-conducting polymeric films have recently attracted increasing interest because of their potential applications in gas sensors, biosensors and as perm selective membranes [183 – 185]. Electropolymerised films of 3-methyl thiophene, aniline, pyrrole, o-toluidine and 1, 3-phenyl diamine on various electrodes such as Pt, Au, GC, ITO, PB/ITO and graphite has been widely applied for electrochemical analysis including pharmaceutical analysis, biosensors etc recently. Conducting polymers possess both protonic and electronic conductivity that makes them a better catalyst support than the common carbon based materials.

Among these conducting polymers poly (o-PDA) is of special interest because of their unique properties. Poly (o-PDA) can be prepared electrochemically in acid, neutral and alkaline solution and is very stable in both aqueous solutions and air [186 – 188]. It is either a ladder polymer with phenazine rings [189] or a 1, 4 - substituted benzene-quinonoid open structure [190]. Poly (o-pda) films can be used to immobilize enzymes and to prevent interference and fouling of the electrode surface. Also, this polymeric film has been used as a perm selective membrane for halogenide ions. As opposed to poly (aniline) or poly (pyridine), poly (o-PDA) shows the conductivity in its reduced state, whereas its oxidized state is insulating.

There are a few reports in the literature on the electropolymerisation of o-PDA and their electrochemical application. Sayyah et al reported the electropolymerisation of poly (o-PDA) on platinum electrode from aqueous acidic solution and explained the kinetics mechanism, electrochemical study and characteristic properties of the polymer obtained [191]. Ekinici et al electrochemically prepared and voltammetrically characterized poly (o-pda) film as a dopamine selective polymeric membrane [192].

Ozkan et al has already reported the voltammetric determination of TAM on a glassy carbon disc electrode [193]. Laina et. al [194] reported the oxidation of TAM at multi walled carbon nanotube modified glassy carbon electrode. There are no reports in the literature for the electro oxidation of TAM at a GE sensor. Hence the present work is aimed to study the voltammetric behavior and oxidation mechanism of TAM at a GE modified with a film of poly (o-PDA) using SWV. After optimizing the various experimental parameters, application studies of the developed sensor was carried out in urine.

7.2 Experimental

7.2.1 Preparation of poly (o-pda)/GE

Prior to modification, GE was polished with alumina (< 50 nm) slurries, rinsed with double distilled water and methanol, and then ultrasonicated for 5 minutes in a water bath. It was then subjected to electrochemical cleaning in 0.5 M H₂SO₄ by CV in the range of 0 - 1500 mV.

Electropolymerisation of o-PDA on GE [191] was carried out from the deoxygenated aqueous solution containing 0.5 M HCl, 0.08 M monomer unit of o-PDA and 0.1 M Na₂SO₄ at a potential between 0 - 800 mV with a scan rate of 100 mV/s. Prior to modification the monomer was purified by twice crystallization from water [195]. If the polymerization is carried out at higher pH, the extent of conjugation may be diminished by the increasing number of -NH₂ groups at the electrode surface [196]. After electro polymerization, the resulting poly (o-PDA) coatings were rinsed with deionized water for subsequent voltammetric studies.

7.2.2 Analytical Procedure

Electrochemical measurements were made on CH Instruments Electrochemical Analyzer (USA) interfaced to a PC. A conventional three electrode system, including poly (o-PDA) modified GE as working electrode, a Pt wire counter electrode and an Ag/AgCl reference electrode were employed. The pH measurements were carried out on a Metrohm pH meter.

Stock solutions of TAM (1×10^{-2} M) were prepared in Milli - Q water. It was then diluted to the required concentration by adding the appropriate amount of supporting electrolyte. The analyte solution was taken in the electrochemical cell and the SWV was then recorded from 600-1200 mV/s at a scan rate of 100 mV/s for concentration study. For the electrode regeneration several cyclic scans were carried out in the blank electrolyte solution until a stable voltammogram was obtained. To study the influence of scan rate on peak current, Linear Sweep Voltammetric (LSV) technique was adopted.

7.2.3 Analysis of urine sample

The feasibility of the poly (o-PDA)/GE for the determination of TAM in urine sample was analyzed. Various concentrations of the drug solution in acetate buffer containing fixed amount of urine sample was prepared. The electrochemical behavior of the prepared solution on the modified electrode was studied by SWV and the unknown concentrations were determined from the calibration graph.

7.3 Results and Discussions

7.3.1 Electropolymerisation of o-PDA and mechanism

Figure 7.2 represents the voltammogram obtained for the electro polymerisation of (o-PDA) on GE surface which exhibited a distinct, irreversible anodic peak at 680 mV. Visual inspection revealed the formation of a thin and homogeneous polymeric film of brownish color on the electrode surface. The anodic peak corresponds to the oxidation of o-PDA monomer by the removal of an electron from the nitrogen atom of the amino group to form a radical cation. The cation then interacts with another monomer molecule to form a dimer radical cation, trimer radical cation and so on; finally results in a 1, 4-substituted benzenoid open structure as in Figure 7.3 [197].

The surface modification of GE with o-PDA is established by surface area study and SEM images. In order to calculate the surface areas of both bare and modified electrodes, the CV of these electrodes were carried out in 2 mM $K_3[Fe(CN)_6]$ at different scan rates (Figure 7.4). In Figure 7.5 the relation between peak current and square root of scan rate obtained from CVs are plotted. Knowing the slope of this linear curve and substituting in Randles Sevcik equation,

$$i_p = 2.69 \times 10^5 \text{ An}^{3/2} \text{D}^{1/2} \text{cv}^{1/2}$$

the effective surface area of GE doubled on modifying with o-PDA from 0.97 cm^2 to 1.77 cm^2 .

SEM images (Figure 7.6) established the fact that surface modification has occurred which can enhance the oxidation of TAM at poly (o-PDA)/GE.

7.3.2 Voltammogram of TAM

The electrochemical response of TAM was first studied on a polyaniline modified Pt electrode but no response was obtained. At the poly(o-PDA)/GE, TAM exhibited a sigmoidal oxidation peak at 864 mV, which was a 100 mV less than for the bare electrode (Figure 7.7). The sigmoidal curve is indicative of a slow electron transfer rate at the surface. The peak current showed a 10 times enhancement on modified electrode. The presence of neutral or protonated $-NH_2$ groups of the polymer may be responsible for the interaction with the analyte molecule and the better response of TAM on the modified electrode [198]. The absence of a reduction peak for TAM in the reverse sweep establishes the irreversibility of the electrochemical process.

7.3.3 Optimization of experimental parameters

The influences of various operational parameters on the developed sensor were studied and the conditions which gave the best peak response for TAM oxidation were chosen for the analysis.

7.3.3.1 Effect of supporting electrolyte

The electrochemical behavior of 1×10^{-3} M TAM was studied by SWV in 0.1 M concentration of different electrolytes such as KNO_3 , H_2SO_4 , NaOH, phosphate buffer and acetate buffer solution. As TAM gave the best oxidation peak in acetate buffer, it was used as the supporting electrolyte throughout the experiment.

7.3.3.2 Effect of pH

Linear sweep voltammogram (LSV) of TAM at all pH values in the range 2 to 9 established one distinct and well-defined anodic peak. The peak

current for TAM oxidation showed a maximum at pH 5 of the supporting electrolyte (Figure 7.8). So pH 5 was selected as the optimal pH.

7.3.3.3 Effect of the number of cycles for polymerization

Figure 7.9 shows the relation between the peak current of TAM and number of cycles for electropolymerisation. The curve showed maximum current corresponding to 20 cycles and thereafter it decreased. Thus the film thickness is optimal for TAM oxidation when the polymerization is carried out in 20 cycles. The decrease in the peak currents with the number of cycles during electro polymerization is indicative of the formation of a non electroactive polymeric film which may be explained by blockage of the access of the monomer to the gold electrode surface on the subsequent scans. Thereafter the modified electrode gave a significant response for the electroactive TAM.

7.3.3.4 Effect of scan rate

Scan rate studies (Figure 7.10) were performed to assess whether the processes at poly (o-PDA)/GE was under diffusion or adsorption controlled. When the scan rate was varied from 40 - 400 mV/s in 1×10^{-3} M solution of TAM, a linear dependence of peak intensity upon the square root of scan rate $v^{1/2}$ was found, demonstrating a diffusional behavior (Figure 7.11).

The relationship between the peak potential and v was also examined. It was found that the potential varies linearly with $\ln v$ (Figure 7.12). The number of electrons involved in the reaction can be calculated from the slope of the plot according to $b=RT/\alpha n_a F$, where b is the slope and α of the totally irreversible electrode process is assumed as 0.5. The obtained value for n_a is 2, which indicates that two electrons are involved in the oxidation of TAM.

7.3.3.5 Interference study

The interference from various species such as urea, glucose, Na⁺, Cl⁻, K⁺, SO₄²⁻ and ascorbic acid in the determination of TAM was systematically studied (Table 7.1). A 100- fold excess of all these compounds does not interfere with the analysis of TAM. But ascorbic acid interfered severely.

7.3.3.6 Calibration curve

Under the optimized conditions, the dependence between the TAM concentration and peak current was studied. A linear relation (Figure 7.13) was found in the concentration range between 8×10^{-7} M and 1×10^{-5} M indicating that the response was diffusion controlled in this range. Above 1×10^{-5} M concentration, a loss of linearity may be attributed to the adsorption of TAM on the electrode surface. The lower limit of detection was found to be 7.4×10^{-8} M (Figure 7.14) and compared with the other reported works (Table 7.2)

7.4 Probable Mechanism for TAM Oxidation

From the scan rate study it was confirmed that two electrons are involved in TAM oxidation which gives an anodic peak in acetate buffer solution at poly (o-PDA)/GE. TAM belongs to the class of alkoxybenzenes and so the probable mechanism involves the oxidation to the corresponding quinone [199] as given in Scheme 7.1. Uslu et al reported that TAM oxidation may be occurring at the methoxy group [200] which is the electro active centre both in acidic and less basic media. Anodic oxidation of alkoxy benzenes in aqueous acidic medium leads to loss of the alkoxy substituent, involving an

ipso-substitution on the radical-cation by water as proposed by Grimshaw et. al [201].

7.5 Application in Urine Sample

The developed sensor was applied for the determination of TAM in spiked urine samples as given in section 7.2.3. The recovery percentage of TAM in urine at the modified electrode was found to be 97.2 – 102.9 % (Table 7.3).

7.6 Conclusions

The electro activity of TAM on poly (o-PDA)/GE was studied by SWV. TAM exhibited an irreversible oxidation involving a two electron mechanism and a diffusion controlled process. The poly (o-PDA) film on GE acts as a conducting polymer layer for both electron and proton. The developed sensor proved to be successful in oxidizing TAM easily, characterized by the enhancement of the peak current and reduction of peak potential for TAM. The electrochemical reduction is attributed to the oxidation of the alkoxy groups on TAM. Thus a very sensitive, rapid and simple method for the determination of TAM was developed.

Table 7.1 Interference by the foreign species in the determination of TAM

Foreign species	Signal change (%)
K ⁺	0.18
Na ⁺	2.78
SO ₄ ²⁻	0.18
Cl ⁻	2.78
Urea	2.17
Glucose	0.34
Ascorbic acid	50

Table 7.2 Comparison of the developed method with the reported works for TAM determination

No:	Method adopted	Lower detection limit (M)
1	Liquid Chromatography [175]	1.0×10^{-8}
2	Radio receptor assay [177]	1.22×10^{-7}
3	Spectrofluorimetry [178]	1.07×10^{-7}
4	RP-HPLC [180]	1.21×10^{-6}
5	Spectrophotometry [182]	1.96×10^{-7}
6	Voltammetry [193]	3.34×10^{-7} (DPV) 2.45×10^{-7} (SWV)
7	Voltammetry [194]	9.8×10^{-8}
8	Voltammetry (<i>Present method</i>)	7.4×10^{-8}

Table 7.3 Recovery % of TAM in urine sample at poly (o-PDA)/GE

GF added (M)	GF found (M)	Recovery %
3×10^{-6}	2.98×10^{-6}	99.3
7×10^{-6}	7.21×10^{-6}	102.9
9×10^{-6}	8.75×10^{-6}	97.2

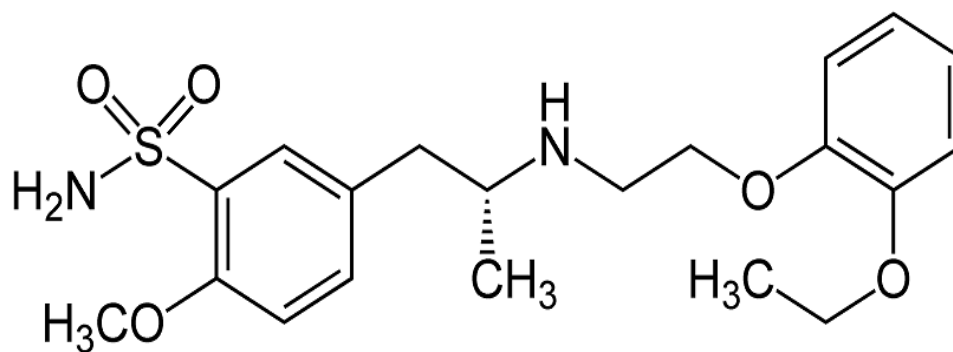


Figure 7.1 Structure of Tamsulosin

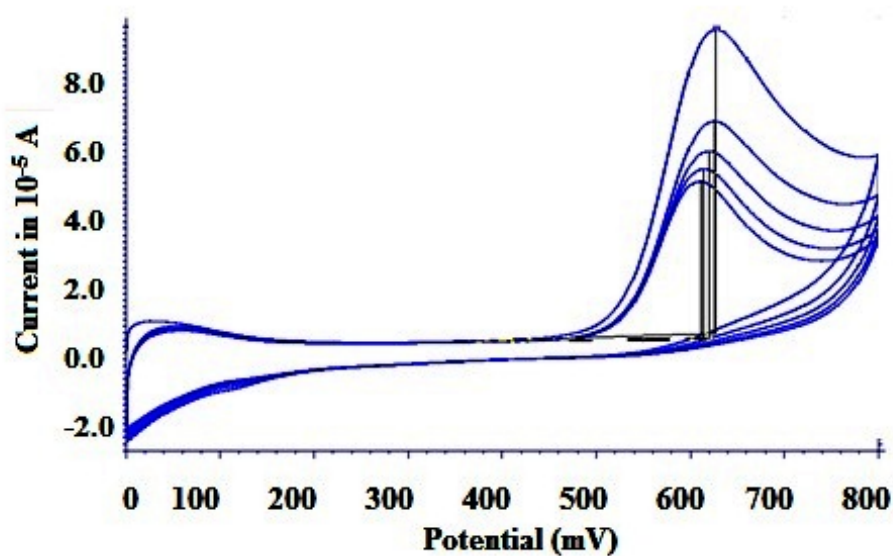


Figure 7.2 Electropolymerisation of o-PDA on GE in 20 cycles

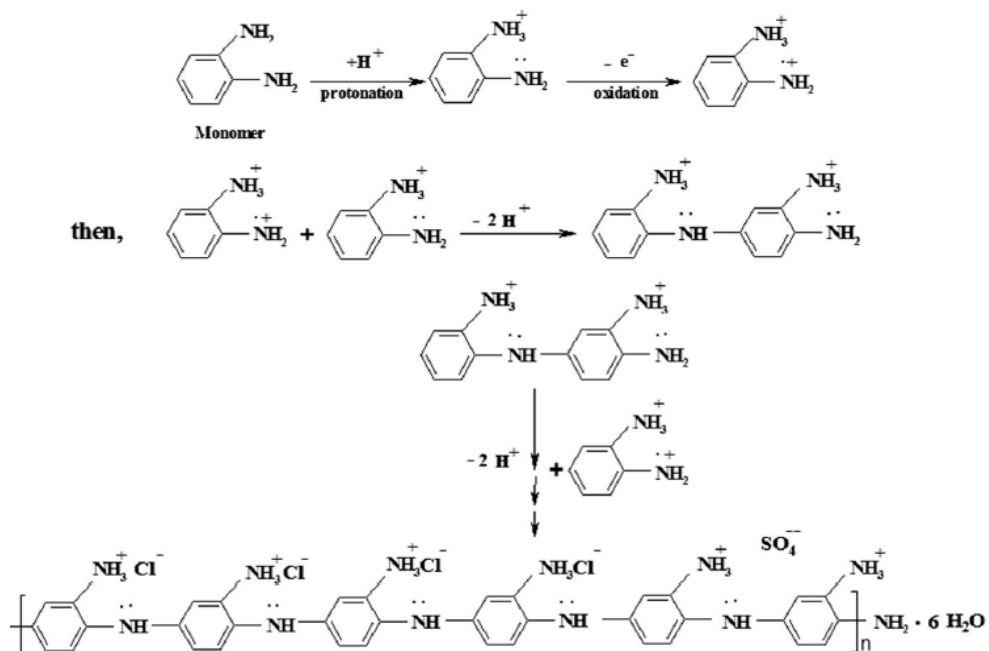
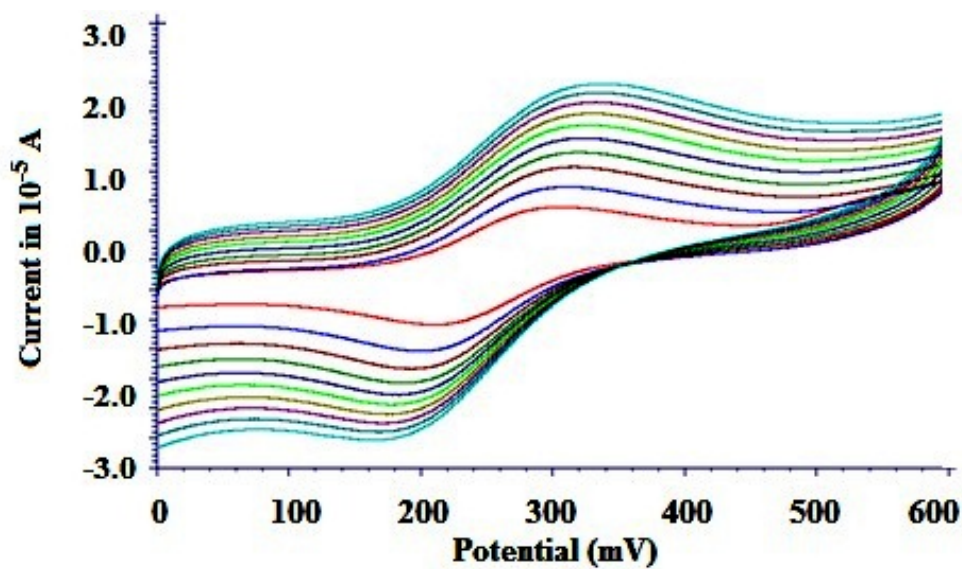
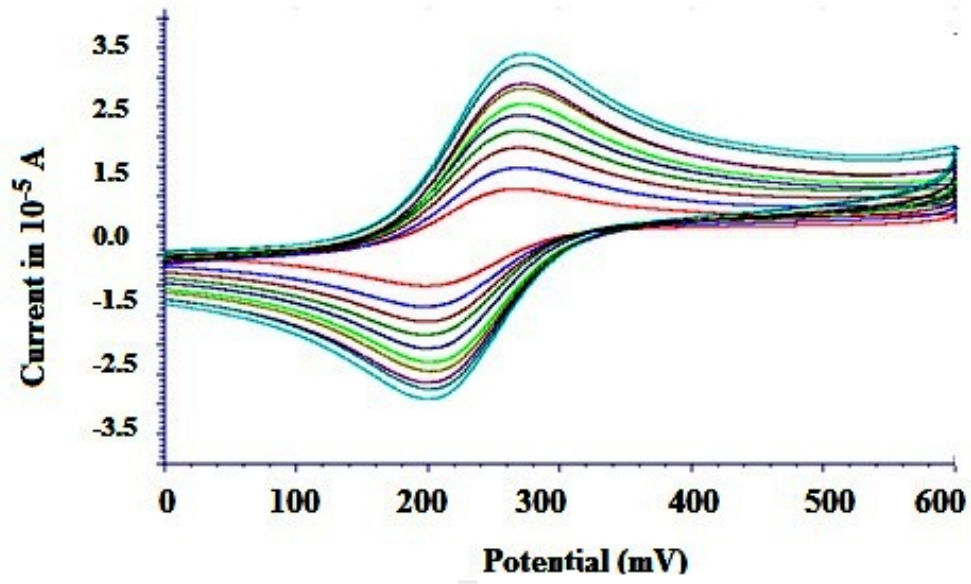


Figure 7.3 Mechanism for the polymerisation of o-PDA on GE

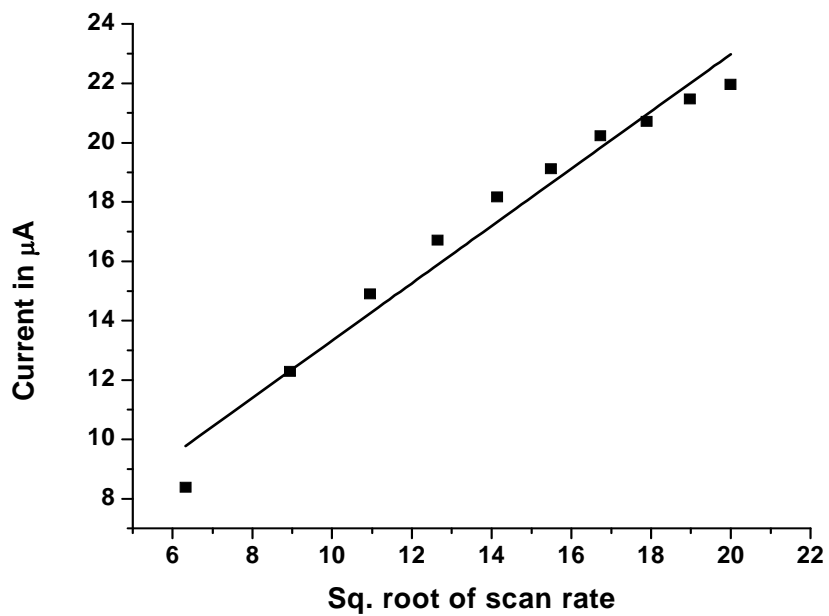


(a)

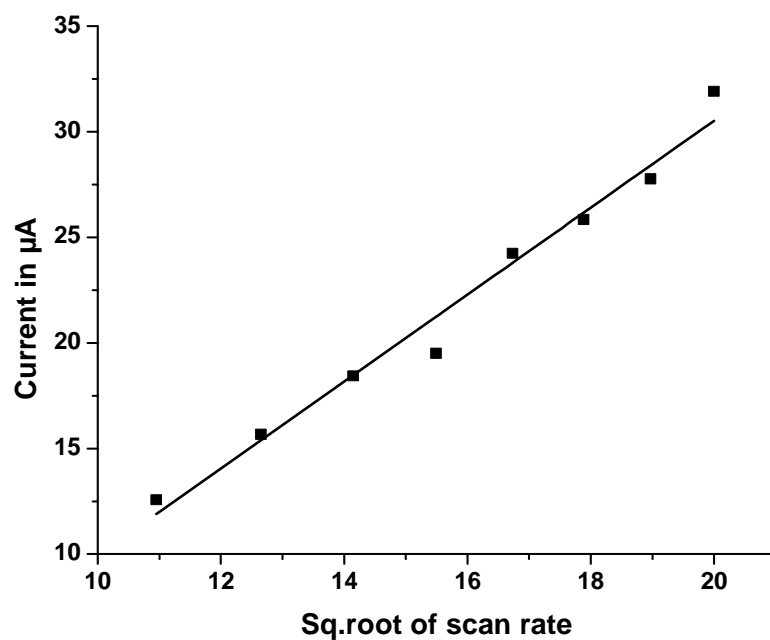


(b)

Figure 7.4 Overlay of CVs of 2 mM $K_3[Fe(CN)_6]$ at a) Bare GE b) poly (o-PDA)/GE



(a)



(b)

Figure 7.5 Variation of peak current of TAM with sq.root of scan rate at a) Bare GE b) poly (o- PDA)/GE

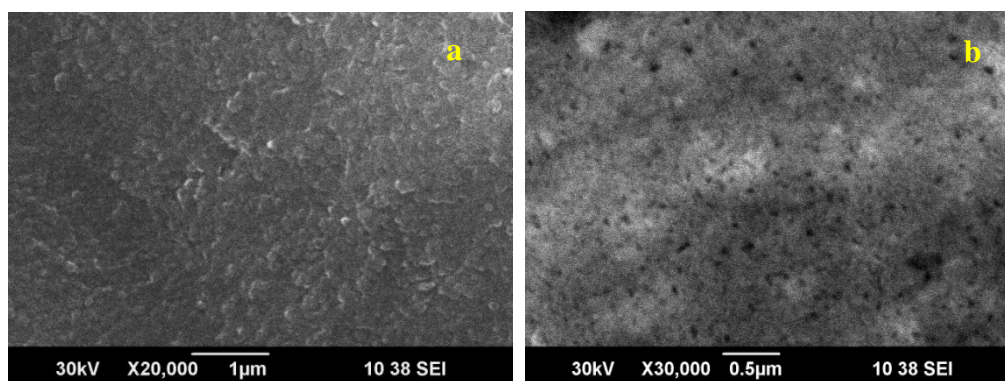


Figure 7.6 SEM images of a) Bare GE b) poly (o-PDA)/GE

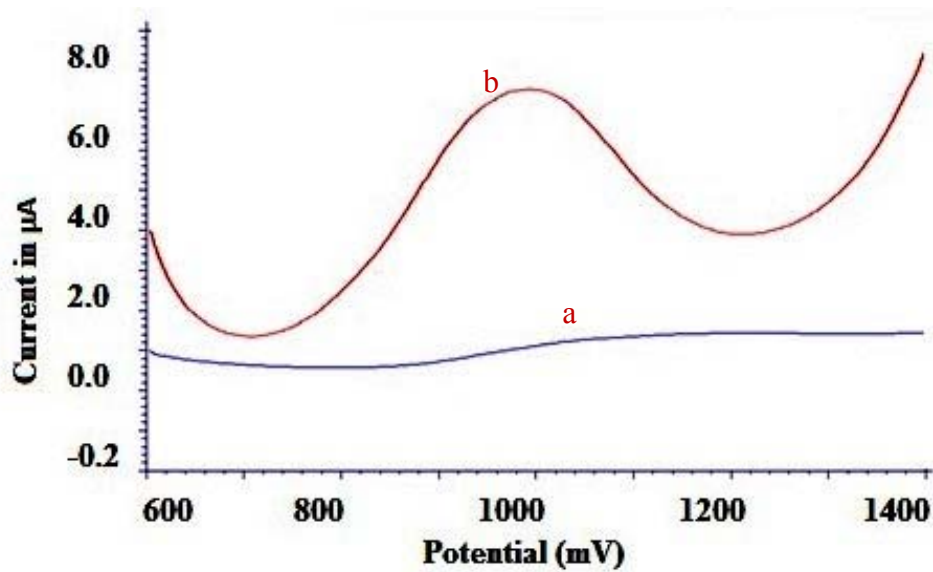


Figure 7.7 Voltammogram of TAM at a) Bare GE b) poly (o-PDA)/GE

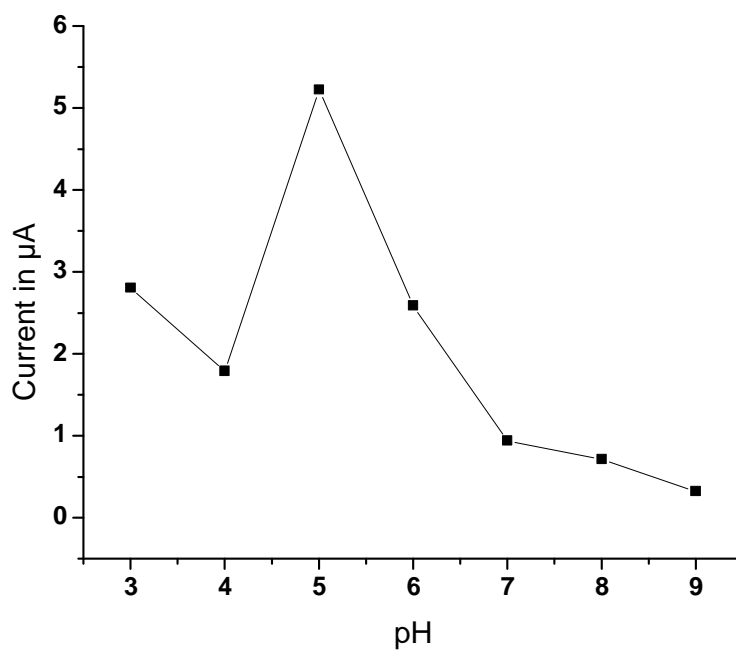


Figure 7.8 Effect of pH on TAM Oxidation

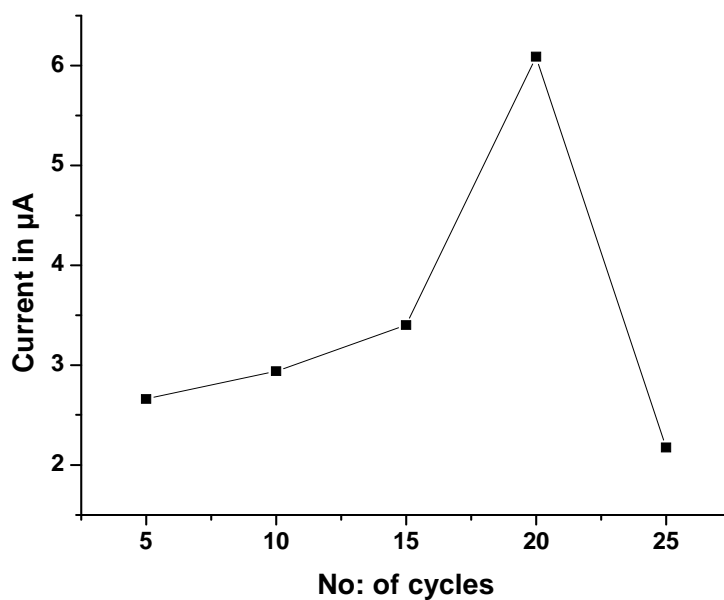


Figure 7.9 Effect of number of cycles of polymerization on TAM oxidation

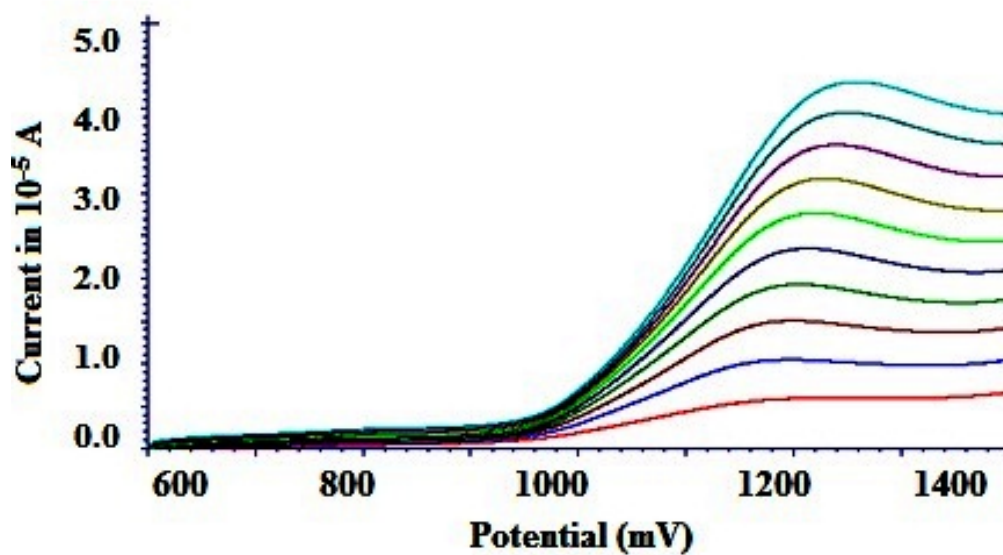


Figure 7.10 Effect of scan rate on TAM oxidation at poly (o-PDA)/GE

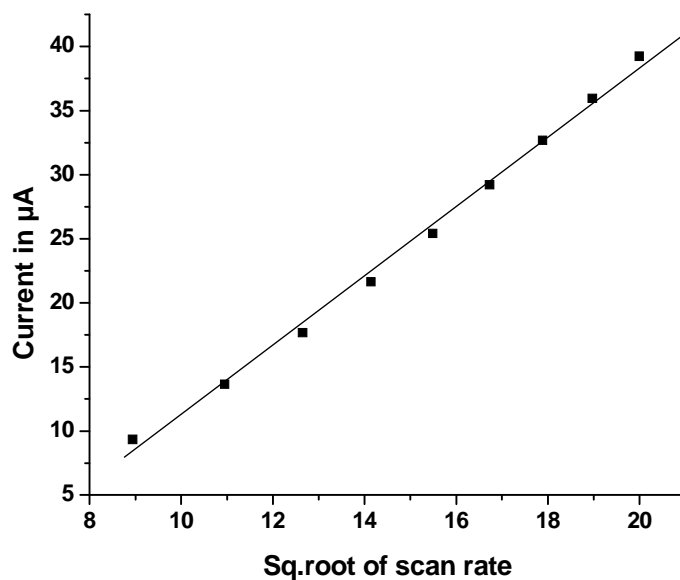


Figure 7.11 Dependence of peak current on square root of scan rate

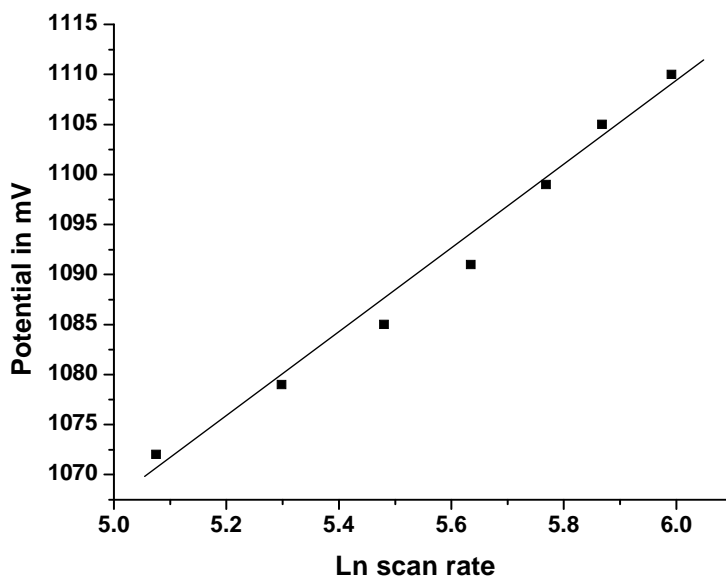


Figure 7.12 Plot of peak potential against \ln (scan rate)

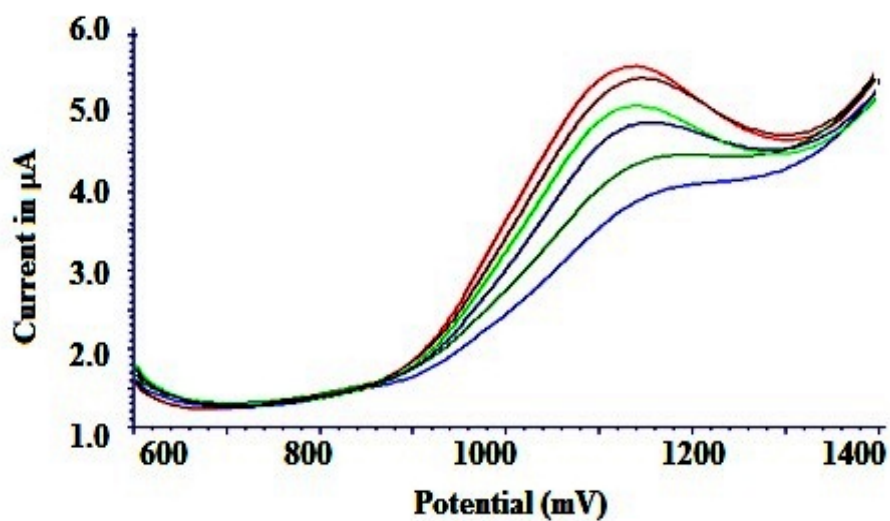


Figure 7. 13 Overlay of SWVs of TAM in the concentration range $8 \times 10^{-7} - 1 \times 10^{-5} \text{ M}$

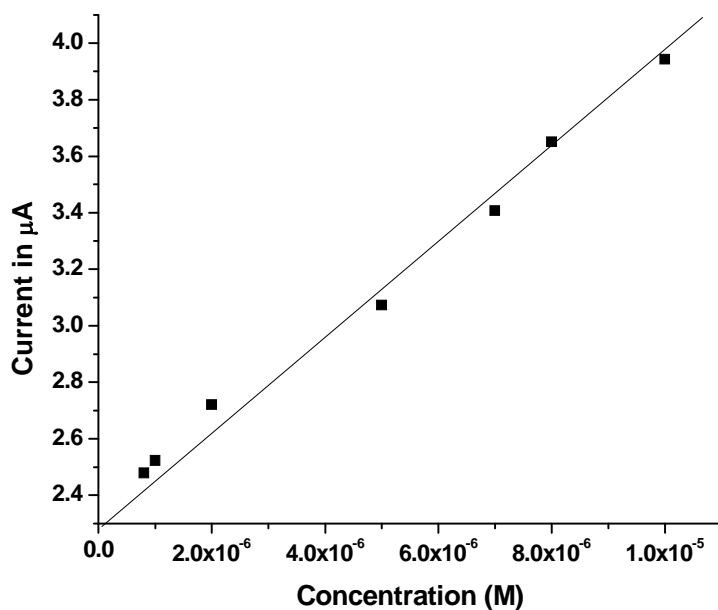
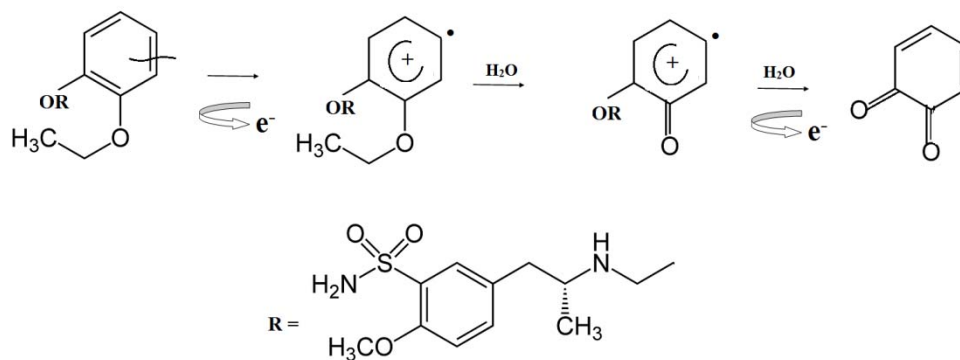


Figure 7.14 Calibration curve of TAM concentration and oxidation peak current



Scheme 7.1 Mechanism for TAM oxidation



VOLTAMMETRIC SENSORS FOR TINIDAZOLE

Contents

8.1	Introduction
8.2	Materials and method
8.3	Results and Discussion
8.4	Determination of Analytical Figures of Merit
8.5	Proposed Scheme for TIN Reduction
8.6	Analytical Application in Real Samples
8.7	Conclusions

This chapter explains the development of two different sensors for the determination of tinidazole (TIN). The electrochemical reduction of TIN, an anti – parasitic drug on a voltammetric sensor fabricated using a glassy carbon electrode (GCE) covalently bound with a polymer layer of L-Cys was studied by square wave voltammetry (SWV). The subsequent modification of poly (L-Cys)/GCE with gold nanoparticles (AuNPs) significantly enhanced the surface activity of the electrode for TIN determination due to the synergistic effect of these double layers on GCE. The modified electrode surfaces were characterized by Scanning Electron Microscope (SEM) and the experimental parameters for the determination of TIN on these electrodes were optimized. Application studies of both the developed sensors were carried out in pharmaceutical tabulations and spiked urine samples.

8.1 Introduction

Tinidazole (TIN) (Figure 8.1) 1-[2-(ethylsulfonyl)ethyl]-2-methyl-5-nitroimidazole, a second-generation 2-methyl-5-nitroimidazole, developed in 1967 is an antibacterial, anti protozoa and anticancer drug. TIN is used to treat trichomoniasis, amebiasis and giardiasis. Chemically, TIN is very much similar to metronidazole, a drug with unpleasant side effects. The mechanism of nitroimidazole activity involves the generation of free nitro radical. The species thus generated is responsible for the cytotoxicity activity [202] of this class of drugs.

Due to its low molecular weight, TIN can easily penetrate into the cell membranes of both aerobic and anaerobic micro organisms. After diffusing into the cells, the nitro group of TIN is reduced to a short – lived toxic free radical by a ferridoxin mediated transport system. These radicals bind to DNA damaging it and ultimately cell death [203].

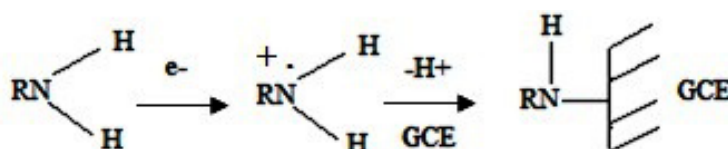
Due to its important role in numerous pathological processes, detection and quantification of TIN is relevant in pharmaceutical and clinical procedures. Several methods are reported for the determination of TIN, including spectrophotometry [204, 205], chromatography [206, 207], capillary electrophoresis [208] and voltammetry [209 -212].

Chemically Modified Electrodes (CMEs) are one among the most researched area in the field of electrocatalytic and electroanalytical chemistry. Bare electrodes may be modified physically or chemically with modifiers such as organic molecule, inorganic species, metal nanoparticles, polymers or biomolecules tailoring to its surface forming monofilm, multilayer film or array. Due to this, the electrode activity may be enhanced significantly in

terms of selectivity, stability, sensitivity etc. These CMEs may be widely applied for the analysis of active ingredients of pharmaceuticals, food additives, metal ions, pesticides etc [213 – 216].

The ability to modify GCE with various amines through the electrochemical oxidation of functionalities attached to it was reported by Randall et. al [217]. Among the various amine modifiers, L-Cysteine polymer layer formation on electrode surface is of great utility as it can form a chemically stable covalent linkage between the nitrogen atom of the amine group and the edge plane sites at the electrode surface.

As proposed by Barbier et. al, initially there is a one electron oxidation of amine functionality to the corresponding radical cation and then form a chemically stable covalent linkage between nitrogen and carbon by the removal of a proton [218]. They also concluded that the electro oxidation of primary amines yielded an excellent surface coverage and can be applied for electrocatalytic and biosensor purposes.



Very recently there are reports on the voltammetric determination of various analytes such as metronidazole, sunset yellow and dopamine [219 - 221] based on L-Cys modified GCE. All these are based on the formation of a negatively charged film by L-Cys due to the deprotonation of the radical cation on the surface of GCE and the selective sensing of the analyte molecule.

The integration of nanotechnology with electrochemical analysis is much advantageous due to their enhanced electron transfer rate and electrocatalytic ability. AuNPs are of much importance as they offer mainly three functions: improved mass transport, high effective surface area and catalytic properties. Currently the focus is on multi layer deposition rather than a monolayer of AuNPs on GCE for the electrochemical analysis of pharmaceuticals. Ozkan et. al reported the voltammetric determination of riluzole [222] based on gold nanoparticles/ ionic liquid/chitosan composite modified GCE. A voltammetric sensor for salbutamol on MWNT/nano Au composite was developed by Yinfeng Li et al. [223]. A double layer electrodeposition on GCE by nano structured thin film (modifier) on a conducting polymer layer of L – Cys has not been reported previously for the determination of TIN.

The present work is targeted to develop two different electrochemical sensors for TIN, based on the electrodeposition of L-Cys and a double layer of poly (L-Cys)/AuNP on GCE. The electrochemical deposition method is chosen as it can control the size and distribution of particles on electrode surface by varying potential, time or solution concentration. Further, optimization of various experimental parameters and application studies of the developed sensors were conducted.

8.2 Materials and Method

8.2.1 Apparatus

All electrochemical experiments were performed with a CH Instrument in a conventional three electrode cell using modified GCE as the working electrode, platinum wire as the auxiliary electrode and Ag/AgCl as

the reference electrode. SEM images were recorded on a JOEL 6390 LV. The pH measurements were carried out on an ELICO LI 120 pH meter.

8.2.2 Cleaning of GCE

GCE was polished with 0.05 μm alumina slurry on a polishing pad and rinsed thoroughly with water. Polished GCE was then sonicated in methanol, 1:1 HNO_3 and acetone consecutively, washing with water each time.

8.2.3 Fabrication of L-Cys/GCE

The cleaned GCE was immersed in 0.1 M phosphate buffer solution (PBS) containing 5 mM L-Cys. The film of L-Cys was grown on the electrode surface by 30 segments of cyclic voltammetric scan between -0.8 V to 2.0 V [224]. The peak response decreased quickly with the successive scan which may be due to the passivation of the electrode surface on grafting Cys on GCE [225]. Hence poly (L-Cys) was electrodeposited on GCE by 30 segments. The modified electrode was then washed with ethanol and dried in air to form a blue film on the surface (Figure 8.2).

8.2.4 Fabrication of AuNP/L-Cys/GCE

The poly (L-Cys)/GCE was immersed in 0.05 M H_2SO_4 containing 1 mM HAuCl_4 solution. This solution has the ability to obtain AuNPs of high density and small size [226] through electrodeposition on the surface of GCE. 20 cyclic scans were carried out between 1.3 V to 0 V at a scan rate of 0.1 Vs^{-1} [227] to form AuNP/ poly (L-Cys)/GCE (Figure 8.3). A golden coloured film was visible on the surface of GCE after electrodeposition. The modified electrode was then activated in PBS before the determination of TIN.

8.2.5 Preparation of TIN solution

Stock solution of TIN (1×10^{-2} M) was prepared by dissolving 24.7 mg in 10 mL methanol. Standard solutions of varying concentrations were prepared by diluting the stock solution using 0.1 M PBS.

8.2.6 Preparation of tablet solution

Five tablets were finely powdered and weight equivalent to prepare 1×10^{-3} M TIN was dissolved in methanol. After shaking the solution vigorously, it was then filtered to a 25 mL standard flask and made up to the mark. The solution was diluted accordingly to perform the analysis on the modified electrode.

8.2.7 Recording the voltammogram for TIN

The electrochemical behavior of TIN was studied by SWV with a three electrode system set up as described under section 8.2.1. Potential was scanned between 0 and - 800 mV at the modified electrodes with a scan rate of 100 mV/s in the chosen supporting electrolyte.

8.3 Results and Discussion

8.3.1 Morphologies and electrochemical behavior of modified electrodes

The surface morphology of the various modified electrodes used in the current study was characterized using SEM (Figure 8.4). The SEM image of bare GCE (a) displayed a smooth and homogenous surface. On modifying GCE with L-Cys, (b) the surface of the electrode was coated with a layer of poly (L-Cys). The surface acquired a symmetric distribution on depositing AuNPs as a second layer (c) on GCE. As seen in the figure, AuNPs form

spherical particles of diameter in the nano range on the surface. Thus SEM image stands as a strong evidence for surface modification of GCE.

To calculate the effective surface area for both bare GCE and modified electrodes, the cyclic voltammogram of 2 mM potassium ferricyanide were recorded (Figure 8.5) at these electrodes in the potential range 0 mV to 600 mV. The peak current (i_p) varied linearly with the square root of scan rate (ν). The surface area of the electrodes are then estimated from the slope of the curve applying Randles Sevcik equation,

$$i_p = 2.69 \times 10^5 A n^{3/2} D^{1/2} c \nu^{1/2}$$

where A- effective surface area in cm^2 , D- diffusion coefficient in cm^2/s , n – number of electrons transferred per mole of the electroactive species and c – concentration of the solution. The effective surface area of 1.15 cm^2 for bare electrode increased to 1.70 cm^2 with poly (L-Cys) monolayer and is doubled to 2.36 cm^2 on further modification with AuNPs.

Figure 8.6 illustrates the square wave voltammetric response of $1 \times 10^{-5} \text{ M}$ TIN on the surface of bare GCE, poly (L-Cys)/GCE and AuNP/poly (L-Cys)/GCE. In comparison to the bare GCE, a reduction in potential from – 640 mV to – 581 mV for TIN on poly (L-Cys)/GCE may be attributed to the selective reduction of TIN on a film of the polymer. During the electrodeposition of L-Cys on GCE, both cathodic and anodic waves are observed due to the reduction and re-oxidation of carboxylic as well as amine functionalities in the molecule of cysteine bonded onto the surface. The acid groups on the surface of the monolayer are deprotonated resulting in a negatively charged film which has an electrostatic attraction towards the positively charged nitro radical on TIN. Consequently, the modified GCE

selectively sense the free nitro radical which accounts for the current enhancement from 10.5 μA to 19.47 μA on the poly (L-Cys)/GCE surface.

On integrating AuNP on poly (L-Cys)/GCE, the reduction potential is further decreased to - 487 mV, indicating the catalytic role of AuNP in the electro reduction of TIN. The observed lower potential is attributed to a synergistic effect of poly (L-Cys) and AuNP that offers a lower resistance for the electron transfer along the surface. The lower peak current of 15.33 μA for TIN reduction on AuNP/L-Cys/GCE compared to L-Cys/GCE may be due to the absence of the prominent electrostatic interaction between L-Cys and TIN through the nano film layer.

The absence of a peak in the reverse scan of TIN reduction by cyclic voltammetry on both the modified electrodes confirms that the reduction is irreversible.

8.3.2 Optimization of experimental parameters

8.3.2.1 Influence of supporting electrolyte

The cathodic peak current of TIN in 0.1 M solution of KNO_3 , NaOH, acetate buffer solution, PBS and Britton – Robinson buffer (BRB) were studied on both poly (L-Cys)/GCE and AuNP/poly (L-Cys)/GCE. Except in BRB, TIN exhibited a well defined peak for all other electrolytes. Among these the lowest potential and highest current response was observed in PBS and this was chosen as the supporting electrolyte for further studies.

8.3.2.2 Influence of pH on the reduction of TIN

The electrochemical behavior of TIN was investigated in various pH in the range 4 – 9 in 0.1 M PBS by SWV for both the modified electrodes.

From the results of pH investigations (Figure 8.7) it was concluded that maximum current response for TIN was observed at pH 4. Reduction current was much enhanced even below pH 3 and above pH 9. But the response was not stable in highly acidic pH and a higher potential was observed for basic pH. So pH 4 was chosen for the determination of TIN in physiological conditions for both modifications.

8.3.2.3 *Effect of accumulation time*

The effect of accumulation time on the reduction peak current of TIN has been examined. As the peak current almost remained unchanged with the accumulation time it may be concluded that accumulation have no influence on TIN reduction.

8.3.2.4 *Effect of scan rate*

In order to study the effect of potential sweep rate (ν) on the peak current, linear sweep voltammetry (LSV) of the buffered solution containing 1×10^{-5} M TIN were recorded at different potential sweep rates of 40 - 280 mV/s for poly (L-Cys)/GCE and 40 - 400 mV/s for AuNP/poly (L-Cys)/GCE. The overlay voltammograms for the reduction of TIN on different modified electrodes at various scan rates are given in (Figure 8.8). A linear relation between the reduction peak current of TIN and square root of scan rate indicates that the process is diffusion controlled.

However the plot of $\log I_p$ against $\log \nu$ suggested a slight variation from diffusional behavior for TIN determination at the surface of both modified electrodes. A slope of 0.64 and 0.7 was observed in the plot with the modified electrodes, rather than the theoretical value of 0.5 expected for a diffusion controlled process. This may be due to the adsorption of the analyte

species on the modified electrode surface and their diffusion through the porous film [228].

According to Laviron theory, the number of electrons involved in the reduction of TIN may be obtained from the plot of E_p against $\ln v$ (Figure 8.9). The corresponding regression equations on poly (L-Cys)/GCE and AuNP/poly (L-Cys)/GCE respectively are as follows:

$$E_p = 34.28 \ln v + 350.45 \quad (R^2 = 0.9976)$$

$$E_p = 32.69 \ln v + 332.19 \quad (R^2 = 0.9905)$$

The slope obtained

$$b = RT / \alpha nF$$

where R is the Universal gas constant, T is the temperature in K, $\alpha = 0.64$ and 0.7 for poly (L-Cys)/GCE and AuNP/poly (L-Cys)/GCE respectively, $F = 96500 \text{ C}$ and n is the number of electrons involved in the reaction. Using the slope obtained for both modifications, the number of electrons involved in the reduction of TIN is calculated to be 2.

8.3.2.5 Interference study

The effect of various foreign species such as ascorbic acid, dextrose, NaCl, urea and metronidazole on the reduction of TIN at these modified electrodes were determined and is given in Table 8.1. One can see that the peak current of TIN varies only slightly (signal change $< 5\%$) for dextrose, NaCl and urea indicating that these chemicals do not interfere with the determination of TIN. A 100 fold excess of metronidazole interfered severely, as it is chemically much similar to TIN and belongs to the class of nitroimidazole. Ascorbic acid also interfered severely.

8.4 Determination of Analytical Figures of Merit

The analytical performance characteristics such as linear range, detection limit and stability under optimized conditions of the developed sensors were assessed for its practical applicability.

8.4.1 Calibration curve for TIN determination

The peak current increased linearly with TIN concentration for both the modified electrodes which may be due to the increased availability of the electroactive species on the electrode surface. Both the electrodes gave linearity in the range $7 \times 10^{-7} \text{ M} - 1 \times 10^{-5} \text{ M}$ (Figure 8.10) with a detection limit of 73 nM and 63 nM for TIN determination on poly (L-Cys)/GCE and AuNP/poly (L-Cys)/GCE respectively. The plot of peak current against concentration of TIN on poly (L-Cys)/GCE and AuNP/poly (L-Cys)/GCE are given in Figure 8.11. This nano level detection limit augment the novelty of the developed sensors for TIN determination in comparison to other reported works (Table 8.2).

8.4.2 Stability of Modified Electrodes

The long term stability of the modified electrodes was evaluated by measuring the current responses at a fixed TIN concentration of $1 \times 10^{-5} \text{ M}$ over a period of two weeks. The electrodes were used daily and stored in distilled water after use. The deviation in current response was less than 5 % which confirmed the long term stability of the fabricated sensors. But as the procedure of electrode preparation is easy and rapid, it is not so important for the electrode to be stable for a prolonged time.

8.5 Proposed Scheme for TIN Reduction

Generally, the reduction of nitroimidazoles is a complex reaction involving the complete reduction of the nitro groups to amines by accepting six electrons [127]. The electro reduction of TIN may be similar to that of metronidazole involving a four electron reduction of nitro group to hydroxylamine [229]. But as the number of electrons involved in TIN reduction is calculated to be two; the mechanism accepted here is the protonation and reduction of nitro group to the corresponding nitroso group [230] as illustrated in Scheme 8.1.

8.6 Analytical Application in Real Samples

8.6.1 Determination of TIN in pharmaceutical dosage form

The applicability of the proposed voltammetric sensor for drug analysis was conducted in TIN tablets (TINIDAL). From the stock solution (procedure as in the earlier section) the required concentrations were prepared by diluting in PBS. SWV for the reduction of TIN in the tablets were recorded and the unknown concentrations determined graphically from the calibration curve. From the replicate measurements, the coefficient of variance was found to be 0.01 for both the methods and the results are tabulated in Table 8.3.

The proposed method was validated with the standard method [231]. The method is based on the measurement of the absorbance of the signal at 368 nm yielded by bathochromic shift during alkaline hydrolysis of TIN in 0.1 N NaOH.

8.6.2 Determination of TIN in spiked urine samples

The feasibility of fabricated sensors for TIN in urine sample was analysed. Various concentration of the drug solution in PBS containing fixed amount of urine sample was prepared. The electrochemical behaviour of drug solution on the modified electrodes was studied by SWV and the unknown concentrations determined from the calibration graph. The recovery percentage is in the range 96 – 105 %.(Table 8.4)

8.7 Conclusions

Merging the unique properties of AuNPs such as high effective surface area and efficient electron tunneling together with the stable matrix of the polymeric material L-Cys on GCE two new sensors for TIN determination have been developed. These modified electrodes have remarkable electrochemical advantages such as excellent stability, linear dynamic range, nano molar detection limit etc. Due to these unique characteristics, the developed sensors have a potential application for TIN determination both in pharmaceutical formulations and spiked urine samples.

Table 8.1 Effect of interferences on the reduction of TIN at various modified electrodes

Interferents (10^{-3}M)	% signal change for 1×10^{-5} M TIN reduction on	
	Poly (L-Cys)/GCE	AuNP / Poly (L-Cys)/GCE
Na^+	2.6	2.4
Cl^-	2.6	2.4
Dextrose	3.2	1.15
Urea	4.7	2.5
Ascorbic acid	6.95	10
Metronidazole	8.8	7.5

Table: 8.2 Comparison of the developed method for TIN determination with the reported works

No:	Method adopted	Lower detection limit (M)
1	Spectrophotometry [204]	2.2×10^{-6}
2	Spectrophotometry [205]	3.0×10^{-6}
3	RP-HPLC [206]	1.2×10^{-6}
4	HPLC [207]	4.05×10^{-5}
5	Capillary Electrophoresis [208]	4.05×10^{-6}
6	Voltammetry [209]	2.7×10^{-8}
7	Voltammetry [210]	5.0×10^{-8}
8	Voltammetry [211]	1.0×10^{-8}
9	Voltammetry [212]	1.0×10^{-8}
10	Voltammetry (<i>present method</i>)	7.3×10^{-8} , 6.3×10^{-8}

Table 8.3 Determination of TIN in pharmaceutical formulations

Method adopted	Declared amount (mg/tablet)	Found amount (mg/tablet)	S.D.	C.V.
Standard method	300 mg	299 mg	2.7	0.01
Poly (L-Cys)/GCE	300 mg	300 mg	3.0	0.01
AuNP / poly (L-Cys) /GCE	300 mg	302 mg	3.2	0.01

Table 8.4 Determination of TIN in urine sample on modified electrodes

Developed sensor For TIN	Amount of TIN added in urine sample (M)	Amount of TIN found in urine sample (M)	Recovery %
	3.00×10^{-6}	3.15×10^{-6}	105.3
Poly (L-Cys)/GCE	5.00×10^{-6}	4.84×10^{-6}	96.8
	7.00×10^{-6}	7.03×10^{-6}	100.4
	2.00×10^{-6}	2.02×10^{-6}	101.0
AuNP/poly (L-Cys)/GCE	4.00×10^{-6}	3.88×10^{-6}	97.0
	9.00×10^{-6}	9.26×10^{-6}	102.8

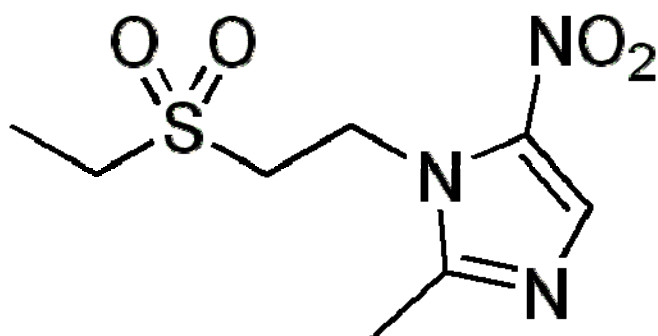


Figure 8.1 Structure of Tinidazole

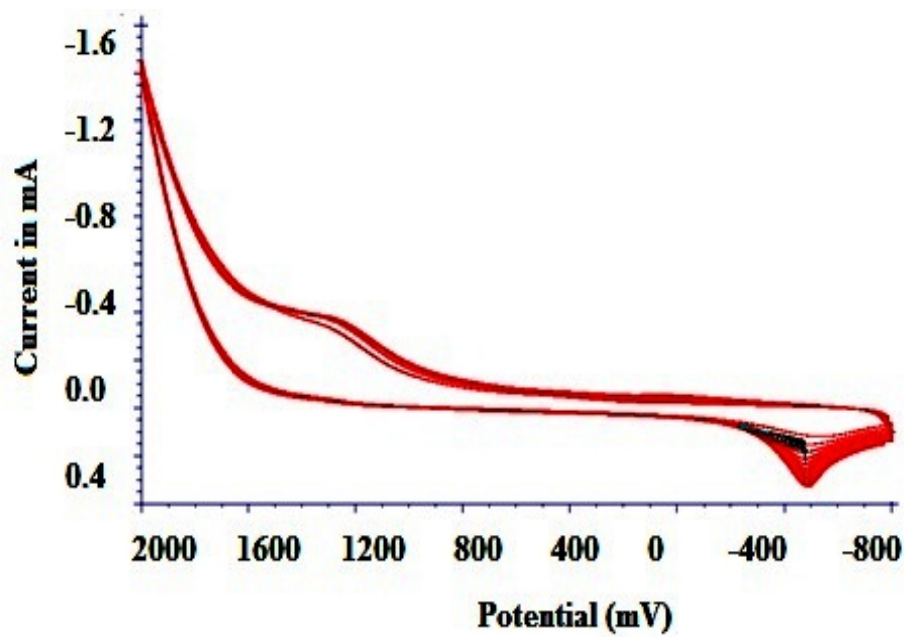


Figure 8.2 Polymerization of L-Cysteine on GCE in 30 segments from 5 mM L-Cys in 0.1 M PBS

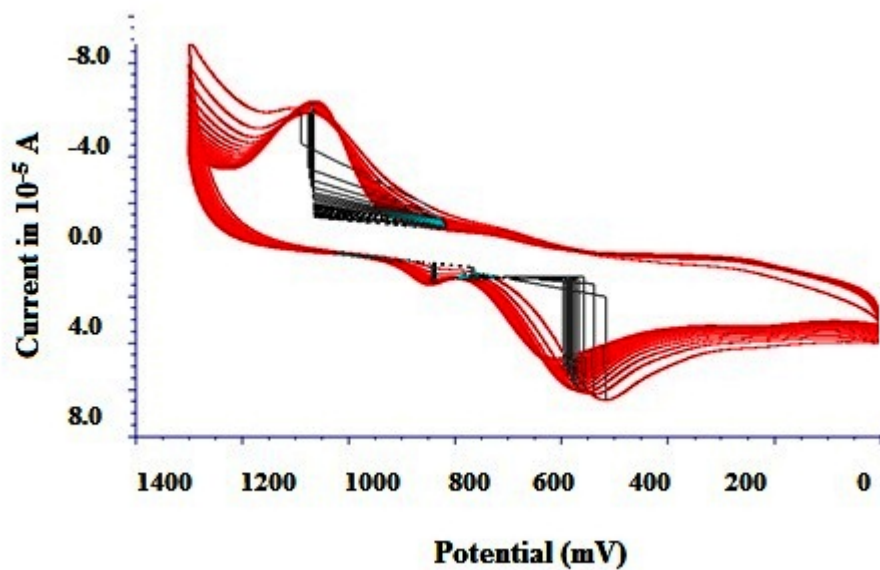
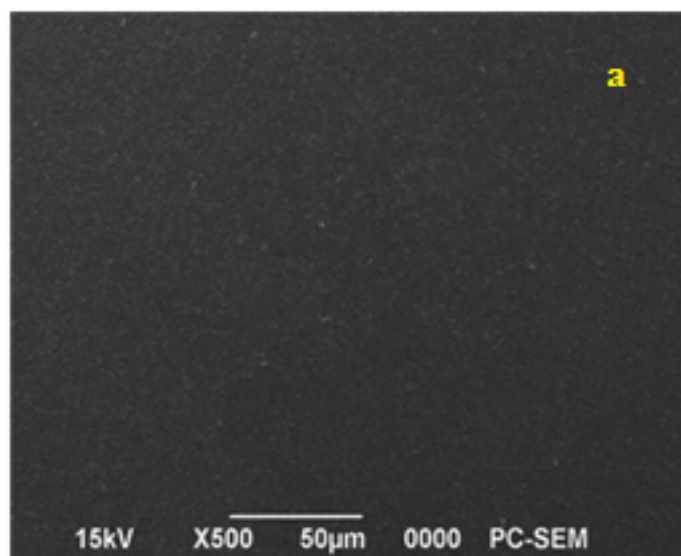


Figure 8.3 Electrodeposition of AuNP on L-Cys/ GCE in 20 cycles



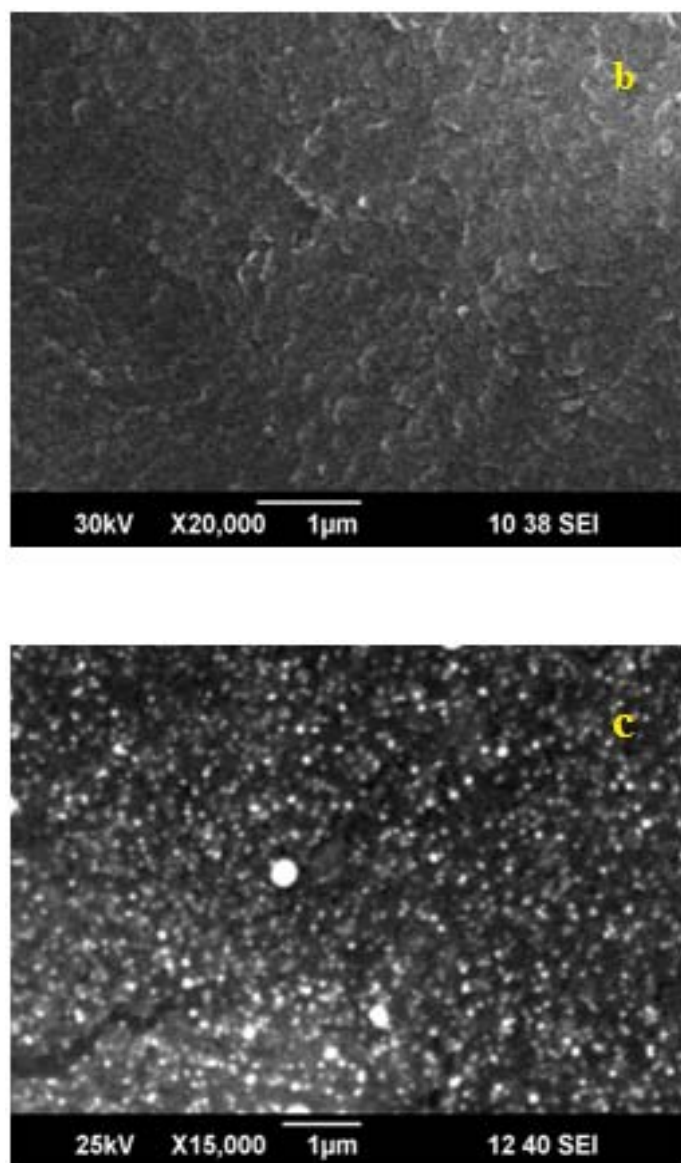
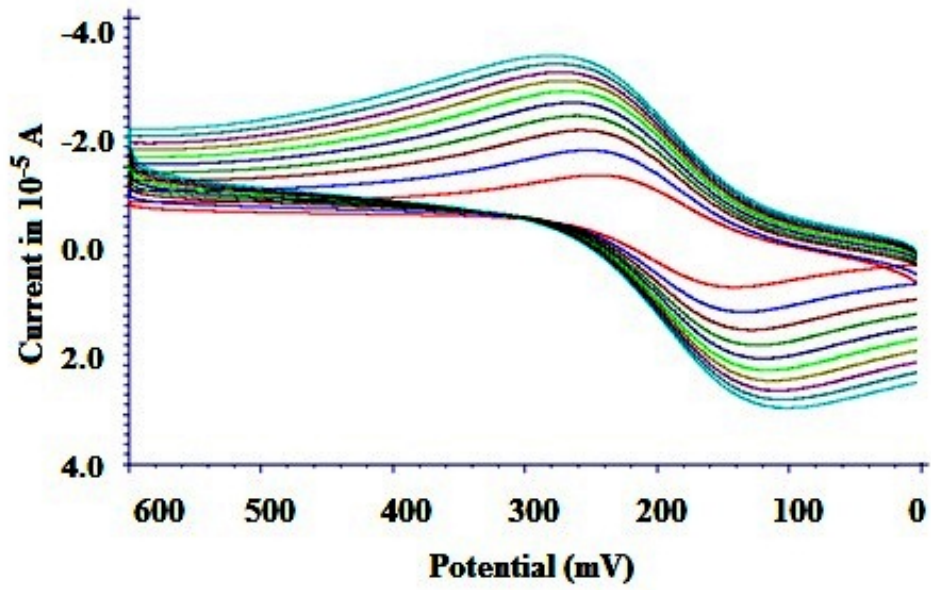
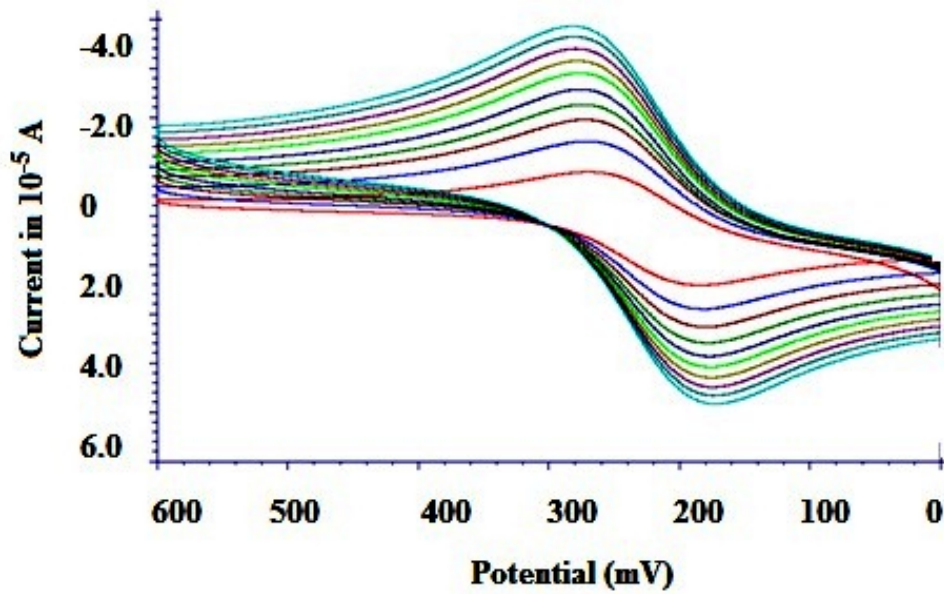


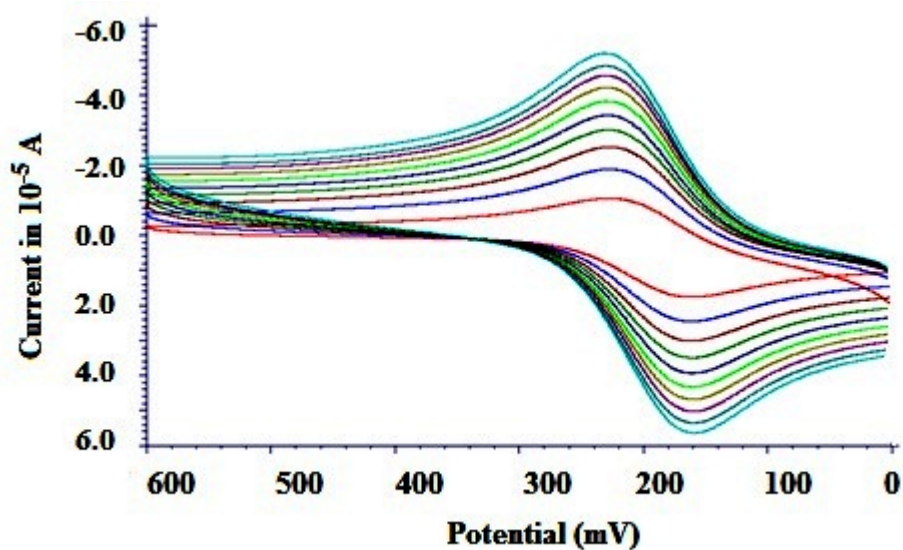
Figure 8.4 SEM images of a) bare GCE b) L-Cys/GCE c) AuNP/L-Cys/GCE



(a)



(b)



(c)

Figure 8.5 CVs of a) Bare GCE b) poly (L-Cys)/GCE c) AuNP/ poly (L-Cys)/GCE in 5 mM $\text{Fe}(\text{CN})_6^{4-/3-}$ at different scan rates

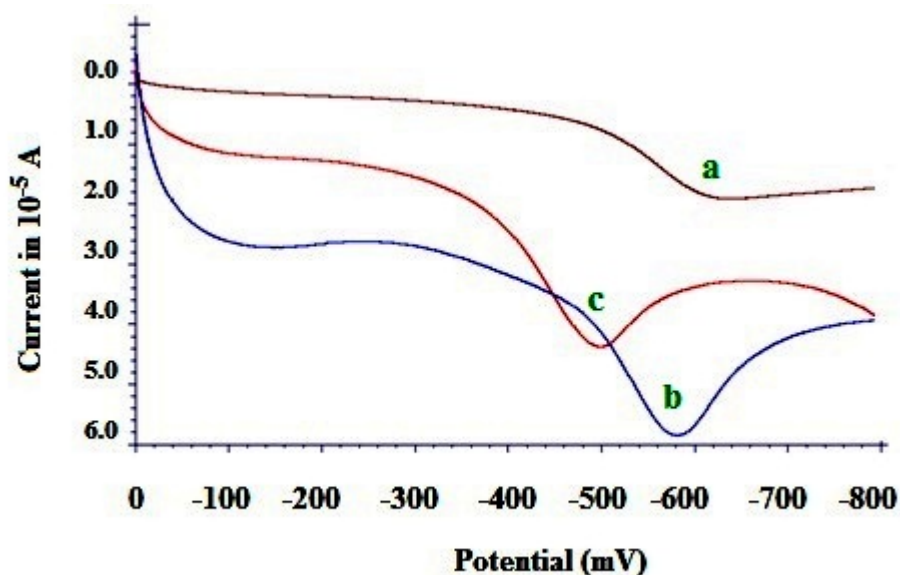


Figure 8.6 Response characteristic of 1×10^{-5} M TIN on a) Bare GCE b) poly (L-Cys)/GCE c) AuNP/ poly (L-Cys)/GCE

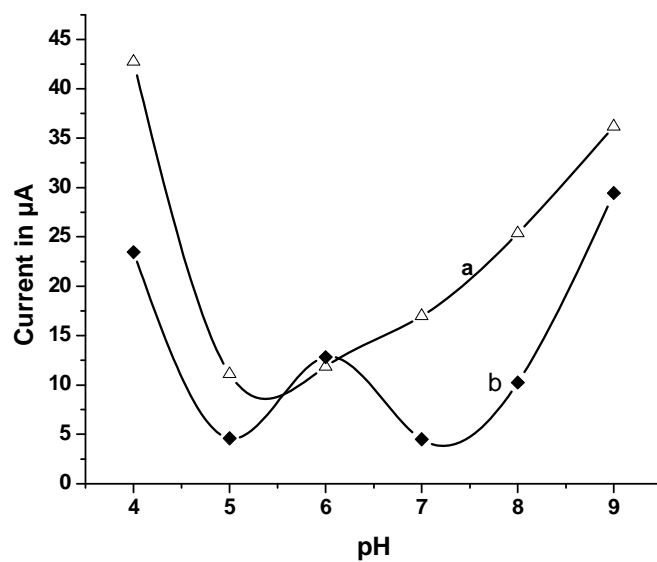
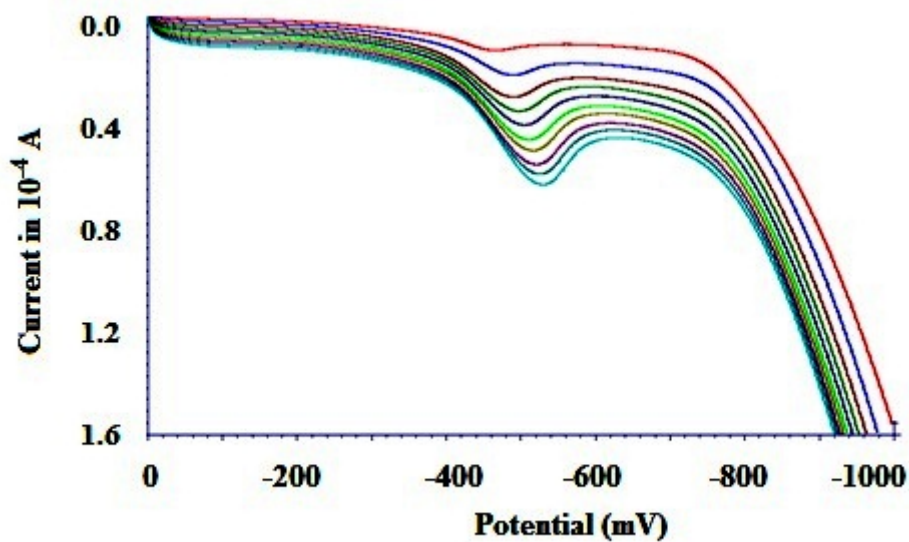
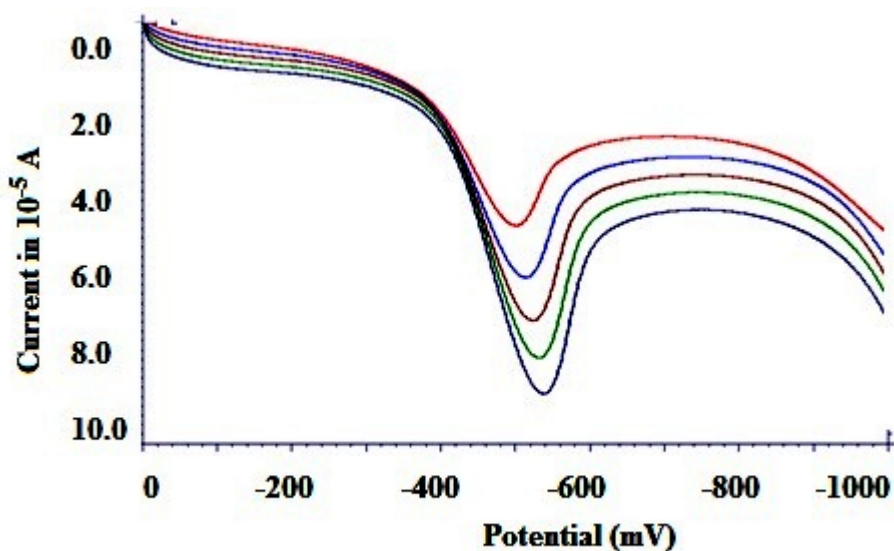


Figure 8.7 pH dependence of TIN reduction on a) poly (L-Cys)/GCE b) AuNP/ poly (L-Cys)/GCE

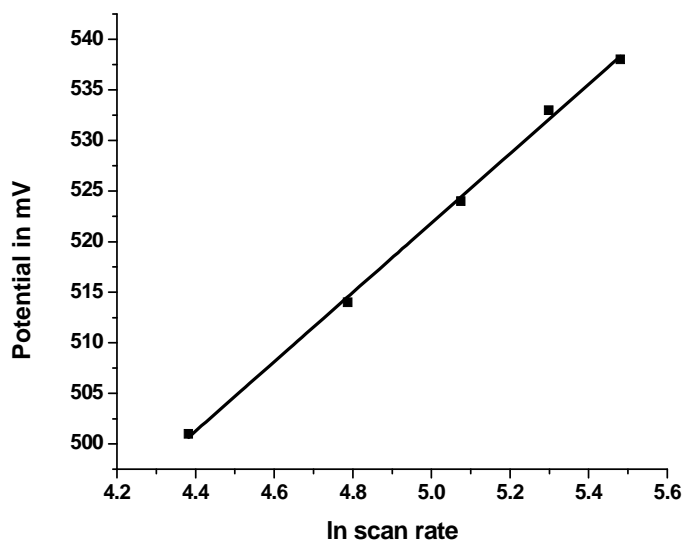


(a)

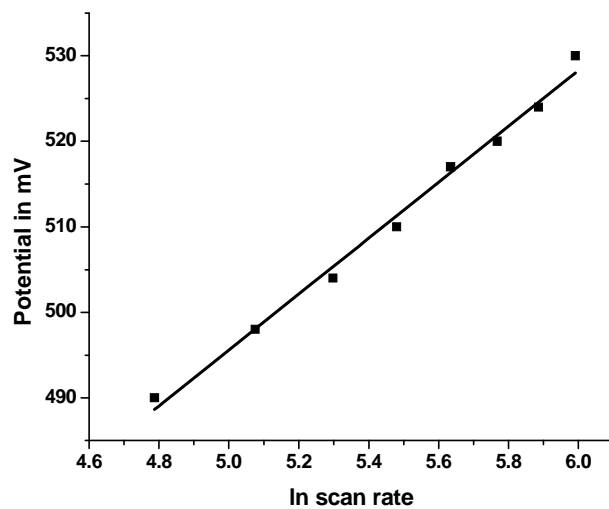


(b)

Figure 8.8 Overlay diagrams for TIN reduction at different scan rates in 0.1 M PBS on a) poly (L-Cys)/GCE b) AuNP/ poly (L-Cys)/GCE

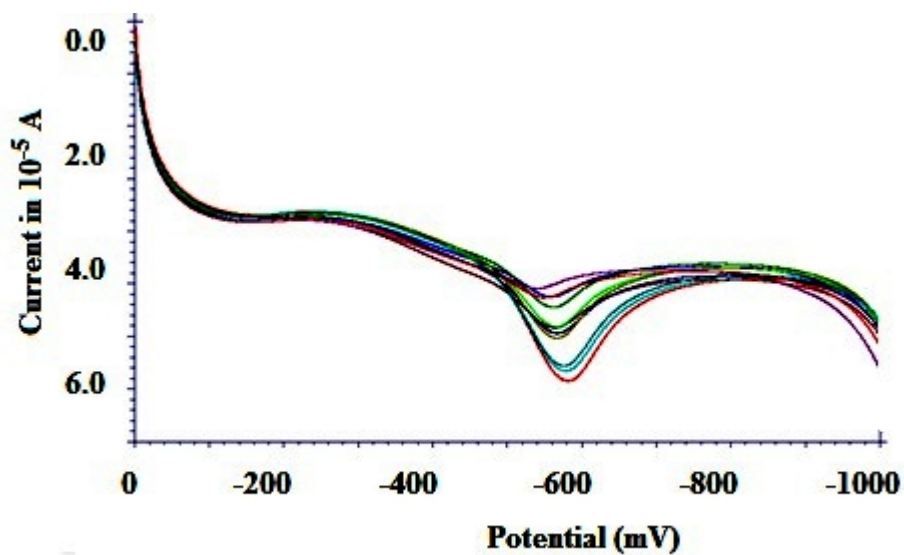


(a)

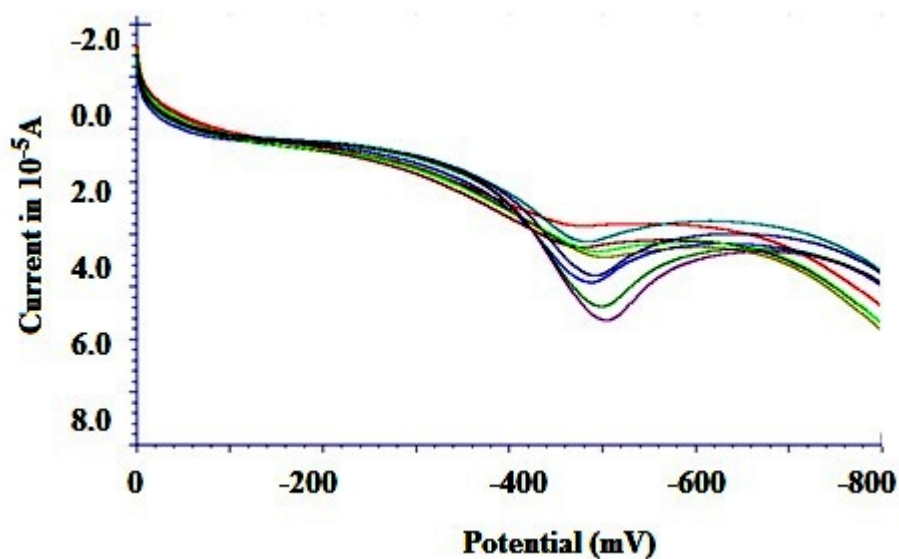


(b)

Figure 8.9 Ep against ln scan rate for TIN reduction on a) poly (L-Cys)/GCE b) AuNP/ poly (L-Cys)/GCE

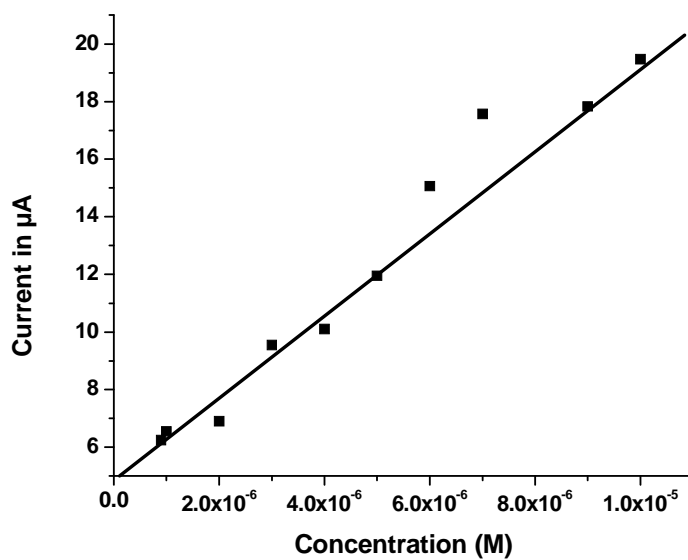


(a)

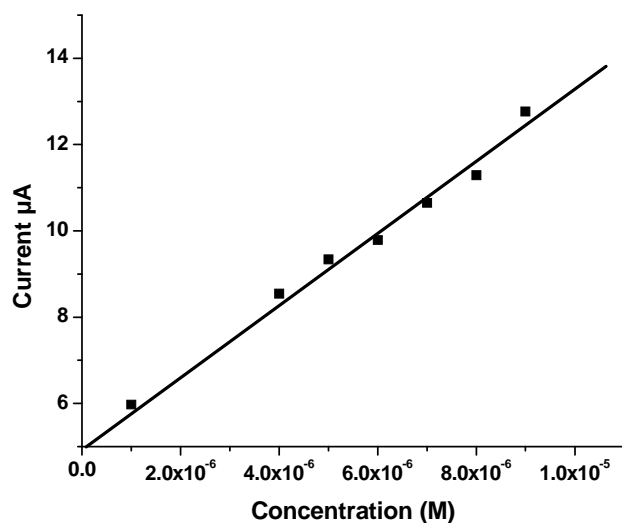


(b)

Figure 8.10 SWV of TIN at different concentrations on a) poly (L-Cys)/GCE b) AuNP/ poly (L-Cys)/GCE

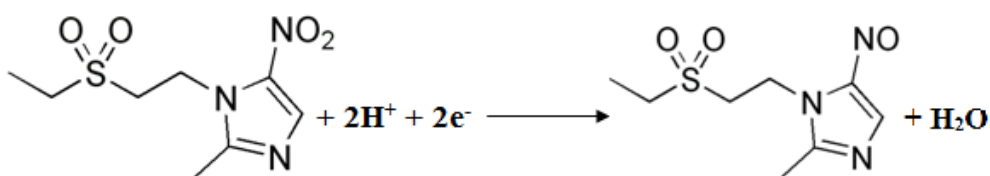


(a)



(b)

Figure 8.11 Calibration curve for TIN on a) poly (L-Cys)/GCE
b) AuNP/ poly (L-Cys)/GCE



Scheme 8.1 Mechanism for Reduction of TIN

SUMMARY AND CONCLUSIONS

9.1	Objectives of the Work
9.2	Summary of the work done
9.3	Conclusions

The objectives of the present work, summary of the findings and conclusions are included in this chapter.

9.1 Objectives of the Work

1. To develop square wave voltammetric sensors based on various modified electrodes for pharmaceutical analysis.
2. Surface characterization of the developed sensors using SEM and electrochemical methods.
3. Optimization of the various performance characteristics of the fabricated sensors.
4. Determination of the lower limit of detection for various analytes on the developed sensors.
5. Predict a plausible mechanism for oxidation/reduction of the analyte species at the electrode surface.

6. Carry out the application studies in spiked urine samples and pharmaceutical formulations.
7. Validate the nobility of the developed sensor with an existing method.

9.2 Summary of the work done

Seven different square wave voltammetric sensors were developed based on chemically modified electrodes. The analytes and sensors with their salient features are compiled in table 9.1.

Table 9.1 Summary of the work done

Analyte	Sensor developed	Supporting electrolyte used	Limit of detection
Metronidazole benzoate	poly(p-TSA)/GCE	0.1 M PBS	6.5×10^{-7} M
PAM chloride	MWCNT/GE	0.1 M PBS	7.8×10^{-8} M
	MWCNT/PB/GE		1.6×10^{-8} M
Guaifenesin	MWCNT/PtE	0.1 M H ₂ SO ₄	1.34×10^{-6} M
Tamsulosin hydrochloride	poly(o-PDA)/GE	0.1 M ABS	7.4×10^{-8} M
Tinidazole	poly(L-Cys)/GCE	0.1 M PBS	7.3×10^{-8} M
	poly(L-Cys)/AuNP/GCE		6.3×10^{-8} M

9.3 Conclusions

Pharmaceutical analysis by electrochemical techniques is quite a promising field as the analysis can be done by simple techniques which are highly sensitive and selective. Nanomolar limit of detection with microelectrodes makes them an excellent platform suitable for drug analysis. The advances in material science further augment the field of electrochemistry for various analysis.

The main focus of the thesis is to fabricate square wave voltammetric sensors for various pharmacologically important drugs and their application in real samples. Both active (Glassy carbon) and inert (Platinum and Gold) electrodes were used as a probe for the present investigations. The efficiency of these electrodes as a Sensor for pharmaceutical analysis can be boosted by modifying its surface chemically with conducting polymers, nanotubes etc using drop casting method or electropolymerisation. This will definitely contribute to Chemically Modified Electrodes in the field of Electrochemical Sensor technology.

Application studies conducted with the developed sensors in real samples open up the possibility of commercializing them. The efficiency of the analytical methods based on these sensors are comparable with the existing standard pharmacopeia methods and are mostly superior to other techniques in terms of detection limit. Hence the analysis of important drugs using a disposable electrode may be expected in the near future.



References

1. R. Greef, R. Peat, L. M. Peter, D. Pletcher, J. Robinson, *Instrumental Methods in Electrochemistry*, John Wiley & Sons, New York, 150 (1985).
2. O. Stern, *Z. Elektrochem.*, **30**, 508 (1924).
3. W. Göpel, T. A. Jones, M. Kleitz, I. Lundström, T. Seiyama, Wiley, *Sensors: A Comprehensive Survey, Chemical and Biochemical Sensors*, **3**, 820 (2008).
4. A. C. Power, A. Morrin, *Electrochemistry: Electroanalytical Sensor Technology*, InTech, 147 (2013).
5. J. Osteryoung, J. J. Odea, *Electroanalytical Chemistry*, (Ed: A. J. Bard), Marcel Dekker, New York, **14**, 209 (1986).
6. G. N. Eccles, *Crit. Rev. Anal. Chem.*, **22**, 345 (1991).
7. M. Lovric', "Square-wave voltammetry", in *Electroanalytical Methods* (Ed: F. Scholz) Springer, Berlin 111 (2002).
8. N. Mirceski, R. Gulaboski, M. Lovric, I. Bogeski, R. Kappl, M. Hoth, *Electroanalysis*, **25**, 2411 (2013).
9. V. Mirceski, R. Gulaboski, *Maced. J. Chem. Chem. Eng.*, **13**, 1 (2014).
10. G. C. Barker, *Congress on Analytical Chemistry in Industry*, St. Andrews, 199 (1957).

11. F. Scholz, *Electroanalytical Methods: Guide to Experiments and Applications*, 2nd revised and extended edition, Springer, 130 (2010).
12. J. G. Osteryoung, R. A. Osteryoung, *Anal. Chem.*, **57**, 101 A (1985).
13. R. Gulaboski, V. Mirceski, I. Bogeski, M. Hoth, *J. Solid State Electrochem.*, **16**, 2315 (2012).
14. S. Kumar, V. Vicente-Beckett, *Beilstein J. Nanotech.*, **3**, 388 (2012).
15. M. A. El Mhammedi, M. Bakasse, R. Bachirat, A. Chtaini, *Food Chem.*, **110**, 1001 (2008).
16. M. Amare, S. Admassie, *Talanta*, **93**, 122 (2012).
17. J. H. Luo, X. X. Jiao, N. B. Li, H. Q. Luo, *J. Electroanal. Chem.*, **689**, 130 (2013).
18. J. A. Ardila, G. G. Oliveira, R. A. Medeiros, O. Fatibello-Filho, *J. Electroanal. Chem.*, **690**, 32 (2013).
19. B. Dogan – Topal, S. A. Ozkan, B. Uslu, *The Open Chemical and Biochemical Methods Journal*, **3**, 56 (2010).
20. X. Tian, C. Cheng, H. Yuan, J. Du, D. Xiao, S. Xie, M. M. F. Choi, *Talanta*, **93**, 79 (2012).
21. L. Wang, H. Chen, X. Huang, J. Nan, *Electroanalysis*, **21**, 755 (2009).
22. X. Huang, L. Wang, S. Liao, *Anal. Chem.*, **80**, 5666 (2008).

References

23. X. Xiao, G. Zhu, L. Liao, B. Liu, Y. Yuan, Y. Wang, J. He, B. He, Y. Wu, *Electrochim. Acta*, **74**, 105 (2012).
24. F. A. Armstrong, "Voltammetry of Proteins", in *Encyclopedia of Electrochemistry*, (Eds: A. J. Bard, M. Stratmann, G. S. Wilson), Wiley VCH, Weinheim, **9**, 33 (2002).
25. F. J. Miller, H. E. Zittel, *Anal. Chem.*, **35**, 1866 (1963).
26. P. R. Moses, L. Wier, R. W. Murray, *Anal. Chem.*, **47**, 1882 (1975).
27. *Pure & Appl. Chem.*, **69**, 1317 (1997).
28. P. Kissinger, W. R. Heineman, *Laboratory Techniques in Electroanalytical Chemistry*, IInd Edition, CRC Press, **405**, 412 (1996).
29. A. K. Bakshi, G. Bhalla, *J. Sci. Ind. Res.*, **63**, 715 (2004).
30. C. K. Chiang, M. D. Drug, S. C. Gan, A. J. Hegger, E. J. Lewis, A. G. Mac Diarmid, Y. W. Park, H. Shirakawa, *J. Am. Chem. Soc.*, **100**, 1013 (1978).
31. J. H. Chen, J. Zhang, Q. Zhuang, S. B. Zhang, X.H. Lin, J. Chen, J. Zhang, Q. Zhuang, S. Zhang, X. Lin, *Talanta*, **72**, 1805 (2007).
32. G.Y. Jin, Y. Z. Zhang, W. X. Cheng, *Sens. Actuat. B*, **107**, 528 (2005).
33. P. Kalimuthu, S. Abraham John, *Bioelectrochemistry*, **77**, 13 (2009).
34. S. Iijima, *Nature*, **354**, 56 (1991).

35. K. S. Novoselov, A. K. Geim, S. V. Morozov, D. Jiang, Y. Zhang, S. V. Dubonos, I. V. Grigorieva, A. A. Firsov, *Science*, **306**, 666 (2004).
36. K. Anazawa, K. Shimotani, C. Manabe, H. Watanabe, M. Shimizu, *Applied Physics Letters*, **81**, 739 (2002).
37. T. Guo, P. Nikolaev, A. Thess, D. T. Colbert, R. E. Smalley, *Chem. Phys. Lett.*, **243**, 49 (1995).
38. L. Vander Wal Randall, J. Hall Lee, M. Berger Gordon, *J. Phys. Chem. B*, **106**, 3564 (2002).
39. L. Vander Wal Randall, M. Ticich, B. Thomas, *J. Phys. Chem. B*, **105**, 10249 (2001).
40. P. C. Ma, J-K Kim, B. Z. Tang, *Carbon*, **44**, 3232 (2006).
41. R. Hirlekar, M. Yamagar, H. Garse, M. Vij, V. Kadam, *Asian J. Pharm. Clin. Res.*, **2**, 17 (2009).
42. J-P Tessonier, D. S. Su, *Chem. Sus. Chem.*, **4**, 824 (2011).
43. T. Yamaguchi, S. Bandow, S. Iijima, *Chem. Phys. Lett.*, **389**, 181 (2004).
44. A. A. Karyakin, E. E. Karyakina, *Russ. Chem. Bull.*, **50**, 1811 (2001).
45. K. Itaya, H. Akahoshi, S. Toshima, *J. Electrochem. Soc.*, **129**, 1498 (1982).

References

46. X. Wu, M. Cao, C. Hu, X. He, *Crystal Growth and Design*, **6**, 26 (2006).
47. B. Haghghi, S. Varma, F. M. Alizadeh Sh, Y. Yigzaw, L. Gorton, *Talanta*, **64**, 3 (2004).
48. N. F. Zakharehuk, B. Meyer, H. Henning, F. Scholz, A. Jaworksi, Z. Stojek, *J. Electroanal. Chem.*, **398**, 23 (1995).
49. Z. Fen – Fen, W. Xia – Qin, M. Xiao – Yun, G. Xiao – Ming, Z. Zong – Rang, *Acta. Phys. Chim. Sin.*, **17**, 788 (2001).
50. R. Yang, Z. Qian, J. Deng, *J. Electrochem. Soc.*, **145**, 2231 (1998).
51. V. D. Neff, *J. Electrochem. Soc.*, **125**, 886 (1978).
52. R. Vittal, K. J. Kim, H. Gomathi, V. Yegnaraman, *J. Phys. Chem. B*, **112**, 149 (2008).
53. N. Zhang, G. Wang, A. Gu, Y. Feng, B. Fang, *Microchim. Acta*, **168**, 129 (2010).
54. A. M. Gurban, T. Noguer, C. Bala, L. Rotariu, *Sensor. Actuat. B - Chem.*, **128**, 536 (2008).
55. F. Ricci, G. Palleschi, *Biosens. Bioelectron.*, **21**, 389 (2005).
56. A. M. Farah, F. T. Thema, E. D. Dikio, *Int. J. Electrochem. Sci.*, **7**, 5069 (2012).
57. T. R. L. C. Paixao, M. Bertotti, *Sensor. Actuat. B - Chem.*, **137**, 266 (2009).

58. M. F. de Oliveira, R. J. Mortimer, N. R. Stradiotto, *Microchem. J.*, **64**, 155 (2000).
59. S. S. Kumar, J. Joseph, K. L. Phani, *Chem. Mater.*, **19**, 4722 (2007).
60. J. Kulys, R. Stupak, *The Open Nanoscience Journal*, **2**, 34 (2008).
61. M. Faraday, *Philos. Trans. R. Soc., London*, **147**, 145 (1857).
62. A. Bonanni, M. Pumera, Y. Miyahara, *Phys. Chem. Chem. Phys.*, **13**, 4980 (2011).
63. R. A. Reynolds, C. A. Mirkin, R. L. Letsinger, *J. Am. Chem. Soc.*, **122**, 3795 (2000).
64. A. Ambrosi, F. Airo, A. Merkoci, *Anal. Chem.*, **82**, 1151 (2010).
65. A. Ambrosi, M. T. Castañeda, A. J. Killard, M. R. Smyth, S. Alegret, A. Merkoçi, *Anal. Chem.*, **79**, 5232 (2007).
66. M. Ozsoz, A. Erdem, D. Ozkan, P. Kara, H. Karadeniz, B. Meric, K. Kerman, S. Girousi, *Bioelectrochemistry*, **67**, 199 (2005).
67. J. Turkevich, P. C. Stevenson, J. Hillier, *J. Phys. Chem.*, **57**, 670 (1953).
68. Y. Sun, Y. Xia, *Science*, **298**, 2176 (2002).
69. G. G. Wildgoose, C. E. Banks, R. G. Compton, *Small*, **2**, 182 (2006).
70. U. S. Mohanty, *J. Appl. Electrochem.*, **41**, 257 (2011).
71. W. Cai, T. Gao, H. Hong, J. Sun, *Nanotechnol. Sci. Appl.*, **1**, 17 (2008).

References

72. C. Wang, F. Wang, C – Y. Li, S. Hu, *Microchim. Acta*, **154**, 275 (2006).
73. Y. Li, L. Zou, G. Song, K. Li, B. Ye, *J. Electroanal. Chem.*, **709**, 1 (2013).
74. H-S Wang, T – H Li, W-L Jia, H-Y Xu, *Biosens. Bioelectron.*, **22**, 664 (2006).
75. D. D. Santos, M. F. Bergamini, M. V. B. Zanoni, *Sensor. Actuat. B-Chem.*, **133**, 398 (2008).
76. P. Gupta, R. N. Goyal, *Electrochim. Acta*, **151**, 1 (2015).
77. Y. Ya, D. Luo, G. Zhan, C. Li, *Bull. Korean Chem. Soc.*, **29**, 928 (2008).
78. S. Kozlovskaja, G. Baltrunas, A. Malinauskas, *Microchim. Acta*, **166**, 229 (2009).
79. I. Biryol, B. Uslu, Z. Kucukyavuz, *J. Pharm. Biomed. Anal.*, **15**, 371 (1996).
80. H. Ghadini, R. M. A. Tehrani, A. S. Mohamed Ali, N. Mohamed, S. Ab Ghani, *Anal. Chim. Acta*, **765**, 70 (2013).
81. S. Issac, K. Girish Kumar, *Anal. Methods*, **2**, 1484 (2010).
82. F. Zhang, S. Gua, Y. Dinga, Z. Zhang, L. Li, *Anal. Chim. Acta*, **770**, 53 (2013).
83. R. Ojani, J. Raoof, S. Zamani, *Talanta*, **81**, 1522 (2010).

84. P. Xiao, W. Wu, J. Yu, F. Zhao, *Int. J. Electrochem. Sci.*, **2**, 149 (2007).
85. V. K. Gupta, A. K. Jain, S. K. Shoorra, *Electrochim. Acta*, **93**, 248 (2013).
86. C. Wang, X. Shao, Q. Liu, Q. Qu, G. Yang, X. Hu, *J. Pharm. Biomed. Anal.*, **42**, 237 (2006).
87. Z. Z. Stoiljkovic, M. L. Avramov Ivic, S. D. Petrovic, D. Z. Mijin, S. I. Stevanovic, U. C. Lacnjevac, A. D. Marinkovic, *Int. J. Electrochem. Sci.*, **7**, 2228 (2012).
88. T. A. Silva, H. Zanin, F. C. Vicentini, E. J. Corat, O. Fatibello – Filho, *Analyst*, **139**, 2832 (2014).
89. B. Dogan – Topal, B. Bozal – Palabiyik, B. Uslu, S. A. Ozkan, *Sensor. Actuat. B - Chem.*, **177**, 841 (2013).
90. A. Veiga, A. Dordio, A. J. Palace Carvalho, D. M. Teixeira, J. G. Teixeira, *Anal. Chim. Acta*, **674**, 182 (2010).
91. Y. Liu, L. Xu, *Sensors*, **7**, 2446 (2007).
92. Y. Yao, X. Bai, K. K. Shiu, *Nanomaterials*, **2**, 428 (2012).
93. L. Lonappan, Ph.D. Thesis: *Voltammetric Sensors for the Determination of Pharmaceuticals*, CUSAT, 109 (2013).
94. B. J. Sanghavi, P. K. Kalamate, S. P. Karna, A. K. Srivastava, *Talanta*, **120**, 1 (2014).

References

95. J. Zhou, Y. Xu, L. Wang, J. Liu, Y. Li, B. Ye, *J. Chinese Chem. Soc.*, **59**, 879 (2012).
96. H. M. Ahmed, M. A. Mohamed, W. M. Salem, *Anal. Methods*, **7**, 581, (2015).
97. A. Veiga, A. Dordio, A. J. Palace Carvalho, D. M. Teixeira, J. G. Teixeira, *Anal. Chim. Acta*, **674**, 182 (2010).
98. N. F. Atta, A. Galal, S. M. Azab, *Electroanalysis*, **24**, 1431 (2012).
99. M. Shamsipur, R. Saber, M. Emami, *Anal. Methods*, **6**, 7038 (2014).
100. E. Arkan, Z. Karimi, M. Shamsipur, R. Saber, *Anal. Sci.*, **29**, 855 (2013).
101. E. Honarmand, M. H. Motaghedifarda, M. Ghamarib, *RSC Adv.*, **4**, 35511 (2014).
102. L. Rajith, A. K. Jissy, K. Girish Kumar, A. Datta, *J. Phys. Chem. C*, **115**, 21858 (2011).
103. R. Joseph, K. Girish Kumar, *Anal. Sci*, **27**, 67 (2011).
104. D. Thomas, L. Lonappan, L. Rajith, S. T. Cyriac, K. Girish Kumar, *J. Fluores.*, **23**, 473 (2013).
105. A. E. Vikraman, D. Thomas, S. T. Cyriac, K. Girish Kumar, *J. Electrochem. Soc.*, **161**, B305 (2014).
106. Z. Rasheed, A. E. Vikraman, D. Thomas, J. S. Jagan, K. Girish Kumar, *Food Anal. Methods*, **8**, 213 (2015).

107. A. Thomas, D. Thomas, A. E. Vikraman, K. Girish Kumar, *Food Anal. Methods*, (2015 - in press).
108. J.A. Alden, A.M. Bond, R. Colton, R.G. Compton, J. C. Eklund, Y. A. Mah, P. J. Mahon, V. Tedesco, *J. Electroanal. Chem*, **447**, 155 (1998).
109. C. P. Smith, H. S. White, *Anal. Chem.*, **65**, 3343 (1993).
110. C. Amatore, M. R. Deakin, R. Wightman, *J. Electroanal. Chem.*, **225**, 49 (1987).
111. A. J. Bard, L. R. Faulkner, *Electrochemical Methods, Fundamentals and Applications*, 2nd ed., John Wiley & Sons Inc., Hoboken, NJ, 613 (2001).
112. F. G. Cottrell, *Z. Phys. Chem.*, **42**, 385 (1903).
113. P. Speelman, *Antimicrob. Agents Chemother.*, **27**, 227 (1985).
114. M. La-Scalea, S. Serrano, E. Ferreira, A. Oliveira Brett, *J. Pharm. Biomed. Anal.*, **29**, 561 (2002).
115. Y. Lin, Y. Su, X. Liao, N. Yang, X. Yang, M. M. F. Choi, *Talanta*, **88**, 646 (2012).
116. H. M. Maher, R. M. Youssef, *Chromatographia*, **69**, 345 (2009).
117. A. A. Salem, H. A. Mossa, *Talanta*, **88**, 104 (2012).
118. O. I. Zheltvai, I. I. Zheltvai, V. V. Spinul, V. P. Antonovich, *J. Anal. Chem.*, **68**, 600 (2013).

References

119. Y. Gu, W. Liu, R. Chen, L. Zhang, Z. Zhang, *Electroanalysis*, **25**, 1209 (2013).
120. S. Lu, K. Wu, X. Dang, S. Hu, *Talanta*, **63**, 653 (2004).
121. R. Joseph, K. Girish Kumar, *Anal. Lett.*, **42**, 2309 (2010).
122. J. Peng, C. Hou, X. Hu, *Sensor. Actuat. B - Chem.*, **169**, 81 (2012).
123. A. M. O. Brett, S. H. P. Sherrano, I. G. R. Gutz, M. A. La-Scalea, *Electroanalysis*, **9**, 110 (1997).
124. P. F. Huang, L. Wang, J. Y. Bai, H. J. Wang, Y. Q. Zhao, S. D. Fan, *Microchim. Acta*, **157**, 41 (2007).
125. C. Nabais, R. P. S. Fartaria, F. M. S. S. Fernandes, L. M. Abrantes, *Int. J. Quantum Chem.*, **99**, 11 (2004).
126. D. Dumanovic, J. Jovanovic, D. Suznjevic, M. Erceg, P. Zuman, *Electroanalysis*, **4**, 795 (1992).
127. D. Dumanovic, J. Ciric, *Talanta*, **20**, 525 (1973).
128. P. Zuman, Z. Fijalek, D. Dumanovic, D. Suznjevic, *Electroanalysis*, **4**, 783 (1992).
129. Sindhu Issac, Ph.D. Thesis: *Fabrication of Electrochemical Sensors for Various Pharmaceuticals*, CUSAT, 137 (2011).
130. European Pharmacopeia, European Directorate for the Quality of Medicines & Healthcare, Strasbourg, France :5th Edition, (2004).

131. S. S. Simoes, E. P. Medeiros, E. N. Gaiao, W. S. Lyra, P. N. T. Moreira, M. C. U. Araujo, E. C. Silva, V. B. Nascimento, *J. Braz. Chem. Soc.*, **17**, 609 (2006).
132. K. Farhadi, S. Bahar, *J. Chin. Chem. Soc.*, **54**, 1521 (2007).
133. K. Siddappa, M. Mallikarjun, P. T. Reddy, M. Tambe, *Eclet. Quim.*, **33**, 41 (2008).
134. D. K. Bempong, R. G. Manning, T. Mirza, L. Bhattacharya, *J. Pharm. Biomed. Anal.*, **38**, 776 (2005).
135. S. Ashour, N. Kattan, *Int. J. Biomed. Sci.*, **6**, 13 (2010).
136. A. M. Frasey, A. B. Grand, M. P. Pouget, B. Vennat, C. Lartigue, M. J. Galmier, *Microchim. Acta*, **144**, 171 (2004).
137. E. Roy, S. Maity, S. Patra, R. Madhuri, P. K. Sharma, *RSC Adv.*, **4**, 32281 (2014).
138. K. Karljickovic Rajic , B. Stankovic, A. Granov , *J. Pharm. Biomed. Anal.*, **8**, 735 (1990).
139. H. Kalasz , E. Szoko, T. Tabi , G. A. Petroianu, D. E. Lorke, A. Omar, S. Alaffi, A. Jasem, K. Tekes, *Med. Chem.*, **5**, 237 (2009).
140. M. Bodioga, D. Agbaba, D. Zivanov-Stakic, R. Popovic, *J. Pharm. Biomed. Anal.*, **12**, 127 (1994).
141. H. John, M. Eddleston, R. Eddie Clutton, F. Worek, H. Thiermann, *Drug Test. Anal.*, **4**, 169 (2012).

References

142. Z. Koricanac, B. Stankovic, Z. Binenfeld, *Vojnosanit Pregl.*, **40**, 168 (1983).
143. S. Issac, K. Girish Kumar, *Anal. Methods*, **2**, 1484 (2012).
144. L. Lonappan, K. Girish Kumar, *Sensor Lett.*, **9**, 541 (2011).
145. R. Joseph Ph.D. Thesis: *Development of Electrochemical Sensors for Various Pharmaceuticals*, CUSAT 117 (2012).
146. Z. Li, J. Chen, W. Li, K. Chen, L. Nie, S. Yao, *J. Electroanal. Chem.*, **603**, 59 (2007).
147. A. M. Farah, N. D. Shooto, F. T. Thema, J. S. Modise, E. D. Dikio, *Int. J. Electrochem. Sci.*, **7**, 4302 (2012).
148. K. Itaya, N. Shoji, I. Uchida, *J. Am. Chem. Soc.*, **106**, 3423 (1984).
149. K. Honda, J. Ochiai, H. Hayashi, *Chem. Commun.*, **2**, 168 (1986).
150. K. Itaya, H. Akahoshi, S. Toshima, *J. Electrochem. Soc.*, **129**, 1498 (1982).
151. C. Cai, H. Ju, H. Chen, *J. Electroanal. Chem.*, **397**, 185 (1995).
152. A. A. Karyakin, *Electroanalysis*, **13**, 813 (2001).
153. A. Abbaspour, M. A. Kamyabi, *J. Electroanal. Chem.*, **584**, 117 (2005).
154. M. Valearcel, S. Cardenas , B. M. Simonet, *Anal. Chem.*, **79**, 4788 (2007).

155. V. A. Petrosyan, M. E. Niyazymbetov, V. Ulyanova, *Russ. Chem. Bull.*, **39**, 546 (1990).
156. H. Luo, Z. Shi, Z. Gu, Q. Zhuang, *Anal. Chem.*, **73**, 915 (2001).
157. Pharmacopoeia of India, 3rd edition, Controller of Publications, Government of India, Delhi, 407, (1985).
158. V. Z. Shahabadi, M. Shamsipur, B. Hemmatenejad, M. Akhond, *Anal. Lett.*, **43**, 687 (2010).
159. O. Abdallah, *Int. J. Anal. Chem.*, **10**, 5 (2010).
160. A. R. Lee, T. M. Hu, *J. Pharm. Biomed. Anal.*, **12**, 747 (1994).
161. N. B. Pappano, Y. C. D. Micalizzi, N. B. Debbatista, F. H. Ferretti, *Talanta*, **44**, 633 (1997).
162. J. B. Aluri, S. Stavchansky, *J. Pharm. Biomed. Anal.*, **11**, 803 (1993).
163. M. L. Wilcox, J. T. Stewart, *J. Pharm. Biomed. Anal.*, **23**, 909 (2000).
164. R. Pomponio, R. Gotti, M. Hudaib, V. Andrisano, V. Cavrini, *J. Sep. Sci.*, **24**, 258 (2001).
165. I. Tapsoba, J. E. Belgaie, K. Boujlel, *J. Pharm. Biomed. Anal.*, **38**, 162 (2005).
166. Y. J. Kim, T. S. Shin, H. D. Choi, J. H. Kwon, Y. C. Chung, H. G. Yoon, *Carbon*, **43**, 23 (2005).
167. D. Tasis, N. Tagmatarchis, V. Georgakilas, M. Prato, *Chem. Eur. J.*, **9**, 4000 (2003).

References

168. J. Wang, M. Mustaf, L. Yuehe, *J. Am. Chem. Soc.*, **125**, 2408 (2003).
169. Y. Suling, Y. Ran, L. Gang , Q. Lingbo, L. Jianjun, Y. Lanlan, *J. Electroanal. Chem.*, **639**, 77 (2010).
170. B. Sljukić, C. E. Banks, R. G. Compton, *Nano Lett.*, **6**, 1556 (2006).
171. M. Valearcel, S. Cardenas , B. M. Simonet, *Anal. Chem.*, **79**, 4788 (2007).
172. M. B. Gholivand, A. Azadbakht, A. Pashabadia, *Electroanalysis*, **23**, 2771 (2011).
173. H. G. Brittain, *Analytical Profiles of Drug Substances and Excipients*, **25**, 153 (1998).
174. R. Upreti, N. Z. M. Homer, G. Naredo, D. F. Cobice, K. A. Hughes, L. H. Stewart, B. R. Walker, R. Andrew, *J. Chromatogr. B*, **930**, 121 (2013).
175. L. Ding, L. Li, P. Tao, J. Yang, Z. Zhang, *J. Chromatogr. B*, **767**, 75 (2002).
176. Y. Soeishi, M. Kobori, S. I. Kobayashi, S. Higuchi, *J. Chromatogr. B*, **533**, 291 (1990).
177. S. Yamada, C. Tanaka, M. Suzuki, T. Ohkura, R. Kimura, K. Kawabe, *J. Pharm. Biomed. Anal.*, **14**, 289 (1996).
178. A. Karasakal, S. T. Ulu, *Luminescence*, **29**, 239 (2014).
179. D. B. Patel, N. U. Patel, *Int. J. Chem. Tech. Res.*, **2**, 646 (2010).

180. J.G. Chandorkar, V. B. Kotwal, N. S. Dhande, S. G. Gurav, V.V. Pande, P.V. Yadav, *Pak. J. Pharm. Sci.*, **21**, 307 (2008).
181. M. K. Thimmaraju, V. Rao, K. Hemanth, P. Siddartha Kumar, *JAPS*, **8**, 177 (2011).
182. M. Nasare, J. Satish, A. Manikanta Kumar, V. V. L. N. Prasad, M. Sanayaima Huidrom, *Asian J. Pharm. Ana.*, **2**, 73 (2012).
183. V. D. Prakash, S. Dogan, U. Akbulut, T. Yalcin, S. Suzer, L. Toppare, *Synth. Met.*, **60**, 27 (1993).
184. P. N. Bartlett, S. K. Ling-Chung, *Sensor. Actuat. B – Chem.*, **20**, 287 (1989).
185. M. Özden, E. Ekinci, A. E. Karagözler, *J. Appl. Polym. Sci.*, **71**, 2141 (1999).
186. Y. Ohnuki, H. Matsuda, T. Ohsaka, N. Oyama, *J. Electroanal. Chem.*, **158**, 55 (1983).
187. K. Ogura, M. Kokura, J. Yano, H. Shigi, *Electrochim. Acta*, **40**, 2707 (1995).
188. L. L. Wu, J. Luo, Z. H. Lin, *Electroanal. Chem.*, **417**, 53 (1996).
189. K. Chiba, T. Ohsaka, Y. Ohnuki, N. Oyama, *J. Electroanal. Chem.*, **219**, 117 (1987).
190. J. Yano, *J. Polym. Sci. Part A: Polym Chem.*, **33**, 435 (1995).

References

191. S. M. Sayyah, M. M. El-Deeb, S. M. Kamal, R. E. Azooz, *J. Appl. Polym. Sci.*, **112**, 3695 (2009).
192. E. Ekiñci, G. Erdoğan, A. E. Karagözler, *J. Appl. Polym. Sci.*, **79**, 327 (2001).
193. S. A. Ozkan, B. Uslu, H. Y. Aboul-Enein, *Talanta*, **61**, 147 (2003).
194. L. Laina, S. Issac, R. Joseph, D. Thomas, K. Girish Kumar, *Micro Nano Lett.*, **6**, 867 (2011).
195. D. Centonze, C. Malitesta, F. Palmisano, P. G. Zambonin, *Electroanalysis*, **6**, 423 (1994).
196. I. Losito, E. Giglio, N. Cioffi, C. Malitesta, *J. Mater. Chem.*, **11**, 1812 (2011).
197. A. H. Premasiri, W. B. Euler, *Macromol. Chem. Phys.*, **196**, 3655 (1995).
198. I. Losito, F. Palmisano, P. G. Zambonin, *Anal. Chem.*, **75**, 4988 (2003).
199. E. Bermejo, A. Zapardiel, J. A. Perez-Lopez, M. Chicharro, A. Sanchez, L. Hernandez, *J. Electroanal. Chem.*, **481**, 52 (2000).
200. Y. Altun, B. Dogan, S. A. Ozkan, B. Uslu, *Acta Chim. Slov.*, **54**, 287 (2007).
201. J. Grimshaw, *Electrochemical Reactions and Mechanisms in Organic Chemistry*, 1st Ed. Amsterdam: Elsevier Sci. Pub., 201 (2000).
202. D. I. Edwards, *Biochem. Pharmacol.*, **35**, 53 (1986).

203. H. B. Fung, T. Doan, *Clin. Ther.*, **27**, 1859 (2005).
204. N. A. F. Alhemiarya, Mohammed. H. A. Saleh, *Der Pharma Chemica*, **4**, 2152 (2012).
205. O. A. Adegoke, O. E. Umoh, J. O. Soyinka, *J. Iran. Chem. Soc.*, **7**, 359 (2010).
206. M. M. Sebaiy, A. A. El – Shanamany, S. M. El-Adl, L. M. Abdel – Aziz, H. A. Hasheem, *Asian J. Pharma. Ana.*, **1**, 79 (2011).
207. T. G. Venkateshwaran, J. T. Stewart, *J. Chromatogr. B.*, **672**, 300 (1995).
208. A. Alnajjar, H. H. Abu Seashu, A. M. Idris, *Talanta*, **72**, 842 (2007).
209. Y. Gui, Y. N. Ni, S. Kokot, *Chin. Chem. Lett.*, **22**, 591 (2011).
210. C. Wang, F. Wang, C. Li, X. Yu, L. Wang, *Dyes and Pigments*, **75**, 213 (2007).
211. C. Yang, *Anal Sci.*, **20**, 821 (2004).
212. S. Shahrokhian, S. Rastgar, *Electrochim. Acta*, **78**, 422 (2012).
213. G. Yang, L. Wang, J. Jia, D. Zhou, D. Li, *J. Solid State Electrochem.*, **16**, 2967 (2012).
214. M. Chao, X. Mao, *Int. J. Electrochem. Sci.*, **7**, 6331 (2012).
215. Q. Liu, F. Wang, Y. Qiao, S. Zhang, B. Ye, *Electrochim. Acta*, **55**, 1795 (2010).
216. D. Yaico, A. Tanimoto, F.F. Lucas, *Anal. Chim. Acta*, **596**, 210 (2007).

References

217. S. D. Randall, H. Mankit, W.A. James, D. Mare, *Langmuir*, **10**, 1306 (1994).
218. B. Barbier, J. Pinson, G. Desarmot, M. Sanchez, *J. Electrochem. Soc.*, **137**, 1757 (1990).
219. L. Zhang, *Microchim. Acta*, **161**, 191 (2008).
220. Y. Gu, W. Liu, R. Chen, L. Zhang, Z. Zhang, *Electroanalysis*, **25**, 1209 (2013).
221. K. Zhang, P. Luo, J. Wu, W. Wang, B. Ye, *Anal. Methods*, **5**, 5044 (2013).
222. H. E. Satana, B. D. Topal, S. A. Ozkan, *Anal. Lett.*, **44**, 976 (2011).
223. Y. Li, Z. Ye, P. Luo, Y. Li, B. Ye, *Anal. Methods*, **6**, 1928 (2014).
224. C. Wang, C. Li, F. Wang, C. Wang, *Microchim. Acta*, **155**, 365 (2006).
225. K. K. Barnes, C. K. Mann, *J. Org. Chem.*, **32**, 1474 (1967).
226. Y. Y. Tang, C. Po-Yu, *JCSS*, **58**, 723 (2011).
227. X. Dai, R. G. Compton, *Anal. Sci.*, **22**, 567 (2006).
228. R. S. Nicholson, I. Shain, *Anal. Chem.*, **36**, 706 (1964).
229. S. Lu, K. Wu, X. Dang, S. Hu, *Talanta*, **63**, 653 (2004).
230. H. Becker, W. Berger, G. Domschke, E. Fanghänel, *Organikum - Organisch Chemisches Praktikum*, Wiley-VCH Verlag 118 (1999).
231. L. Lopez Martinez, F. J. Luna Varquez, P. L. Lopez-de Alba, *Anal. Chim. Acta*, **340**, 241 (1997).

Research Papers Published

1. Electrochemical Sensing of Tinidazole on Modified Glassy Carbon Electrodes, **T. Jos**, A. R. Jose, U. Sivasankaran, K. Girish Kumar, J. Electrochem. Soc., **162**, B1 (2015).
2. Voltammetric Determination of Guaifenesin on a MWCNT Modified Pt Electrode, **T. Jos**, L. Lonappan, Z. Rasheed, A. E. Vikraman, K. Girish Kumar, Electrochem. Lett., **3**, B23 (2014).
3. Electrocatalysis and Determination of Pyridine-2-aldoxime methochloride using Carbon nanotube-modified Gold Electrode. **T. Jos**, S. Issac, R. Joseph, L. Rajith, K. Girish Kumar, Micro Nano Lett., **7**, 854 (2012).
4. Effect of Anionic Surfactant on the Reduction of Tinidazole at a Gold nanoparticle Modified Glassy Carbon Electrode, **T. Jos**, D. Thomas, S. T. Cyriac, M. Jacob, K. Girish Kumar, Indo American Journal of Pharmaceutical Research, **3**, 8434 (2013).
5. Diffusion Contorlled Process at an AuNP/Pt Electrode Surface for the Voltammetric Determination of TAM, **T. Jos**, L. Lonappan, A.E. Vikraman, Z. Rasheed, K. Girish Kumar, Journal of Pharmaceutical Research and Development, **2**, 224 (2013).

-
6. Spectrophotometric Determination of Metronidazole in Bulk and Dosage Form, **T. Jos**, R. Minju, K.R. Reshma, T. V. Vidya, P. S. Vrinda, T. N. Vrindha, *Int. J. Pharmacol. Pharm. Sci.*, **1**, 11 (2014).
 7. Development of Electrochemical Sensor for the Determination of Amaranth: A Synthetic Dye, S. Chandran, L. Lonappan, D. Thomas, **T. Jos**, K. Girish Kumar, *Food Anal. Methods*, **7**, 714 (2014).
 8. A lead (II) selective PVC Membrane Potentiometric Sensor Based on a Tetraazamacrocyclic Ligand, S. Mathew, L. Rajith, L. Lonappan, **T. Jos**, K. Girish Kumar., *J. Incl. Phenom. Macro.*, **78**, 171 (2014).

Conferences Papers

1. Electrochemical sensing of Metronidazole benzoate on a conducting polymer layer of p-TSA on GCE (*New Frontiers in Chemical Research, Sacred Heart College, Thevara, December 2014*)
2. Electrochemical sensing of Tinidazole on modified glassy carbon electrodes (*24th Swadeshi Science Congress, SSC, Tirur, November 2014*)
3. Electrochemical determination of Guaiphenesin on a Pt electrode incorporating the 1-d character of MWNT (*Current Trends in Chemistry C-TRiC, CUSAT, March 2013*)
4. Voltammetric determination of TAM on a Au electrode coated with a polymeric film of o – phenylene diamine (*Recent Advances in Surface Sciences (RASS), Gandhigram Rural Institute, Dindigul, February 2013*)
5. Voltammetric determination of PAM on MWCNT/Au electrode (*Materials of the millennium MATCON, CUSAT, January 2010*)
6. Voltammetric determination of PAM on MWNT/PB/Au electrode (*Recent Trends in Chemistry, Sidhardata College of Pharmaceutical Sciences, Vijayawada, February 2009*)